VANADIUM ISOTOPIC ANALYSIS OF EXTRACTABLE ORGANIC MATTER AND BULK ROCK SHALE IN THE EAGLE FORD SHALE

A Thesis Presented to

The Faculty of the Department of Earth and Atmospheric Sciences

University of Houston

In Partial Fulfillment

of the Requirements for the Degree

Master of Science

By:

Mariah Michie

May 2019

VANADIUM ISOTOPIC ANALYSIS OF EXTRACTABLE ORGANIC MATTER AND BULK ROCK SHALE IN THE EAGLE FORD SHALE

Mariah Michie

APPROVED:

Dr. John Casey, Chairman

Dr. Alan Brandon

Dr. Yongjun Gao

Dr. Joseph Curiale

Dan E. Wells, Dean
College of Natural Sciences and Mathematics

ACKNOWLEDGEMENTS

I first want to thank my committee advisor, Dr. John Casey for taking me under his wing, and letting me work on a new area of research. My committee members, Dr. Yongjun Gao, Dr. Alan Brandon, and Dr. Joseph Curiale were very encouraging every step of the way. Dr. Gao spent countless hours helping me with the methodology portion, because it was such a new area of study.

I also want to thank Dr. Adry Bissada, Dr. Thomas Lapen, and Dr. Minako Righter for allowing me to use their labs, and assisting me to conduct my experiment.

I want to thank my parents and fiancé for pushing me to the end and being there for me every step of the way, I couldn't have done it without them!

An Abstract of a Thesis

Presented to

The Faculty of the Department of Earth and Atmospheric Sciences

University of Houston

In Partial Fulfillment

of the Requirements for the Degree

Master of Science

By

Mariah Michie

May 2019

Abstract

Crude oils are enriched in a variety of metals (e.g., vanadium, nickel and molybdenum). Advances in instrumentation and research now allow the exploration of more trace elements and unconventional stable isotopic compositions of these metals in oils (e.g., V, Ni, and Mo). Crude oils appear ideal to investigate metal isotope biogeochemistry due to their accessibility and global occurrence. Stable isotopes are subject to mass dependent stable isotope fractionation, which is driven by the differences in chemical and physical properties of the atoms arising from the relative mass difference of a given element. Biodegradation, maturation, valence states/redox conditions can all induce fractionation among vanadium isotopes resulting from the differences in coordination chemistry and bond strength. In this study, a relatively recently developed unconventional stable method of obtaining the precise isotope ratio of $^{51}V/^{50}V$ was used to analyze for the first time the V isotope ratios of thirteen bulk rock shale samples and seven extractable organic matter (EOM) samples. These samples are from a core drilled from the La Salle county, TX in the Eagle Ford Shale. High concentrations and enrichments of metals are shown in the bulk rock shale where high total organic carbon, TOC, also prevails, which appears to indicate highly euxinic conditions. While the metal concentrations are important, the metal ratios, V/Ni and V/(V+Ni), are also important as they are suggested to be paleoenvironmental indicators. The bulk rock shale and EOM samples show very high V/(V+Ni) ratios (~0.9), which is indicative of very anoxic or euxinic (sulfidic) conditions. However, the V/Ni ratio has variations in the bulk rock shale, EOM and the oil.

The $\delta\ ^{51}V/^{50}V$ of the bulk rock shale and EOM samples shows variability and disparity throughout the core. The deepest samples of the bulk rock and EOM show similar values of approximately -0.7‰ +/- 0.2‰, which are close to bulk silicate earth (BSE). However, the EOM samples diverge away from BSE values, and become isotopically lighter up hole. On the other hand, the bulk rock shale samples become isotopically heavier up hole. There lies an array of fractionation processes that could be causing the disparity in isotopic composition between the bulk rock shale and EOM. The fractionation processes include the vanadium speciation and redox conditions at the sea bottom, fractionation during diagenesis, progressive kerogen-crude oil transformation, progressive crude oil expulsion, and catagenesis-related crude oil demetallation.

Table of Contents

CHAPTER 1

INTRODUCTION:

1.1 Petroleum System Elements and Processes

Oil and gas plays consist of both petroleum system elements and processes that must all be present and operative in order for there to be an active play. The petroleum elements include: source rock, overburden rock, reservoir rock, migration route, seal rock, and the trap (Magoon, 1988). The source rock is a rock with abundant hydrocarbon prone organic matter. The overburden rock is the rock lying above the source rock. The reservoir rock is the rock in which the oil and gas migrates and accumulates. The migration route includes the avenues in the rock through which the oil and gas move from the source rock to the trap. The seal rock is an impermeable rock through which oil and gas cannot move effectively, and the trap is a structural and stratigraphic location which acts as a focus for the oil and gas into an accumulation. The petroleum system processes work in conjunction with the petroleum system elements. The petroleum system processes include generation, migration, accumulation, preservation, and timing (Magoon, 1988). Generation is the process of source rock burial at high temperatures and pressures during which conversion of organic matter or kerogen to hydrocarbons takes place. The migration process is the upward and lateral movement of hydrocarbons from the initial location of the source rock to the final location, the trap. The accumulation process includes the quantity of hydrocarbons moving into the trap faster than the quantity of hydrocarbons leaking out of the trap. The preservation process deals with the hydrocarbons remaining in the reservoir and not being subjected to destruction by biodegradation and water washing. Lastly, the timing process lends to the trap forming

either before and during hydrocarbon migration. All of the petroleum system elements and processes must be present in order for an oil accumulation to occur (Magoon, 1988).

More recent advancements indicate the petroleum system can occur in either a conventional or unconventional play (Magoon, 1988). A conventional play occurs when each petroleum system element and process resides as its own entity and oil/gas is extracted laterally by the natural pressure from the wells from a reservoir where oil has migrated and accumulated. An unconventional petroleum system occurs when the source rock, reservoir rock, and trap are all one in the same. If retrieving oil is scarce by conventional ways, an unconventional method can be used. This includes drilling downward, drilling horizontally and subjecting the rock to sufficient pressures by "fracking." This allows oil and gas to flow from very tight, low-porosity shales and sandstones that would not be possible with conventional drilling and recovery techniques.

1.2 Trace Element Geochemistry of Crude Oil

Vanadium, Nickel and Sulfur

Petroleum consists of major components of hydrogen and carbon with lesser amounts of nitrogen, sulfur, and oxygen. These five elements make up the organic molecules of oil. Crude oil also consists of an inorganic component comprising largely of molecules containing vanadium (V), nickel (Ni), and other trace metals (Aleshin et al., 1984; Amorim et al., 2007). Abundances of vanadium and nickel in oil vary depending on the redox conditions, the degree of organic preservation, and metal replenishment from the overlying water column and abundance of the accumulated organic matter at the depositional site (Emerson & Huestes, 1991). Metal enrichment is highest in

euxinic/anoxic environments where organic matter preservation tends also to be highest, and tends to be lowest in oxic environments. Therefore, the concentrations of vanadium and nickel are dependent on source rock composition, depositional environment, basin type, and organic matter type, which all contribute to preservation of certain high metal contents (Lewan & Maynard, 1982; Lewan, 1984; Barwise, 1990). In 1990, Barwise presented a classification scheme relating vanadium, nickel, and sulfur content to source rock lithology and depositional environment. The highest metal abundances commonly exist in marine environments where sea-bottom anoxia often exists, while metal abundances decrease significantly in terrigenous oxic conditions. The abundances of these metals can also be influenced by secondary processes of maturation, biodegradation, and crude oil migration. For example, Barwise (1990) indicated that nickel and vanadium metal concentrations vary with API gravity.

Metal abundance is high in low API gravity, or low maturity crudes, whereas at higher thermal maturities and higher API, metal abundances decrease. The loss of metals with increases of thermal maturation could be due to source rocks subjected to high temperatures over time, resulting in a process called demetallation (Constantinides et al., 1959). However, although abundances of metals are subject to change due to secondary processes, the V/Ni, Ni/V and V/(V+Ni) ratios stay fairly constant for lower degrees of maturity due to the structural similarities among compounds containing vanadium and nickel, ie. until very high maturities are reached (Ro=~1) (Lewan, 1980). The V/Ni and V/(V+Ni) ratios have been used to characterize depositional environment, redox conditions as well as oil-source rock and oil-oil correlations (Moldowan et al.,

1986; Barwise 1990; Sundararaman et al., 1993; Galarraga et al., 2008). Furthermore, geochemical signatures of Ni/V>2 often indicate lacustrine terrigenous oxic source rocks, while Ni/V<2 indicate marine carbonate anoxic source rocks (Barwise, 1990). In crude oil, vanadium occurs mainly as vanadyl ions (VO^{2+}) of organometallic porphyrins and non-porphyrins. Porphyrin structures are initially derived from plant precursors such as chlorophyll (Treibs, 1934, 1936; Lewan, 1984; Baker and Palmer, 1987; Lipiner et al., 1988; Louda et al., 1998). The proportionality of Ni and V in petroleum are controlled by Eh-pH conditions, sulfur availability, and source rock lithology (Lewan & Maynard, 1982; Lewan, 1984).

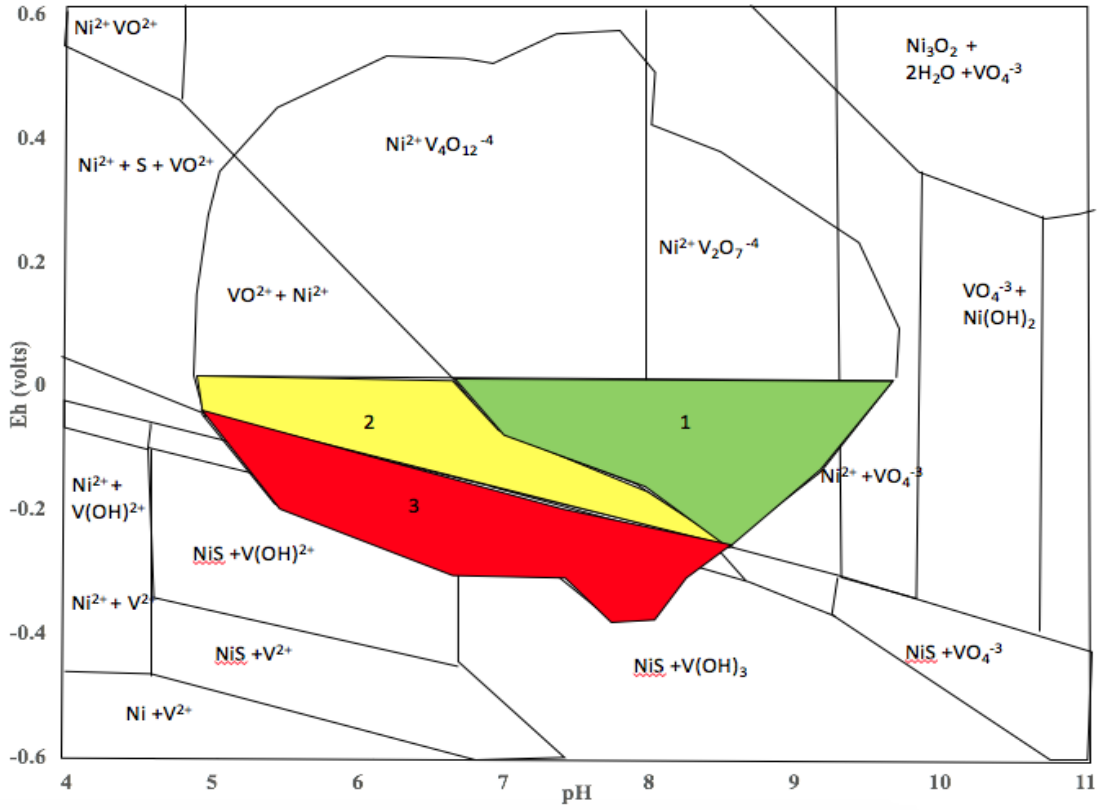

Figure 1.2.1: Three Regimes comparing Eh vs pH for vanadium and nickel speciation. Regime one (green) indicates Ni ions for metalation over V ions. Regime two (yellow) indicates Ni and V ions available for metalation depending on pH conditions. Regime three (red) indicates V ions available for metalation over Ni due to sulfate reduction. (Redrafted from Lewan, 1984).

Lewan, in 1984, established an oil classification scheme consisting of three regimes (Figure 1.2.1). Regime one represents vanadium occurring as a quinquivalent anion where vanadyl cations are not available for metalation into the sediment. On the contrary, nickelous cations are available for metalation giving rise to an overall low V/(V+Ni) ratio, and low sulfur content. In regime two, vanadyl and nickelous cations are available for metalation. In basic (high pH) conditions, nickelous cations dominate for metalation

due to the vanadyl ions being hindered by hydroxide ions. In acidic (low pH) conditions, hydroxide ions do not hinder vanadium, therefore allowing for vanadyl and nickelous cations to be available for metalation. The V/(V+Ni) ratio is usually ~0.1 to 0.5 (Lewan, 1984). Lastly, in regime three vanadyl ions are available for metalation, but nickel is hindered by reduced sulfate. In this regime, sulfate is reduced by sulfate reducing bacteria and nickelous cations have an affinity to bind to the reduced sulfur (and Ni-sulfide production). This results in high V/(V+Ni) and high sulfur content in the crude oil.

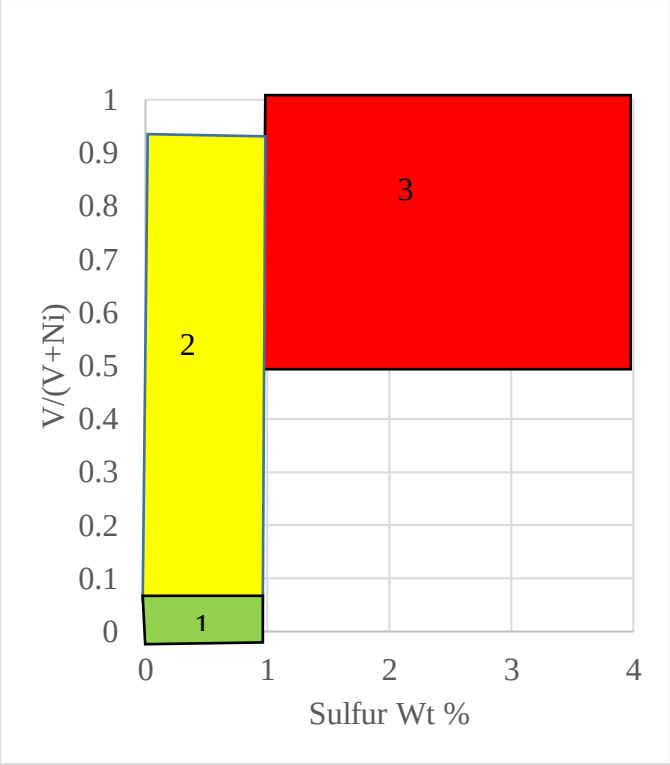

Figure 1.2.2: Three Regimes comparing V/(V+Ni) ratio and sulfur content. Regime one (green) indicates high sulfur content and high V/(V+Ni). Regime two (yellow) indicates low sulfur and variable V/(V+Ni). Regime three (red) indicates low sulfur and low V/(V+Ni). (Redrafted from Lewan 1984; Whisman and Cotton 1971).

In anoxic conditions marine conditions, VO(II) porphyrins predominates over Ni(II) porphyrins due to the fact that in oxygen depleted environments, the bacteria carry out sulfate reduction and bottom waters become H_2S rich. Sulfate is reduced and nickel binds to the free sulfur, leaving vanadium to bind with the free-base porphyrins and other organometallic complexes in the sediment. In other words, there is a positive correlation with sulfur % and vanadium abundance in oils (Barwise, 1990; Figure 1.2.2). On the contrary, in oxic environments, Ni(II) porphyrins predominates over VO(II) porphyrins. Hydroxides in basic conditions hinder the vanadium from binding to the porphyrins and other organometallic complexes, leaving the nickel available for metalation of the porphyrins and organometallic complexes.

1.3 Vanadium Stable Isotopes

While abundances of metals can reveal information about depositional environment, source rock lithology and organic matter type, stable isotope analysis of vanadium could provide additional information, but these studies are in their infancy (Ventura et al., 2015; Gao et al., 2017). Transition metal stable isotopes have a correlation between ocean oxygenation and redox related changes in global oceans (Anbar et al., 2007). Oxygenation in oceans changes over time with oxygen consumption dependent on carbon-rich organic matter from the photic zone, and oxygen supply resulting from water circulation and mixing. Ocean oxygenation is therefore linked with carbon cycling and global climate.

Stable isotope analysis of the metals in crude oils has been of high interest due to the fact that crude oils contain high amounts of transition metals: e.g., V, Ni, Mo

characterized by multiple stable isotopes. Crude oils are important to study stable isotope biogeochemistry due to their availability, and global occurrence (Ventura et al., 2015). They represent one of the most extensive reservoirs of sedimentary organic matter from the past with oils sourced from ancient high organic matter source rocks (Ventura et al., 2015).

Stable isotopes differ from radiogenic isotopes because they are subjected to mass-dependent fractionation, which is driven by the differences in chemical and physical properties of atoms (Hoefs, 2008). Vanadium fractionation is affected by a variety of different processes such as phases/species, valence states, mineral absorption, biological activity, biodegradation, and thermal maturity (Gao et al., 2017). It is also shown that V isotope fractionation occurs within different species of the same valence state with changes in bond lengths and coordination numbers (Wu et al., 2015).

Fractionation can occur in vanadium due to the multiple valence states (V^{+2}, V^{+3}, V^{+4}, V^{+5}) in aqueous environments and consequently isotopic ratios are very sensitive to redox conditions (Ventura et al., 2015). Vanadium follows a two-step reduction process which can lead to the formation of separate vanadium carrier phases of differing solubilities under varying depositional environments (Tribovillard, 2006). V^{+2} compounds are reducing agents, while V^{+5} compounds are oxidizing agents. In oxygen enriched environments, V(V) exists and forms soluble HVO_4^{2-} and $H_2VO_4^{2-}$. As oxygen becomes depleted in anoxic environments, V(V) is reduced to V(IV) and forms vanadyl ions, and insoluble hydroxides ($VO(OH_3)$, $VO(OH)_2$). V(V) and V(IV) are both surface reactive and are subjected to adsorption processes (Tribovillard, 2006; Gao et al., 2017). Depending on the pH of the water and the vanadium stability, V will adsorb to differing

compounds. For example, V(V) being both soluble and mobile, adsorbs to iron and manganese oxides, and clay minerals leading to high vanadium concentrations in seawater (Wu et al., 2015). In euxinic environments, consisting of high sulfur and no oxygen, the presence of H_2S causes the V(IV) to be reduced further to V(III), which precipitates as V_2O_3 and $V(OH)_3$. Changes in redox reactions can cause fractionation of vanadium. These redox reactions affect metal speciation and reactivity to reducing and oxidizing agents, therefore vanadium isotopic fractionation of trace metals in crude oils could have the potential to trace depositional or post sedimentary environments to understand the biogeochemical cycles that lead to oil formation.

Secondly, fractionation between phases/species are controlled primarily by the valence state and binding chemistry. Species with shorter bonds, V-O in this case, tend to be enriched in the heavier isotope (Schauble et al., 2001; Wu et al., 2015). In this case, vanadium occurring as V^{+5} is enriched in the heavier isotope relative to V^{+3} (Schauble et al., 2001; Wu et al., 2015). As valence state increases, the bond length decreases, and the bond strength increases. This applies to most redox related elements such as Cu, Fe, and V (Wu et al., 2015).

Fractionation can also occur between the same species, but differing coordination numbers and structure. For example, in 2015, Wu et al., discovered that significant isotopic fractionation occurred between vanadium occurring as a +5 valence state and a four-fold coordination cluster, and vanadium occurring as a +5 valence state and a six fold coordination cluster. On the contrary, when the valence state and coordination number were the same, the fractionation was very minimal (Wu et al., 2015).

In addition, biodegradation and thermal maturation can induce isotopic fractionation in crude oils. Pr/nC_{17} values as well as gas chromatogram distributions of light organic compounds can indicate biodegradation (Gao et al., 2017). Bacteria in both aerobic and anaerobic environments utilize nutrients and alter petroleum. Microbial activity can also induce changes of the species and coordination geometries of vanadium ions (Gao et al., 2017). The lighter, lower molecular weight vanadium complexes are the first attacked by the bacteria, leaving the higher molecular weight complexes more resistant to attack. The pristine V isotopic compositions can be significantly modified by biodegradation in which the V/V+Ni has a very restricted value with large variation in $\delta^{51}V$. In terms of maturation, as source rocks are subjected to higher pressures and temperatures, thermal maturity increases. During this process, labile portions of crude oils begin to crack and concentrations of metals decrease. This process of demetallation that occurs can cause porphyrin compounds in crude oil to change type, or decompose the metallo-porphyrins, which can lead to free cations that can be occluded into asphaltenes or form a metal sulfide that gets trapped in asphaltene micelles (Filby, 1994). The exchange and transformation of vanadium between different species can induce fractionation resulting from changing bonding strengths among structures. Decreases in $\delta^{51}V$ with increasing thermal maturity could be a result of demetallation loss of ^{51}V or preferential incorporation of ^{50}V into the organometallic complexes (Peters and Moldowan, 1993; Gao et al., 2017; Figure 1.3.1). Lastly, fractionation can also occur due to biological activity as vanadium is an essential growth trace element for many plants and animals. Therefore, the vanadium isotopic composition can be used to track the source or type of biomass (Gao et al., 2017).

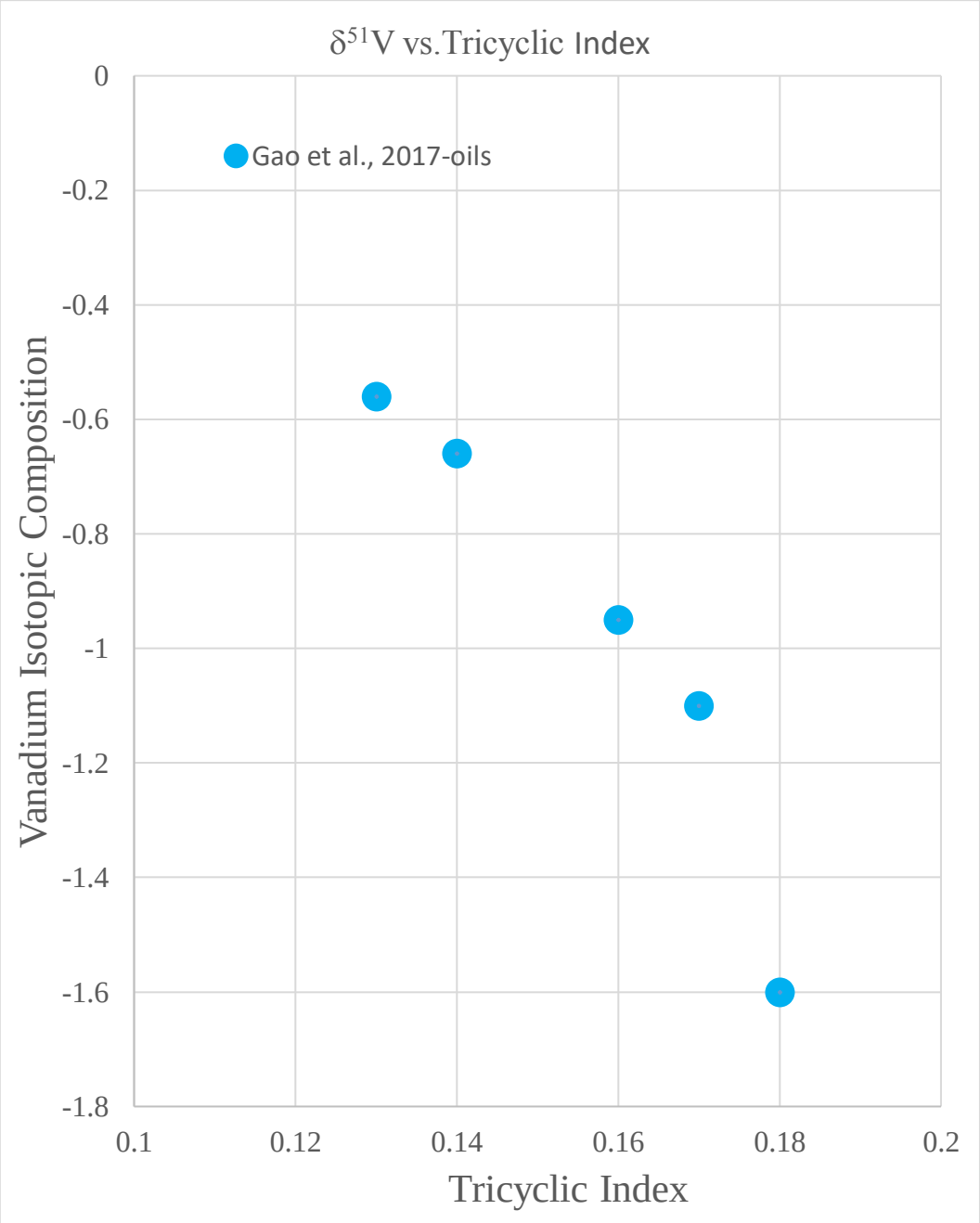

Figure 1.3.1: Vanadium Isotopic Composition vs thermal maturation. $\delta^{51}V$ becomes lighter with increasing thermal maturity. (Redrafted from Gao et al 2017).

1.4 Previous Vanadium Isotopic Work

In 2015, Ventura et al., was one of the first to measure vanadium isotope compositions of crude oils. Discovered in the study was the fact that in crude oils, vanadium isotopic compositions have tremendous variability. He proposed that the data distinguishing two distinct clusters comprise oils with isotopically light compositions and most likely sourced from terrestrial siliciclastic rocks, and a cluster composing of isotopically heavy compositions most likely sourced from carbonate marine rocks (Ventura et al., 2015). It was therefore realized that $\delta^{51}V$ denotes that the isotopic compositions in unaltered crude oils are most likely inherited from the vanadium present during time of deposition. He further verified this concept by comparing metal concentration to the $\delta^{51}V$ for vanadium (Ventura et al., 2015). Once again, two distinct clusters were recognized, where samples more enriched in the heavier $\delta^{51}V$ tend to have igher metal concentrations comprising of the carbonate marine samples. Samples depleted in the heavier $\delta^{51}V$ tend to have lower metal concentrations comprising more of the terrestrial siliciclastic samples (Figure 1.4.1). This indicates that the isotopic signatures are inherited from the primary source which controls the metal availability or the accumulation of heavy isotopes with metal enrichment during diagenesis.

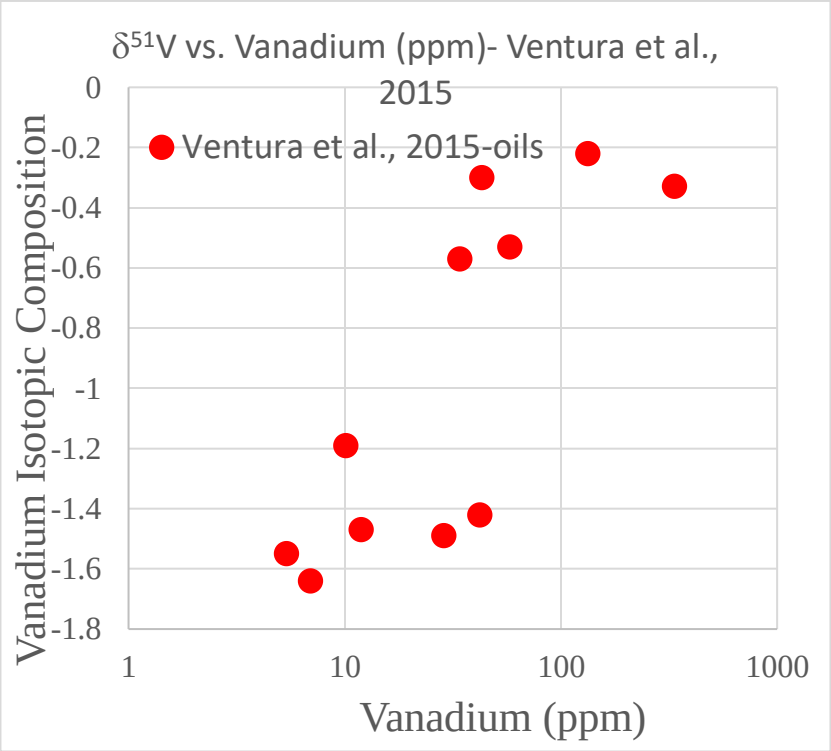

Figure 1.4.1: Vanadium (ppm) vs vanadium isotopic composition. Lower vanadium concentration samples associated with lighter vanadium isotopes, and higher vanadium concentration samples associated with heavier vanadium isotopes. (Redrafted from Ventura et al., 2015).

Gao et al., 2017 measured vanadium isotopic compositions of a different set of crude oils and found similar correlations. There was a first order positive correlation between the vanadium isotopic composition and the redox parameter, V/(V+Ni) in unaltered samples (Gao et al., 2017; Figure 1.4.2). Samples enriched in heavier vanadium isotope compositions exhibit higher V/(V+Ni), while samples depleted in the heavier vanadium isotope compositions show a lower V/(V+Ni) (Gao et al., 2017; Ventura et al., 2015; Figure 1.4.2). Vanadium fractionation was also analyzed for a set of oils from a single oil field, which indicated that both biodegradation and maturation affect not only

vanadium concentration, but isotopic signatures as well. Biodegradation fractionates the vanadium isotope composition to both heavier and lighter values (Gao et al., 2017). Maturation affects the isotopic signature by fractionating to lighter values with increases in thermal maturity.

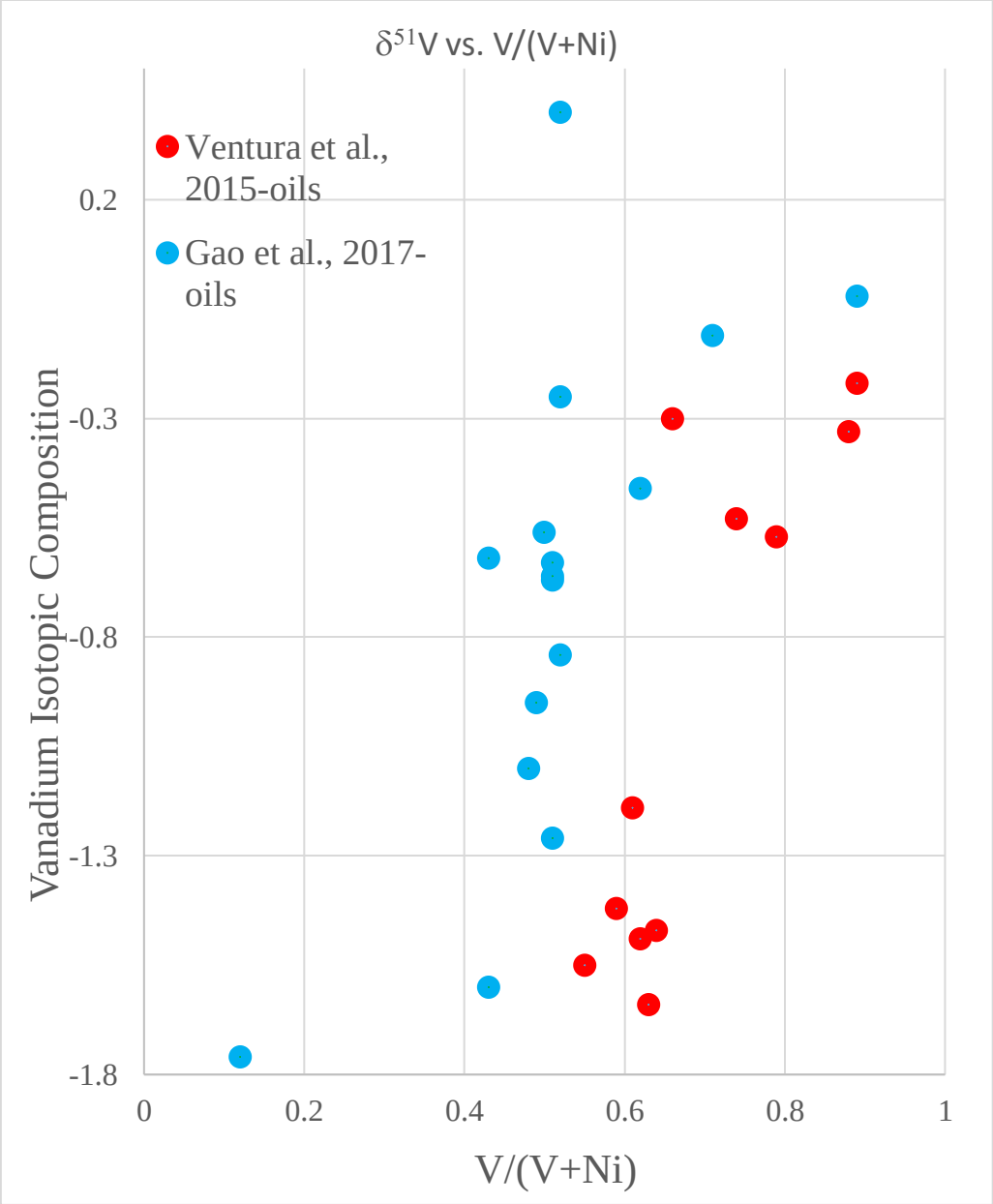

Figure 1.4.2: Positive slope correlation between the V/(V+Ni), redox parameter, and the vanadium isotopic composition. The lighter $\delta^{51}V$ corresponds with lower V/(V+Ni), and the heavier $\delta^{51}V$ corresponds with higher V/(V+Ni) (Redrafted from Ventura et al., 2015; Gao et al., 2017).

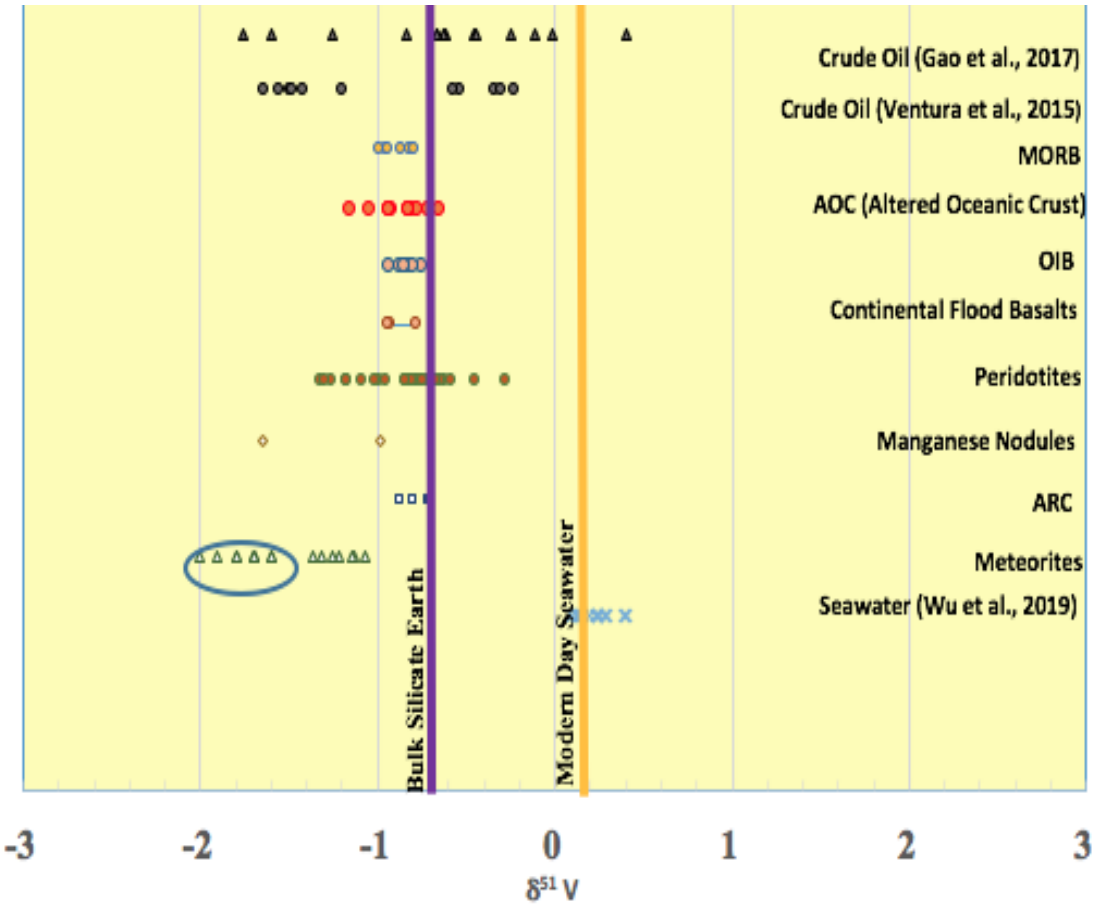

Figure 1.4.3: Crude oil data alongside Terrestrial and Extraterrestrial vanadium isotopic data (Klein and Langmuir, 1987; Fisk and Kelley, 2002; Wanless et al., 2012, Gannoun et al., 2012; Prytulak et al., 2013; Nielsen et al., 2014; Gale et al., 2014; Ventura et al., 2015; Wu et al., 2016; Schuth et al., 2017; Redrafted from Gao et al., 2017; Wu et al., 2018)

In 2017, Gao et al., compared isotopic data to that of Ventura et al., 2015, alongside high-temperature mafic and ultramafic rock data (Figure 1.4.3). The 2017 study showed wider isotopic compositions comparatively to the other study. In the Ventura et al., 2015 study, sulfur was not accounted for and removed by column chromatography before vanadium was measured, which could alter results and lend lighter isotopically.

Contrary to low temperature crude oils, terrestrial and meteorite reservoirs show a much more restricted $\delta^{51}V$ value. Mass fractionation is inversely related to temperature (Gao et al., 2017). The higher the temperature, fractionation diminishes to zero. Therefore, high temperature mafic/ultramafic rocks display a restricted isotopic range centered near the Bulk Silicate Earth (BSE) composition compared to low temperature crude oils (Urey, 1947; Prytulak et al., 2013).

1.5 Samples

Seven extractable organic matter and thirteen shale bulk rock samples from a core (~120 ft) located in La Salle county of the lower Eagle Ford Shale were analyzed. The samples consist of a set of extractable organic matter which is assumed to be "frozen oil" in the rock and a set of bulk rock shales which are described as laminated sedimentary rock formed from mud and clays. The samples were chosen in order to obtain a broad spectrum through the whole 120 ft cored interval. The EOM samples were limited to only seven samples based on the higher vanadium content suitable for V extraction. Low concentrations of vanadium in the EOM limits vanadium isotopic analyses, because higher quantities of extraction are needed. The bulk rock shale samples have very high vanadium concentrations allowing for easier analyses.

CHAPTER 2

GEOLOGIC SETTING

2.1 Eagle Ford Shale, Texas

The Eagle Ford Shale is, by definition, an unconventional reservoir. The source rock, reservoir rock, and trap are within the same formation. In order for the hydrocarbons to be expelled, hydraulic fracturing (fracking), a process where the reservoir undergoes large amounts of fluid pressure, is implemented to fracture the rocks. Although categorized as an unconventional reservoir, the Eagle Ford has generated and expelled oil in a conventional manner, and that oil has migrated to the Austin Chalk reservoirs where it is produced today (Dawson et al., 1995). Thus, it is both a conventional source rock and an unconventional source-rock reservoir.

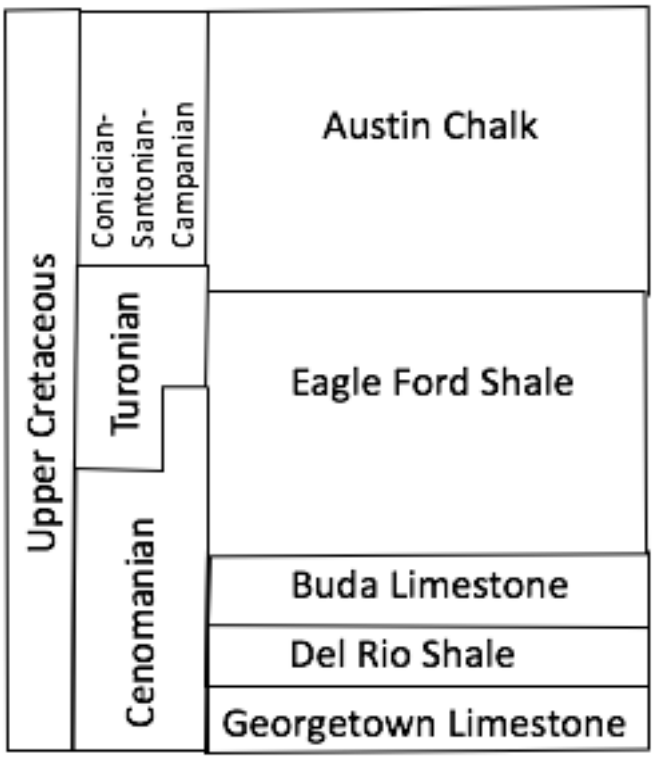

Figure 2.2.1: Lithostratigraphy of the western Eagle Ford Shale. The Eagle Ford shale lies above the Buda Limestone formation and below the Austin Chalk formation. (Redrafted from Hentz and Ruppel, 2010).

The Eagle Ford Shale extends from the Mexican border in West Texas, through Austin, Waco into northwestern Texas, and ending in Louisiana (Hentz and Ruppel. 2010). The Eagle Ford Shale was deposited at the upper Cretaceous Cenomanian-Turonian boundary and lies underneath the Austin Chalk and above the Buda Limestone Formation (Hentz and Ruppel, 2010; Figure 2.2.1). The Eagle Ford shale has two distinct depositional intervals: the upper Eagle Ford Shale and the lower Eagle Ford Shale. The lower transgressive Eagle Ford Shale consists of a low energy, anoxic environment dominated by fossiliferous, little bioturbated high organic carbon shales (Murphy et al., 2013; Donovan and Staerker, 2010). Laminations present throughout rocks show very quiet water conditions with the absence of storms or disruptions. They also indicate the absence of sediment mixing or the involvement of extensive organism activity (Mcgarity, 2013). The upper regressive Eagle Ford Shale consists of a high stand system tract, where the accumulated sediment rates surpass the sea level rise (Martin et al., 2011). Forming at the upper Cretaceous boundary, two separate anoxic events occurred. The more recent anoxic event occurred during extremely warm oceans and an increase in atmospheric carbon dioxide due to the greenhouse effect (Martin et al., 2011). The increase in carbon dioxide resulted in an increase in organic material (Martin et al., 2011). This led to the laminated black shales present throughout the lower transgressive interval in the Eagle Ford, while the upper Eagle Ford is interpreted to have been deposited in a more near-shore environment (Martin et al., 2011).

While the Eagle Ford Shale shows considerable variation in depositional environment, both depth and thickness throughout the shale play change as well

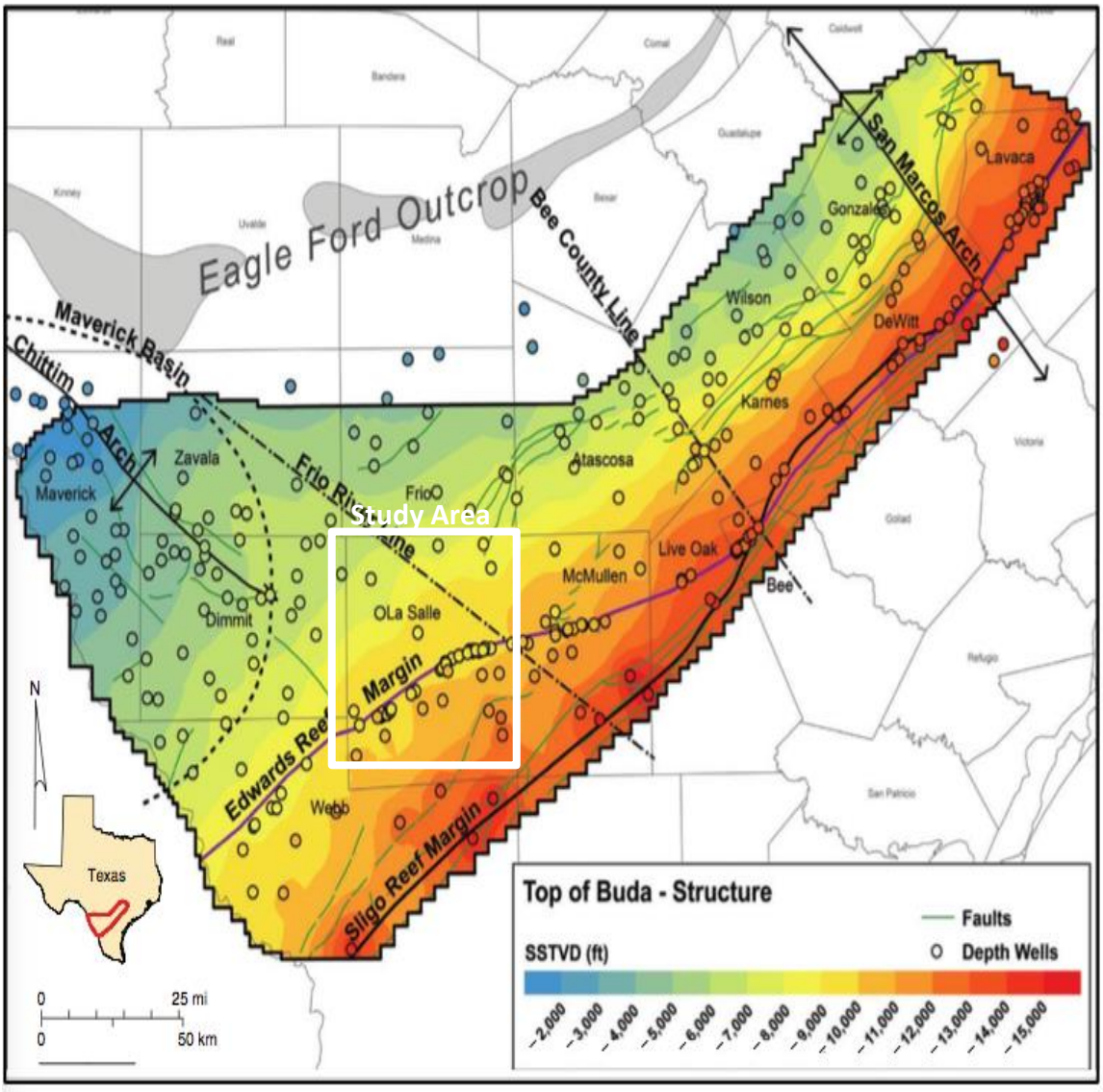

Figure 2.1.2: Eagle Ford Shale formation depth map. The depth of the formation increases as you migrate from the northwest to the southwest. The depths increase from around 1,400 ft in the northwest to >14,000 feet in the southeast (Modified from Hammes et al., 2016)

(Hammes et al., 2016). Starting with the variations in depth, the northwest section of the play shows depths starting at around 1,500 feet and stretching towards the southeast with elevations reaching to depths of 14,000 feet (Hammes et al., 2016, Figure 2.1.2). Thickness variations show more abrupt changes throughout the Eagle Ford Shale (Figure 2.1.3). The thickness is the smallest near the Frio, Atascosa, and Wilson counties in the

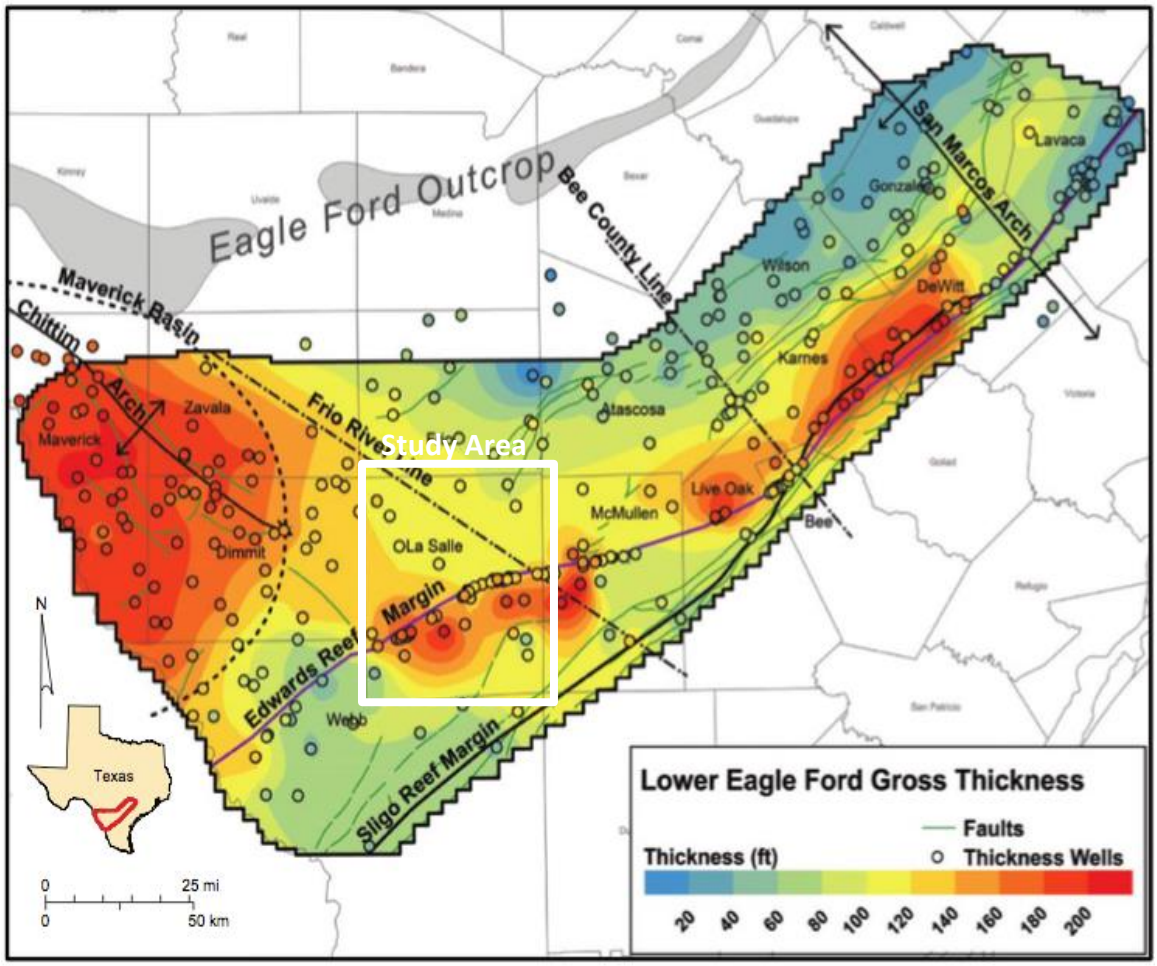

Figure 2.1.3: Lower Eagle Ford Shale formation thickness. The highest thicknesses (>200 ft) exists near the Maverick Basin, and in portions of La Salle, McMullen, and Karnes counties.). Thicknesses vary in other portions of the formation ranging from 20 ft to 400 ft. (Modified from Hammes et al., 2016).

north with ranges of about 20-100 feet (Hammes et al., 2016; Figure 2.1.3). However, to the northwest of the play near the Maverick basin, the thicknesses become >200 ft (Hammes et al., 2016). In addition, to the south the thicknesses increase to nearly 350 ft in parts of La Salle, McMullen and Karnes counties (Hammes et al., 2016; Figure 2.1.3). It is also important to note that the Eagle Ford Shale formation dips to the southeast

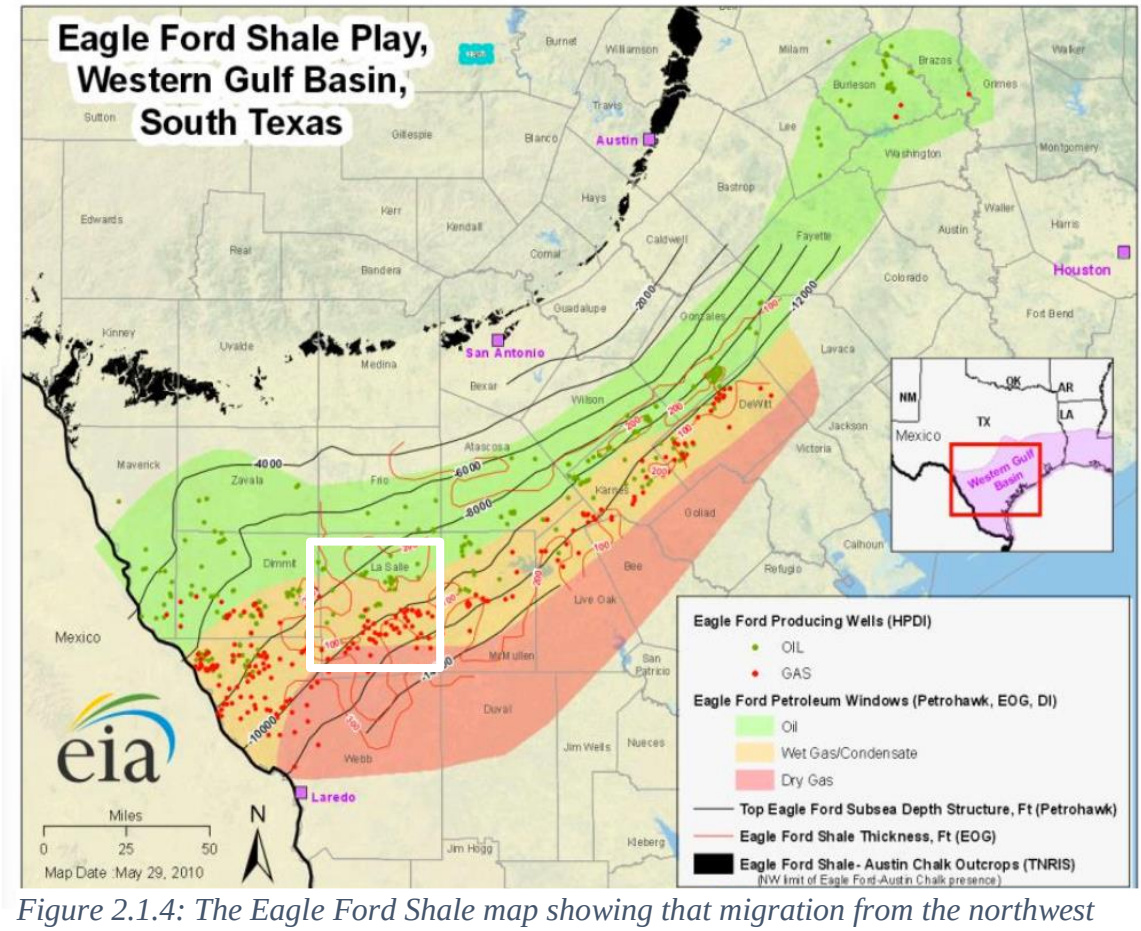

Figure 2.1.4: The Eagle Ford Shale map showing that migration from the northwest section of the play to the southeast, thermal maturation increases. The most thermally immature sediments include the northern most section of the play (green) and the most thermally mature sediments include the most southerly portion of the play (red) (Modified from U.S. Energy Information Administration, 2010).

toward the Gulf of Mexico (Harbor, 2011). As the Eagle Ford formation dips to the southeast, it is evident that the sediments become more mature with depth, crossing through several hydrocarbon generation zones (U.S. Energy Information Administration, 2010; Figure 2.1.4) Hydrocarbon generation is partitioned into five zones based on vitrinite reflectance. Zone one incorporates the biochemical methane generation and dry

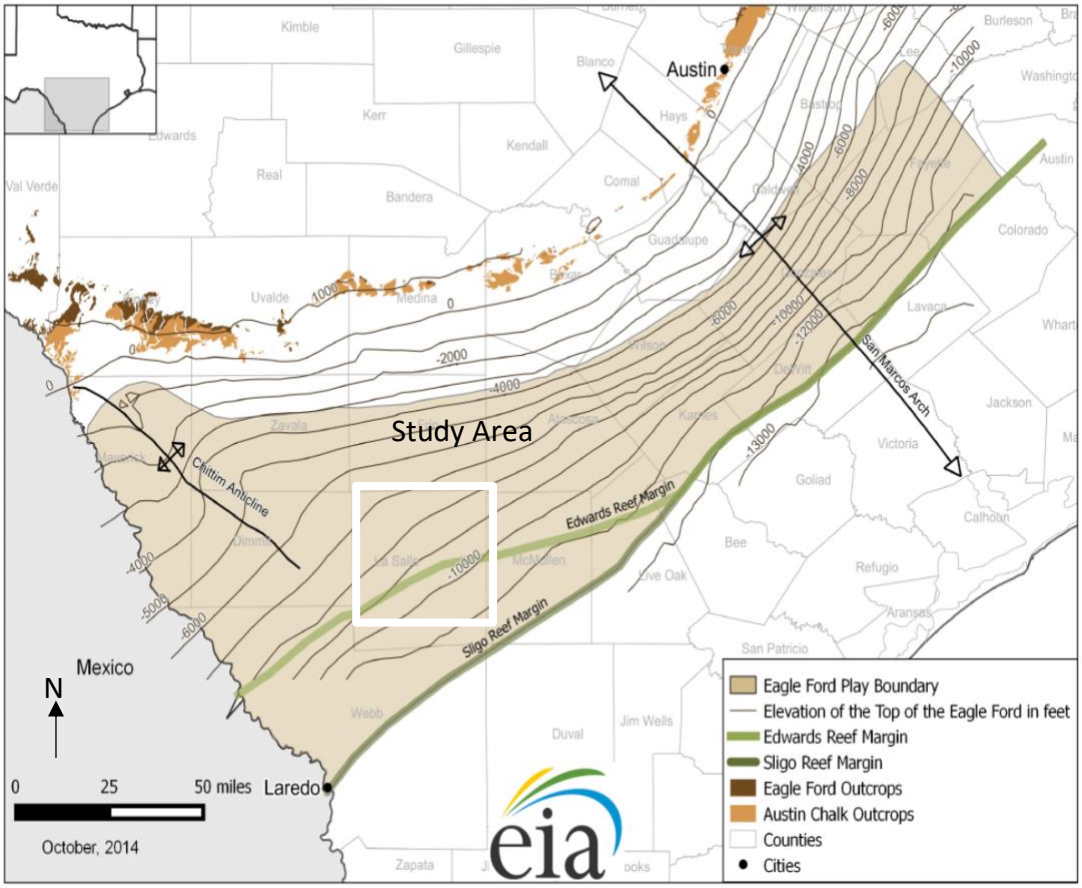

Figure 2.1.5: Eagle Ford Shale formation map showing the splitting of the two reef systems: Edwards and Sligo near the study area of La Salle county. The splitting of the two reef systems creates a structural low in the middle, the Hawkville Trough. (Modified from U.S. Energy Information Administration, 2014).

gas; zone two includes dry and wet gas; zone three consists of the peak oil generation zone; zone four includes condensates mixed with wet and dry gas; zone five includes dry gas (dead carbon) (U.S. Energy Information Administration, 2010). Migrating from one zone to the next in ascending numerical order, the vitrinite reflectance increases showing the most thermally mature sediments in the most southern portion of the play (U.S. Energy Information Administration, 2010; Figure 2.1.4).

The Eagle Ford Shale includes several geological features across the play. The Maverick Basin in the far western portion of Texas. Secondly, the San Marcos Arch

serves as an extension of the Llano Uplift in the northern portion of the play and results in thinning of the Eagle Ford in the region. Two separate embayments are prominent: The Houston embayment and the Rio Grande embayment. The Houston embayment includes east of the San Marcos Arch and the Rio Grande embayment includes west of the San Marcos Arch. The Sligo and Edwards Reef Margin mark the southern boundary of the Eagle Ford and structurally influences the Rio Grande embayment.

The area of research lies in the La Salle county, part of the Rio Grande embayment. In this area the Sligo and Edwards reef margins were originally one reef system, split into two (U.S. Energy Information Administration, 2014; Figure 2.1.5). The splitting of the two reef systems creates two structural highs with a lower silled basin in between, the Hawkville Trough. The deep, weakly restricted Hawkville Trough basin along with high sedimentation rates created very thick sections and high organic content between the two reef margins (Donovan and Staerker, 2010; Gardner et al., 2013; Figure 2.1.5). The Edwards Reef margin and the Sligo Reef margin formed during times of high sea level rise followed by drops in sea level which created oxygen depleted, anoxic environments in the weakly restricted basin due to lower nutrient-rich sediment supply (Donovan and Staerker, 2010). Areas of very high total organic carbon along with a high content of redox related trace metals are evident in portions of the lower Eagle Ford shale (Donovan and Staerker, 2010).

The core studied in this work is from the lower Eagle Ford Shale in the Hawkville Trough between the two reef systems of the La Salle County (Figure 2.1.5).

CHAPTER 3

METHODS

Extractions, Digestions, Multi-step Liquid Chromatography, MC-ICPMS

Vanadium consists of only two stable isotopes: ^{51}V (99.75%) and minor ^{50}V (0.24%). Prior to 2015, V isotopic compositions were measured using thermal ionization mass spectrometry (TIMS) (Premovic et al., 2002). Unfortunately, the analytical uncertainty was high due to polyatomic and isobaric interferences of chromium and titanium as well as the lack of a good reference standard (Gao et al. 2017). In 2015, Nielsen et al., proposed a new high precision analysis of vanadium isotopes, while correctly accounting for fractionation and interferences of Cr and Ni. The new method required analysis on a Multi-Collector Inductively Coupled Plasma Mass Spectrometry (MC-ICP-MS) and the creation of a column chemistry separation technique. V isotopes are now possible with precisions of 0.10% (2σ) in silicate matrices (Nielsen et al., 2011, 2014, 2016). In 2017, Gao et al., proposed a new method taking sulfur interferences into account due to interferences with V isotopes and ^{49}Ti (Gao et al., 2017). To ensure that sulfur has been successfully removed for analysis, a multistep liquid chromatography procedure with combined cation and anion exchange columns was presented for crude oil and silicates (Gao et al., 2017). Although a precise method has been designed, high precision measurement in crude oils is a still a challenge today due to their heavy organic matrix, high sulfur content and variability, and low mass fractions of V in some samples (e.g., mature crude oil).

3.1 Sample preparation

Analysis of both EOM and bulk rock shales requires powdering of the bulk rock using a jaw crusher and a shatter box. This is followed by separating an aliquot of the powder for EOM extraction and an aliquot for bulk rock measurement. For extraction of organic matter, 100 g of the sample was used and crushed to pieces in the skull crusher.

For the organic matter, the EOM samples were introduced into the shatter box to grind the sample into a fine powder and weighed (referred to as "extracted"; Table 3.1.1). Dichloromethane (DCM) was added to a flask and the sample in a styrofoam thimble and set up in the extraction. The process took around a week as the temperature reaches the boiling point of the DCM and the organic matter was completely extracted. The thimbles were removed and dried overnight. Next, the flask was introduced into the rotary evaporator (rotovap) to remove the solvent from the sample and to isolate the EOM. Lastly, the EOM was transferred into small glass vials along with DCM (referred to as "vial+bitumen"; Table 3.1.1). The vials were set on a hot plate to evaporate the DCM prior to the digestion process. The sample bitumen was then weighed prior to the microwave digestion process. The EOM samples after DCM evaporation weighed near 1g each (Table 3.1.1).

Table 3.1.1: EOM samples ending up with ~1g of bitumen after organic matter extraction

Sample	Native(g)	Extracted (g)	Vial+Bitumen (g)	Vial (g)	Bitumen (g)
8	101.46	99.19	13.82	12.75	1.069
16	94.17	91.38	14.04	12.79	1.248
18	94.74	92	14.17	12.88	1.286
22	99.05	95.71	14.35	12.8	1.548
26	91.96	87.51	14.67	12.92	1.751
30	103.13	99.43	14.84	12.8	2.044
44	100.93	98.32	13.64	12.85	0.79

3.2 Digestion (EOM)

Crude oils have a very heavy organic matrix that causes polyatomic and isobaric interferences. Therefore, a mineralization procedure was developed to destroy organic

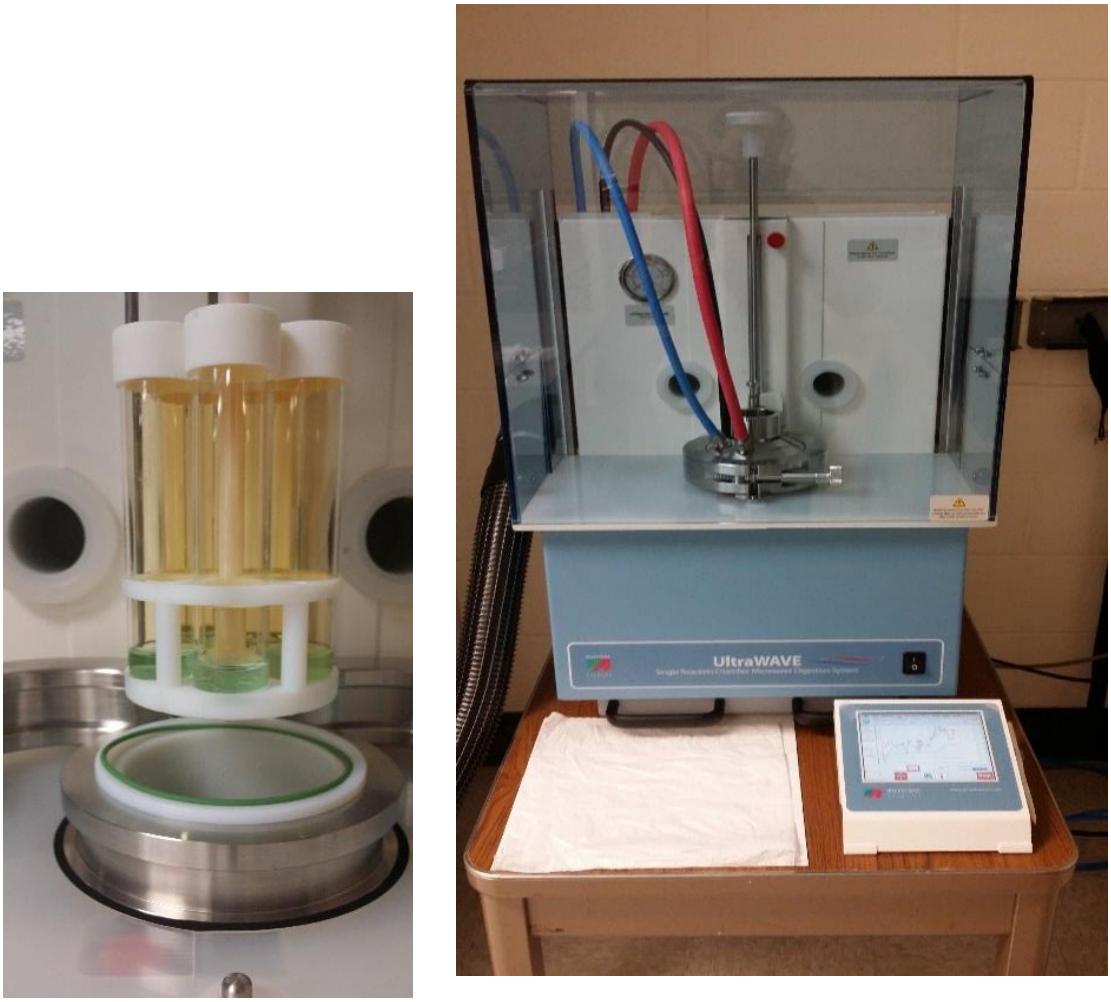

Figure 3.2.1: Milestone Ultrawave Single reaction chamber (SRC) microwave system

structures in the EOM and oil with strong oxidizing acids in pressurized vessels with the single reaction chamber microwave digestion system using the Milestone Ultrawave Single reaction chamber (SRC) microwave system (Casey et al., 2016; Wang et al., 2014, Figure 3.2.1). In the EOM digestion process, the EOM samples were pipetted out of the

glass vials into the digestion tubes. DCM was added to each of the glass vials in order to ensure that the EOM was completely removed from the vial and into the tubes. The milestone Ultrawave holds five quartz glass sample tubes at a time. The digestion tubes with samples were first placed on the hot plate at 40 ºC for 20 min to ensure that the DCM is completely evaporated. Then 1 mL of 16 N HNO_3, 1 mL of 12 N HCl, 1 mL of H_2O_2 were added to do a pre-digestion for about 10 min and then 4 mL of 16 N HNO_3 were added prior to microwave digestion. The sample tubes were then loaded into the single reaction chamber for microwave digestion. The tubes were loaded into a cylindrical shaped Teflon container where the tubes were submerged into a tub of 130 mL of H_2O, and 5 mL 16 N HNO_3. After tubes were securely in place and the machine was locked, the pre-programmed method selection of "Long Condensate.mpr" was selected for EOM samples (Table 3.2.1).

Table 3.2.1: Ultrawave Microwave Digestion Long Condensate.mpr and Rock Digestion.mpr temperature/pressure

	Long Condensate.mpr	
Time (min)	Temperature ºC	Pressure (bar)
10 min	0-100	0-150
5min	100	150
5min	120	150
10 min	180	150
10 min	180	150
10 min	250	150
45 min	250	150
	Rock Digestion.mpr	
Time (min)	Temperature ºC	Pressure (bar)
5 min	150	150
5 min	180	150
10 min	250	150
30 min	250	150
5 min	230	150
5 min	250	150
30 min	250	150

The pressure gauge was opened slowly until 40 bars were met, and the digestion process started. Once digestions were complete and samples were cooled and depressurized, the samples were returned from the tubes into clean PFA beakers and the digestion tubes were rinsed thoroughly with 2% HNO_3 and then decanted to the beakers to ensure that all the digested material was transferred into the new PFA beakers. The sample in the beakers were dried down. After dry-down, 10 mL of 2% HNO_3 was added to the beakers, capped and left on the hot plate overnight at 100 ºC. The samples were then transferred into glass test tubes. If the EOM samples have a milky white color, they are centrifuged for ~30-45 min to separate the wax precipitate from the clear liquid. The sample was then taken from the test tube and returned back to the beakers, leaving behind

the solid precipitate produced from the centrifuge. The samples were dried down once again, and 6N HCl was added to the beakers before column chemistry begins.

3.3 Digestion (Bulk Rock)

For the whole rock powder, samples were loaded into Teflon digestion tubes and weighed. The Teflon tubes rather than quartz glass are required for the use of HF acids to digest whole rock powders. First, 100 mg of weighed powder was transferred into PFA beakers for a pre digestion step with 2 mL HF and 1 mL HNO_3. They were placed on a hot plate overnight at 120 ºC. The solutions were dried down and 2 mL HF and 2 mL Aqua Regia (HNO_3 and HCl) were added into the beakers and transferred to the Teflon Digestion tubes. The Teflon Digestion tubes were placed into the single reaction chamber for microwave digestion. The tubes were loaded into a cylindrical shape Teflon container where the tubes are submerged into a tub of 130 mL of H_2O, and 5 mL 16N HNO_3. The microwave digestion was conducted using the pre-set "rock digestion.mpr (Table 3.2.1).

When the digestion process was complete, the sample solutions were transferred into the PFA beakers that were originally used and washed with 2% HNO_3 to ensure complete recovery of the sample. The samples were dried down on a hot plate at 110 ºC. 2 mL 16 N HNO_3 was added and put back on hot plate to dry down. Once the sample was completely dried, another 1 mL of 16 N HNO_3 was added and dried down again. Then, 2 mL of 12 N HCl was added and the sample capped and left on hot plate at 110 ºC overnight. The cap was removed, dried down again and then 1 mL 16 N HNO_3 was added. This process was repeated three times. Next, 4 mL 8 N HNO_3 was added, capped and cooked for 2-3 h until the solution was clear. Lastly, an acid cleaned 125 mL LDPE

bottle was obtained, and labeled with sample numbers. The capped bottle was weighed, and then samples were transferred into the bottle. The

solution was in 2% HNO_3. Once the solutions were in 2% HNO_3, a concentration check was performed on the samples in order to determine the amount of vanadium solution to use in column chemistry to obtain about 4-5 ug/g of V. The required amount of sample solutions were then dried down once again and 2 ml HNO_3, was added before column chemistry began.

3.4 Vanadium Purification by Column Chemistry (EOM and Bulk Rock)

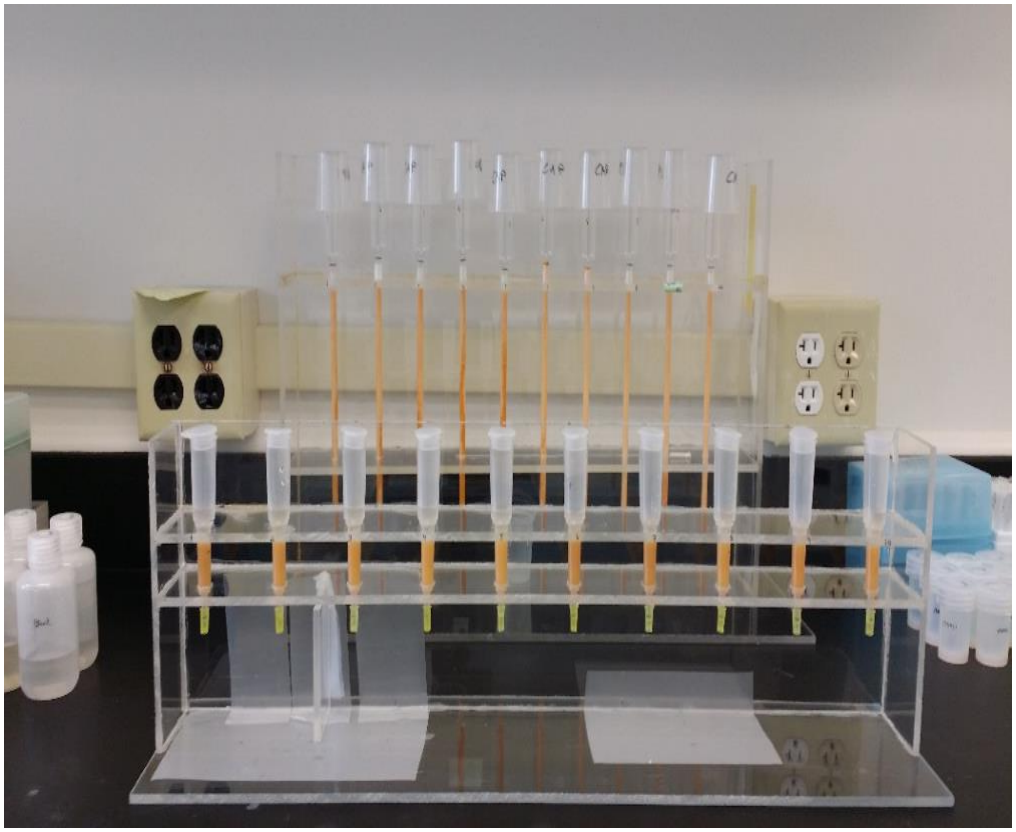

Figure 3.4.1: Liquid Chromatography Cation and Anion Column Chemistry

In order to precisely analyze vanadium isotopes, V in the prepared samples needs to be pre-concentrated and separated from other elements by liquid chromatography. A chemical purification process containing a multi-step liquid chromatography process with combined cation and anion columns was used to isolate vanadium from sulfur, titanium, chromium, and other major elements for vanadium isotope analysis (Gao et al., 2017; Figure 3.4.1).

3.5 First Column Chemistry

The first column was used to remove sulfur along with major and trace elements. Before the resin was loaded into the columns, it was leached with 6N HCl. The 1 mL of wet Bio-Rad AG 50W X-12 cation exchange resin was inserted into the column and washed with 3 mL of 6 N HCl and 3 mL of Milli-Q H_2O. The resin was then conditioned with 3 mL 0.2 N HCl. The 2 mL sample was loaded into the column in 0.2 N HCl onto the resin. The resin was washed with 4 mL of Milli-Q H_2O and 4 mL of 0.2 N HCl to remove the S and major elements. Lastly, the vanadium was washed out of the column with 11 mL of 1 N HCl. Sulfur along with other cations (Mg, Ca, Fe, Al, Si, and Cr) were all separated from the vanadium by being held in the resin due to higher distribution coefficients (Gao et al., 2017). A portion of the collected solution was measured using the ICP-MS QQQ to ensure that vanadium was near ~100% completely recovered. The samples were dried down repeatedly three times in reducing 6N HCl to reduce V^{5+} to V^{4+}.

3.6 Second Column Chemistry

The second column was used to separate titanium from vanadium. The 1 mL of anion exchange resin AG1 X8 was loaded into the columns and cleaned with 10 mL of 1 N HCl. The resin was then conditioned with 5 mL of 2 N HF. The 2 mL sample was then added to the column in 2 N HF, and the vanadium was washed out with 18 mL of 0.3 N HCL in 1 N HF. The sample was dried down repeatedly three times in 16 N HNO_3 to oxidize V to V^{5+}.

3.7 Third Column Chemistry

The third column was used to further purify V from the rest of the cations, mainly K and minor Cr remaining in the vanadium. The 1 mL AG1 X8 resin was washed with 5 mL of 2 N HNO_3 and 3 mL of Milli-Q H_2O, and then conditioned with 3 mL of 0.01 N HNO_3/3% H_2O_2. The 2 mL sample was loaded into the column in 0.01 N HNO_3/ 3% H_2O_2. The cations do not absorb onto the resin due to the formation of a polyvandate complex inside the anion exchange resin particles with a matrix of weak acid containing H_2O_2, so the vanadium stays inside the resin while the cations are washed through. Finally, 10 mL of 0.01 N HNO_3/3% H_2O_2 was added to wash down all cations before the 14 mL of 1 N HNO_3 was added to wash out the purified vanadium from the column. The samples were dried down repeatedly three times in 2% HNO_3.

3.8 Elemental Analysis

3.8.1 ICP-MS

Figure 3.8.1: Agilent 8800 ICP-MS

Concentrations of major elements, V, Ni, and S were determined by the triple Quadrupole (QQQ) ICP-MS after each column chemistry (Figure 3.8.1). Each time the sample was run through the column (three times in all), a concentration check was enforced. This is to ensure that vanadium isn't lost and that the major elements and S are removed. The recovery rate of vanadium in the EOM and bulk rock samples averaged between 99-100%. The 8800 Agilent Triple Quadrupole ICP-MS consists of an ionization source, a collision cell, and two quadrupole mass filters. The sample enters into the ionization source and the first quadrupole mass filter, Q1, is the primary m/z selector

where ions that do not exhibit the m/z ratios other than what is selected will not be able to penetrate Q1. Q2, is also known as the collision cell. This is where fragmentation of the sample occurs in an inert gas, argon in this case. Due to the collisions in argon with the analyte, a daughter ion is produced. After the collision cell, the fragmented ions travel into the Q3, quadrupole mass filter where m/z selection occurs once again. The triple quadrupole is a scanning instrument so it detects ions one m/z at a time.

3.8.2 Multi collector Inductively Coupled Mass Spectrometer

Figure 3.8.2: Nu Plasma II MC-ICP-MS- University of Houston

For vanadium isotope analysis, the high resolution Nu Plasma II Multi Collector Inductively Coupled Mass Spectrometer at the University of Houston was used (Gao et al., 2017; Figure 3.8.2). The bulk rock shale and EOM samples were introduced through a nebulizer at a concentration of 700 ng/g of V in 2% HNO_3 (Gao et al., 2017). Samples were bracketed by a 700 ng/g in house standard (IVU) (Gao et al., 2017).

During the analysis, the samples were introduced into the inductively coupled plasma, which stripped off electrons creating positively charged ions. Once the ions were produced, they were accelerated and focused to produce a beam. The ion beam passed through an energy filter and then through a magnetic field where the ions were separated by their mass to charge ratio. The mass resolved beams were then directed into collectors where the ion beams were measured simultaneously. Isotopic compositions were first calculated relative to the UH in house standard ($\delta^{51}V_{UH}$) in parts per thousand, $\delta^{51}V= 1000x[(^{51}V/^{50}V_{sample}/^{51}V/^{50}V_{IVU})-1]$, and then converted relative to the ($\delta^{51}V_{AA}$) in parts per thousand, $\delta^{51}V= 1000x[(^{51}V/^{50}V_{sample}/^{51}V/^{50}V_{AA})-1]$ (Nielsen et al 2011; Gao et al., 2017). The solutions with 700 ng g^{-1} V and an uptake rate of 40 ul min^{-1} yielded a ^{51}V intensity of about 40-45 volts (Gao et al., 2017). Masses 49, 50, 51, 52 and 53 were also collected to examine isobaric interferences on ^{50}V. Isobaric interferences from Ti and Cr on minor V were corrected by monitoring masses 49 and 53 with values of 0.9725 for $^{50}Ti/^{49}Ti$ and 0.4574 for $^{50}Cr/^{53}Cr$ (Niederer et al., 1985; Shields et al., 1966).

3.9 Accuracy and Precision

When performing isotopic analysis, it is important to use a variety of standards in order to check for accuracy and precision. Precision is replicating the standard multiple times and maintaining a value 2sd of 0.3 or less, and accuracy has to do with the mean value of the standard replications similar to the already published value. To measure the vanadium isotopic composition of the EOM and bulk rock shale, three different types of USGS standards were used: rock (basalt), oil, and pure vanadium solution (Table 3.9).

Table 3.9: USGS standard data (Wu et al., 2016; Nielsen et al., 2011; Gao et al., 2017)

Sample Frequency	Standard	Standard Type	$\delta^{51}V$	2 sd	published	2sd
n=3	BCR-2	Basalt	-0.78	0.09	-0.78	0.08
n=3	BIR-1	Basalt	-0.97	0.14	-0.92	0.09
n=5	RM8505	Oil	0.03	0.40	-0.02	0.3
n=13	AA*	V Solution	-0.06	0.22	0	
n=13	BDH*	V Solution	-1.35	0.34	-1.19	0.12
n=13	BDH**	V Solution	-1.29	0.34	-1.19	0.12
* Calibrated with UH Vanadium						
** Calibrated by AA Vanadium						

The USGS standards used include BCR-1 (basalt), BCR-2 (basalt), RM8505 (oil), AA (pure vanadium solution), and BDH (pure vanadium solution). The rock samples were used with the bulk shale samples because they are the most similar standard to a bulk shale rock, and the oil sample was used with the EOM samples because EOM is most similar to oil.

In terms of accuracy and precision, BCR-1 and BCR-2 were both used three times. For BCR-2 the mean $\delta^{51}V$ value was -0.78 with a 2σ error of 0.09. Precision was

almost identical with the published $\delta^{51}V$ value of -0.78 and 2σ error or 0.08 (Wu et al., 2016). For BCR-1 the mean $\delta^{51}V$ value was -0.97 with a 2σ error of 0.14. Precision was almost identical with the published $\delta^{51}V$ value of -0.92 and 2σ error or 0.09 (Wu et al., 2016). The oil, RM8505, was used five times. The mean $\delta^{51}V$ value was 0.03 with a 2σ error of 0.4. Precision was very high with the published $\delta^{51}V$ value of -0.02 and 2σ error or 0.3 (Gao et al., 2017). The pure vanadium solutions were used thirteen times each. The pure vanadium solutions usually give the best results as they lack metals that can cause interferences in measurement and consist of just vanadium. The vanadium solution, AA, has a mean $\delta^{51}V$ value of -0.06 with a 2σ error of 0.22. Precision was very high with the published $\delta^{51}V$ value of 0 (Nielsen et al., 2011). The vanadium solution, BDH, was first calibrated with the UH vanadium. The mean $\delta^{51}V$ value was -1.35 with a 2σ error of 0.34. The published $\delta^{51}V$ value of -1.19 and 2σ error of 0.12 (Nielsen et al., 2011). BDH was then calibrated with the AA standard with a mean value of $\delta^{51}V$ of -1.29 and 2σ of 0.34.

Overall, both the accuracy and precision for the USGS standards and pure vanadium solutions were very high. The standard values were very reproducible and showed low errors when compared to published USGS data values.

CHAPTER 4

EOM & BULK ROCK SHALE TRACE ELEMENT AND ISOTOPIC ANALYSES DISCUSSION

4.1 Vanadium Isotopic Analysis

Performing vanadium isotopic analysis on both the EOM and the bulk rock shale came about after examining trends in trace element concentrations and certain metal ratios such as V/Ni, V/(V+Ni), and vanadium and molybdenum enrichment factors in the shale. Metals such as V and Mo each have more than a single isotope and are in high abundance in shales and sometimes crude oils specifically, leading to new types of unconventional isotopic analysis for shales, EOM, and crude oils (Ventura et al., 2015; Gao et al., 2017). To date, there are two studies of vanadium isotopic work that have been performed on a set of global crude oils from different parts of the world (Ventura et al., 2015; Gao et al., 2017). Ventura et al., 2015 studied crude oils from sedimentary basins located in Russia, Kuwait, Venezuela Brazil and the U.S. Gao et al., 2017 studied crude oils from sedimentary basins in Venezuela, Russia, U.S., and oils from off the island of Barbados. This study represents the first time that both bulk rock shale and their associated extractable organic matter (EOM) have been analyzed from any hydrocarbon play.

4.2 Sample Data- Bulk Rock and EOM in the Eagle Ford Shale

Table 4.2.1: Bulk shale data. Each sample includes the depth (ft) of sample, the TOC, the vanadium concentration (µg/g), the V/Ni ratio, and the V/(V+Ni) ratio

Rock (shale)	Depth (ft)	Leco TOC (wt%)	V (µg/g)	V/Ni	V/(V+Ni)
EP8	17.23	3.41	385	8.4	0.89
EP16	39.2	5.37	877	9.9	0.90
EP18	44.69	4.99	854	8.6	0.89
EP22	55.69	6.28	540	5.2	0.83
EP24	61.18	6.06	649	7.4	0.88
EP26	66.67	6.39	577	6.8	0.87
EP28	72.16	7.59	713	6.4	0.86
EP30	77.65	7.73	1056	6.9	0.87
EP32	83.1	1.82	155	8.0	0.88
EP34	88.64	6.6	529	6.5	0.86
EP36	94.08	6.5	546	5.8	0.85
EP38	99.6	5.84	363	5.3	0.84
EP44	116.06	3.69	252	4.8	0.82

Table 4.2.2: EOM data. Each sample includes the depth (ft) of sample, the TOC, the vanadium concentration (ng/g), the V/Ni ratio, and the V/(V+Ni) ratio

EOM	Depth (ft)	V (ng/g)	V/Ni	V/(V+Ni)
EP 8	17.23	1437	8.2	0.89
EP 16	39.2	3345	29	0.97
EP 18	44.69	2026	18.8	0.95
EP 22	55.69	1634	24.7	0.96
EP 26	66.67	4742	5.9	0.86
EP 30	77.65	3481	41.2	0.98
EP 44	116.06	3436	10.4	0.91

4.3 Vanadium Metal Concentrations

Vanadium and molybdenum have high concentrations in the studied shales. These enrichments typically correlate with high organic matter preservation and more reducing conditions, thus their abundances and ratios are very important to examine (Trivobillard et al., 2006; Algeo et al., 2012; Takahashi et al., 2014; Table 4.2.1). In Figure 4.3.1, the bulk rock shale data show that vanadium abundances change downhole with depth. The depth profiles do not display the true depth, but are a modified distance down core. Rather than reporting true depth, 0 ft marks the top of the core, and 120 ft marks the bottom of the core. Vanadium abundances in shales vary from roughly 400 µg/g at the top of the core to 800-1000 µg/g in the middle section, returning to lower concentrations of 225 µg/g at the bottom of the core. The total organic carbon (TOC) diagram in shale is plotted alongside the vanadium abundance diagram. As shown, the high abundances of vanadium in the bulk rock coincide with high TOC. Figure 4.3.2 shows a similar pattern of bulk rock shale data for molybdenum. Molybdenum concentrations vary from roughly 18 µg/g at the top of the core, climbing to concentrations of 100 µg/g in the middle section, and returning to lower concentrations of 20 µg/g at the bottom of the core (Figure 4.3.2). Molybdenum also shows high abundances in the middle section of the core where the TOC is high (Trivobillard et al., 2006; Algeo et al., 2012; Takahashi et al., 2014).

In Figure 4.3.3, EOM vanadium concentrations are plotted against depth. EOM sample concentrations are significantly lower than the high values (155 µg/g to 1056 µg/g) in the bulk rock shale. The EOM samples exhibit vanadium concentrations of (1437 ng/g to 4742 ng/g) (Table 4.2.2). There does not seem to be a distinct increase in

vanadium concentration in the middle of the core as seen in the vanadium and molybdenum bulk rock shale data. This could be due to the fact that overall, the kerogen or EOM have lesser amounts of vanadium than the bulk rock shale or EOM has evolved as a crude oil expulsion event occurred or maturity increased. Also, the EOM samples do not show a correlation with high concentrations coinciding with higher TOC values.

The oil produced from the borehole is extremely mature with very low concentrations of metals. The source rock with the oil with high thermal maturity, ~R_o=1.1, has vanadium concentrations of only 20 ng/g, even much less than the EOM (eg., personal communication). However, a less mature oil with similar (V/V+Ni) characteristics and ratios in the La Luna shales from Venezuela deposited at about the same time as Eagle Ford Shale, RM 8505, has very high metal concentrations. (Gao et al., 2017). This suggests that less mature oils expelled from the Eagle Ford shales with similar V/V+Ni may have been more enriched.

Combining the three possible reservoirs of V in the bulk shale, siliciclastic component, EOM component, and kerogen component in the rock, it is evident that the the EOM component now contains extremely minor vanadium and the crude oil produced (Well) has even smaller amounts.

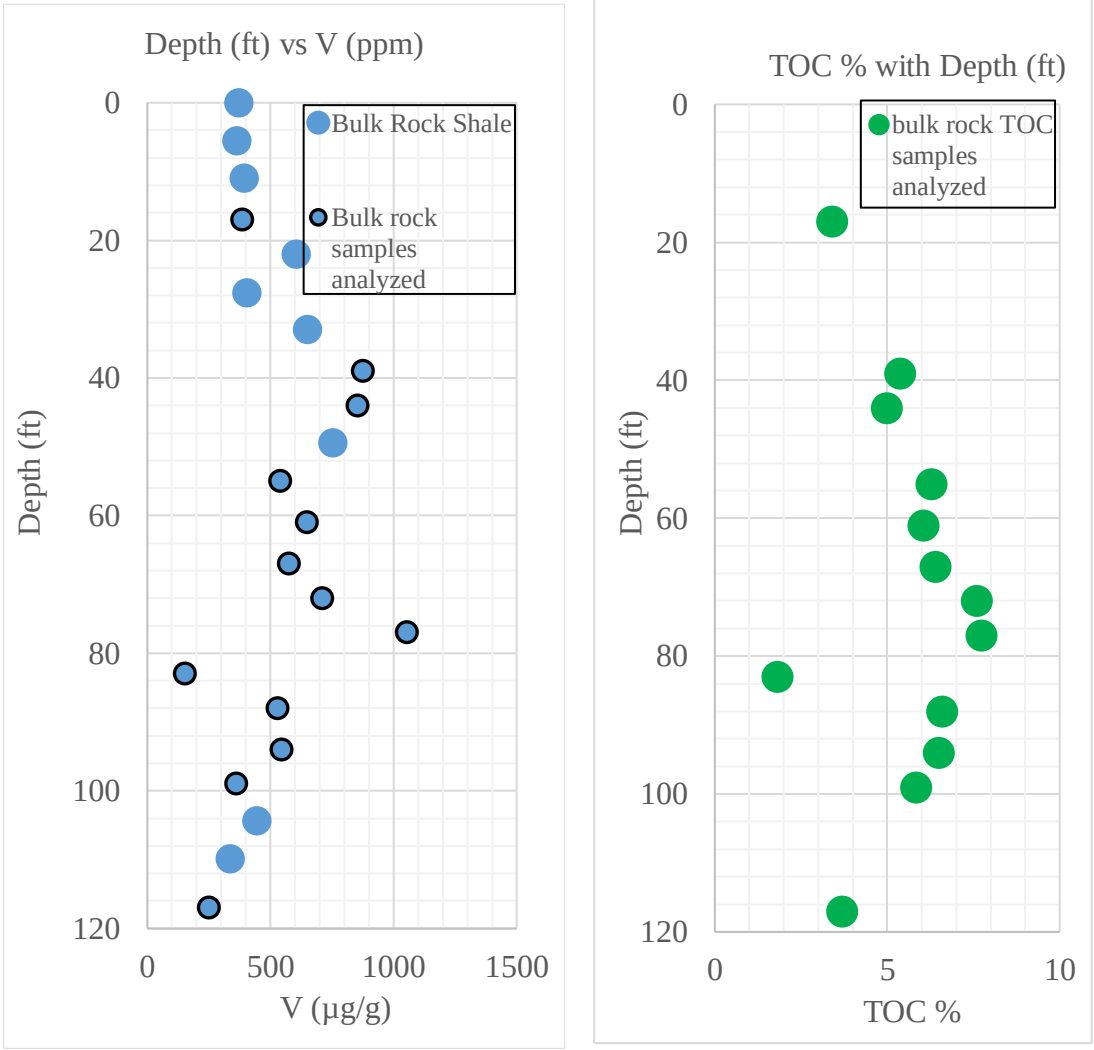

Figure 4.3.1: Bulk rock shale vanadium (µg/g) vs depth (ft) alongside TOC vs depth (ft). Lower vanadium concentrations dominate the top and bottom of the core, with enrichments in the middle sector for the shales. The higher concentrations coincide generally with the >5 TOC. Depth profiles display a modified depth, not true depth.

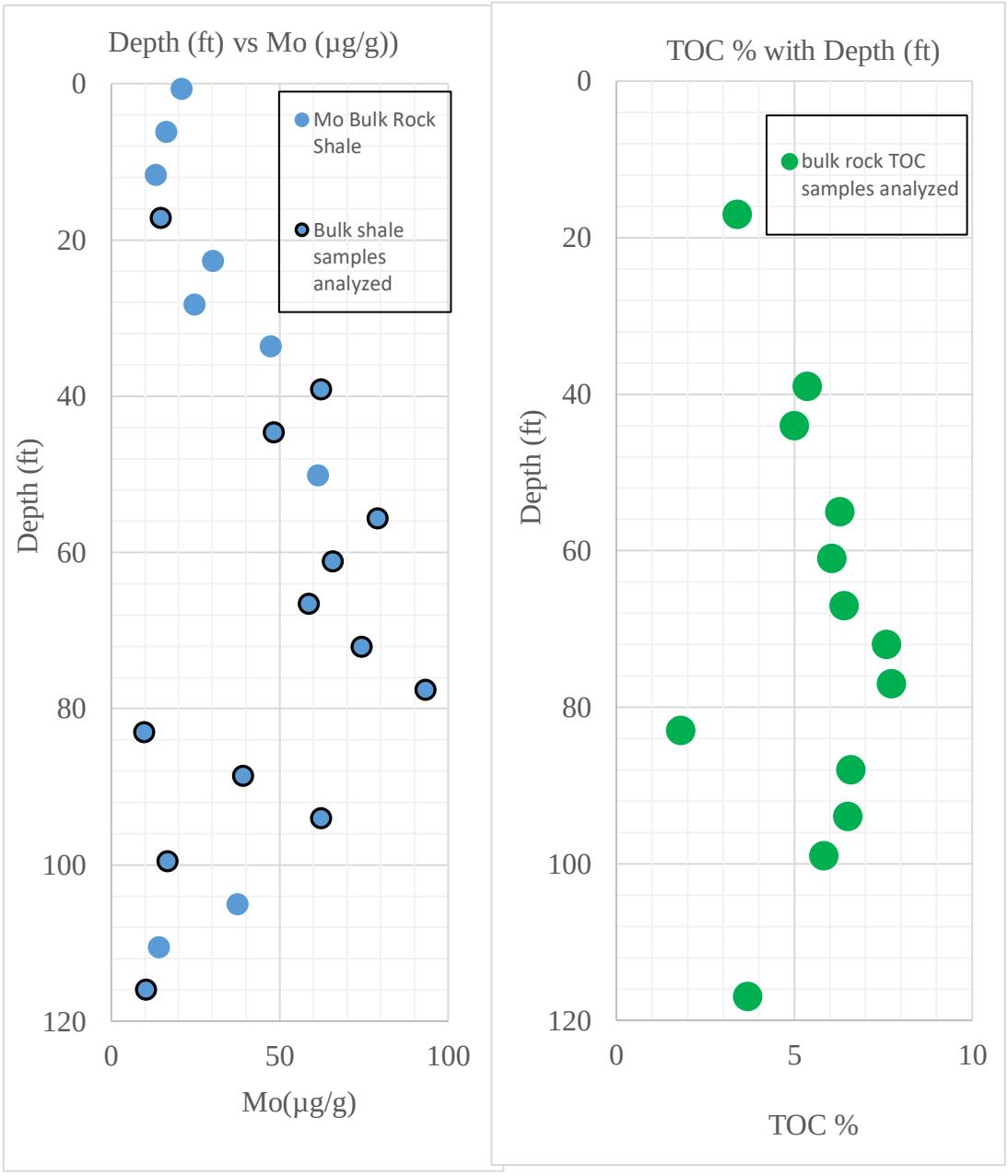

Figure 4.3.2: Bulk rock shale molybdenum (µg/g) vs depth (ft) alongside TOC vs depth (ft) Lower molybdenum concentrations dominate the top and bottom of the core, with enrichments in the middle sector for the shales. The higher concentrations generally coincide with >5TOC. Depth profiles display a modified depth, not true depth.

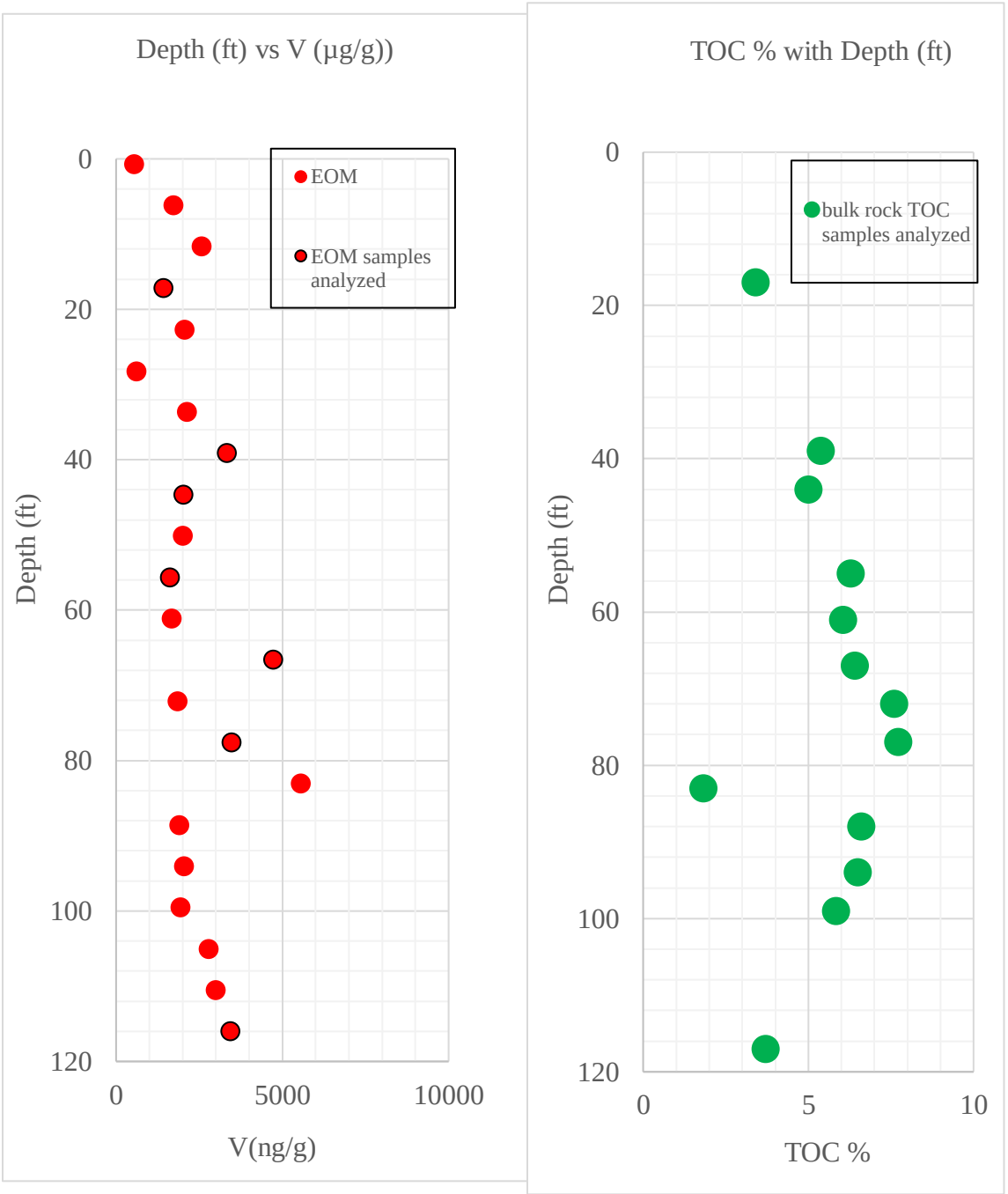

Figure 4.3.3: EOM vanadium (ng/g) vs depth (ft) alongside TOC vs depth (ft). There does not seem to be a correlation between higher EOM concentrations and higher TOC. Depth profiles display a modified depth, not true depth.

4.4 Vanadium Concentrations vs TOC

Vanadium and molybdenum metal concentrations and enrichments generally correlate with the high total organic carbon interval (Figure 4.4.1; Figure 4.4.2). This correlation has also been observed in other locations (Trivobillard et al., 2006; Algeo et al., 2012; Takahashi et al., 2014). As shown in Figure 4.4.1 and Figure 4.4.2, there is a positive correlation between the highest concentrations of vanadium and molybdenum in the bulk rock shale with the TOC

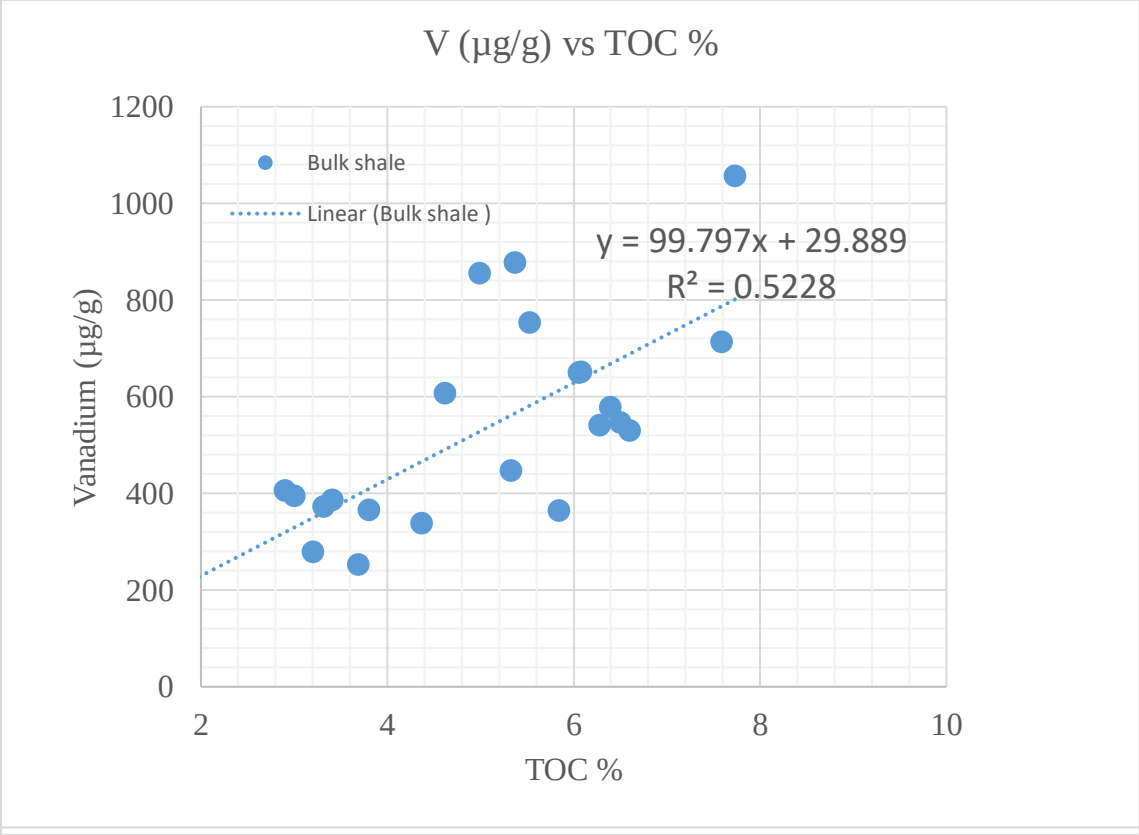

Figure 4.4.1 Bulk rock shale vanadium (µg/g) vs TOC. There is a positive correlation between vanadium concentration and TOC.

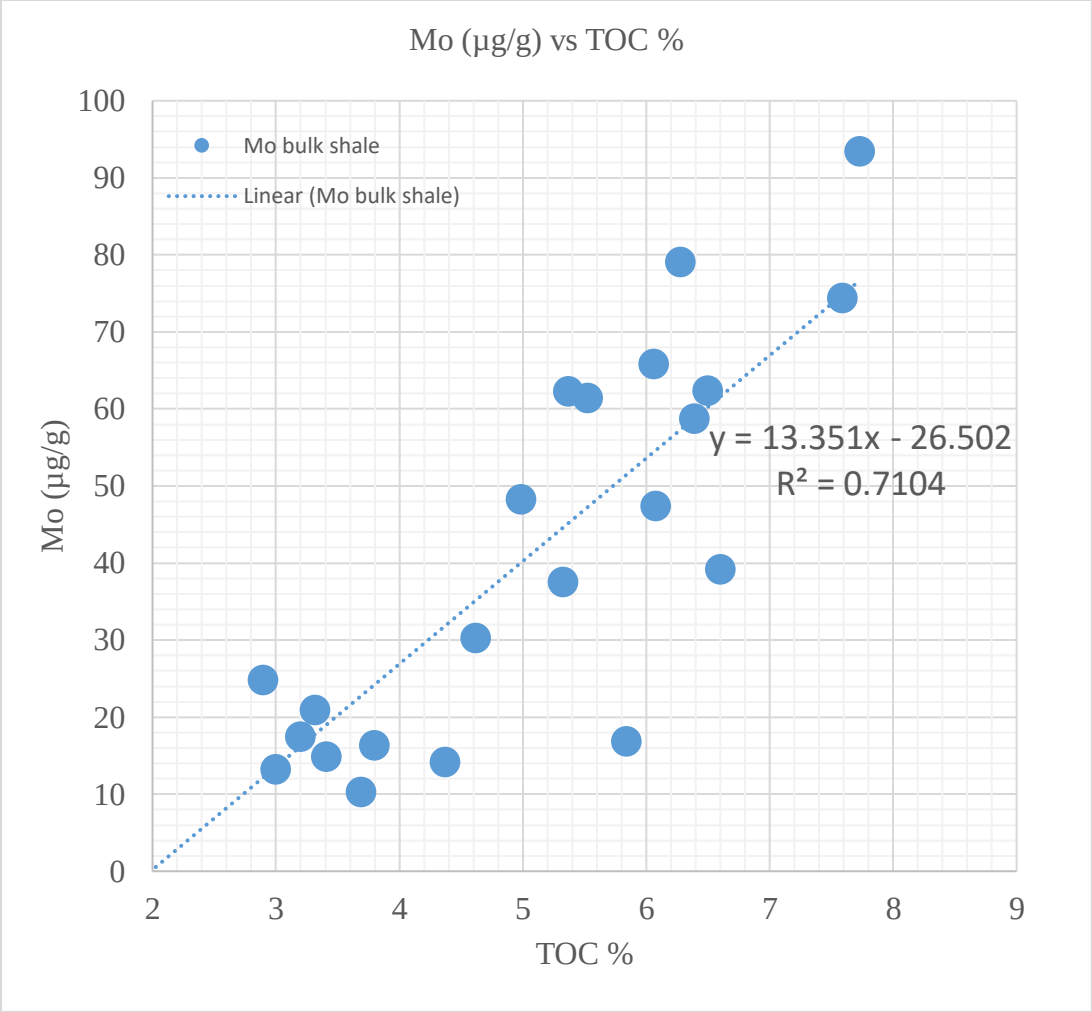

Figure 4.4.2 Bulk rock shale molybdenum (µg/g) vs TOC. There is a positive correlation between vanadium concentration and TOC.

4.5 V and Ni Fractionation

In addition to the mass fractions of metals, it is also important to examine the ratios of metals such as V/Ni and V/(V+Ni) in the oil, EOM and shale, which have been related to Eh-Ph and redox conditions during deposition and early diagenesis of the shale (Lewan 1984). V/(V+Ni) or V/Ni is often used as a paleoenvironmental redox proxy for

crude oil, with higher V/(V+Ni) values indicating the most reducing conditions and lower V/(V+Ni) values indicating more oxidizing conditions (Lewan, 1984; Ventura el al., 2015; Gao et al., 2017). The paleoenvironmental indicator indicating reducing or oxidizing conditions is only true if the only factor controlling the ratio is redox conditions. However, the type of free base porphyrin that is eventually metallated at the seabottom is also a controlling factor, as are others. There are many first order controlling conditions on the ratio besides redox.

In Figure 4.5.1, the V/(V+Ni) is plotted against depth for both the bulk rock shale and EOM. As shown in Figure 4.5.1 the V/(V+Ni) values do not vary much between the EOM and bulk rock shale. The V/(V+Ni) value is relatively high and similar for EOM (0.77-0.99) and for shale (0.82-0.91). Since V/(V+Ni) is a paleoenvironmental indicator of the depositional environment, high V/(V+Ni) ratios can indicate very reducing conditions (Lewan, 1984; Gao et al., 2017). The bulk rock shale and EOM samples exhibiting this high ratio indicates Eh/pH conditions of a very sulfidic environment.

In Figure 4.5.2, V/Ni is plotted against depth for both the bulk rock shale and EOM. The V/Ni ratio does vary in the EOM and bulk rock shale. The bulk rock shale exhibits V/Ni ratios within a narrow range from (4.8-9.9) and the EOM exhibits V/Ni ratios within a much wider range of (3.3- 41.2). The bulk rock shale and EOM not only show differences between the two, but also large variation between individual samples of EOM and bulk rock shale. In addition, the crude oil produced from the drill hole also shows much lower values than the bulk shale values.

In Figure 4.5.3, although similar, the V/Ni is plotted against the V/(V+Ni) for both the EOM and bulk rock shale samples and of course are well correlated. In the

Figure 4.5.3, the bulk rock shale samples plot within a narrow range of variation in V/(V+Ni) and V/Ni. The EOM samples plot with not much variation in V/(V+Ni), yet somewhat higher than the bulk shale composition, but with large variation in V/Ni. Also plotted on the diagram are two oils. One is from the borehole drilled in the Eagle Ford where samples were collected (Well), which is the very mature oil producing today, and exhibits extremely low V/(V+Ni) (.02) and V/Ni ratios (.03). The second oil is RM 8505, is a NIST standard reference material -- Venezuela crude oil -- that is, in turn, immature and has similar ratios of V/(V+Ni) (.89) and V/Ni ratios (8.0) to the Eagle Ford Shale sample ratios analyzed here and its source rock, the Venezuelan La Luna Formation. The La Luna Formation was deposited during the same peak in Cretaceous sea level, and has the same approximate age as the Eagle Ford sampled here. RM 8505 is a high V immature crude oil, which we assume may be similar to the early crude oils expelled from the Eagle Ford Shale based on their similar V/Ni and V/(V+Ni).

Within Figure 4.5.3, all the samples plot on a forced correlated parabolic line with the EOM samples showing the highest V/Ni ratios, the bulk rock shales and RM 8505 plotting in the middle, and the mature produced Well oil exhibiting the lowest V/Ni ratio, apparently severely fractionated with respect to the EOM and shale ratio values. This difference could indicate oil-expulsion fractionation events between the early oil and EOM/kerogen, which created the large observed variations in the V/Ni ratios.

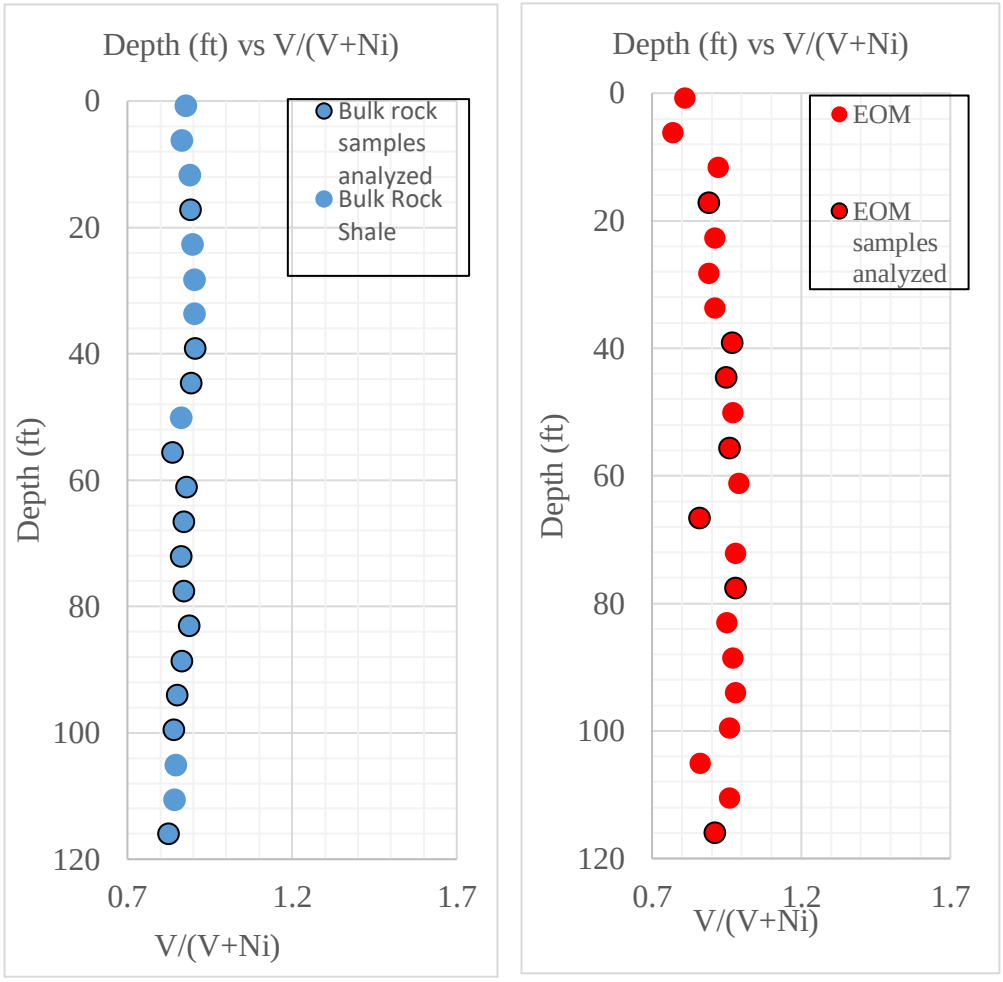

Figure 4.5.1: Bulk rock shale and EOM depth vs V(V+Ni). The bulk rock shale and EOM show very similar V/(V+Ni) ratios ~0.9. Depth profiles display a modified depth, not true depth.

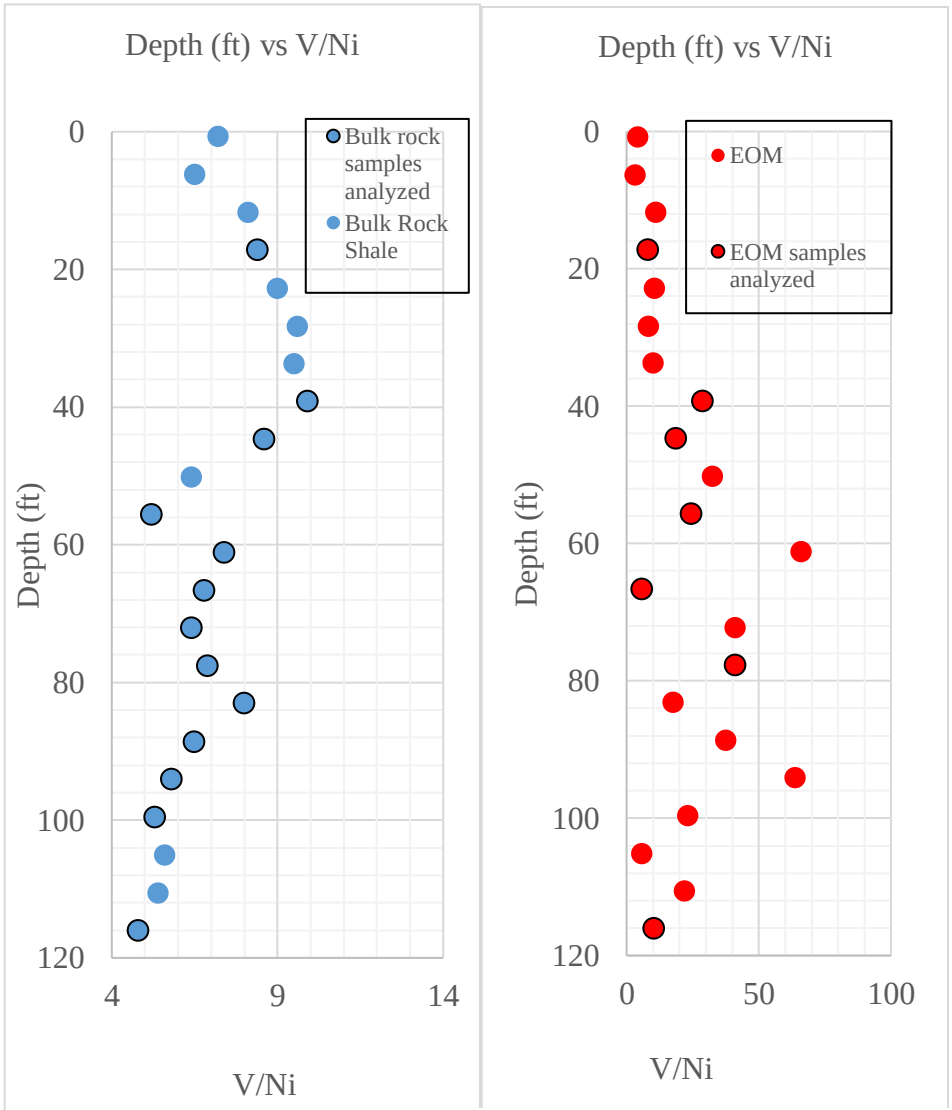

Figure 4.5.2: Bulk rock shale and EOM depth vs V/Ni. The V/Ni ratio shows variation between bulk rock shale and EOM and within bulk rock shale and EOM. Depth profiles display a modified depth, not true depth.

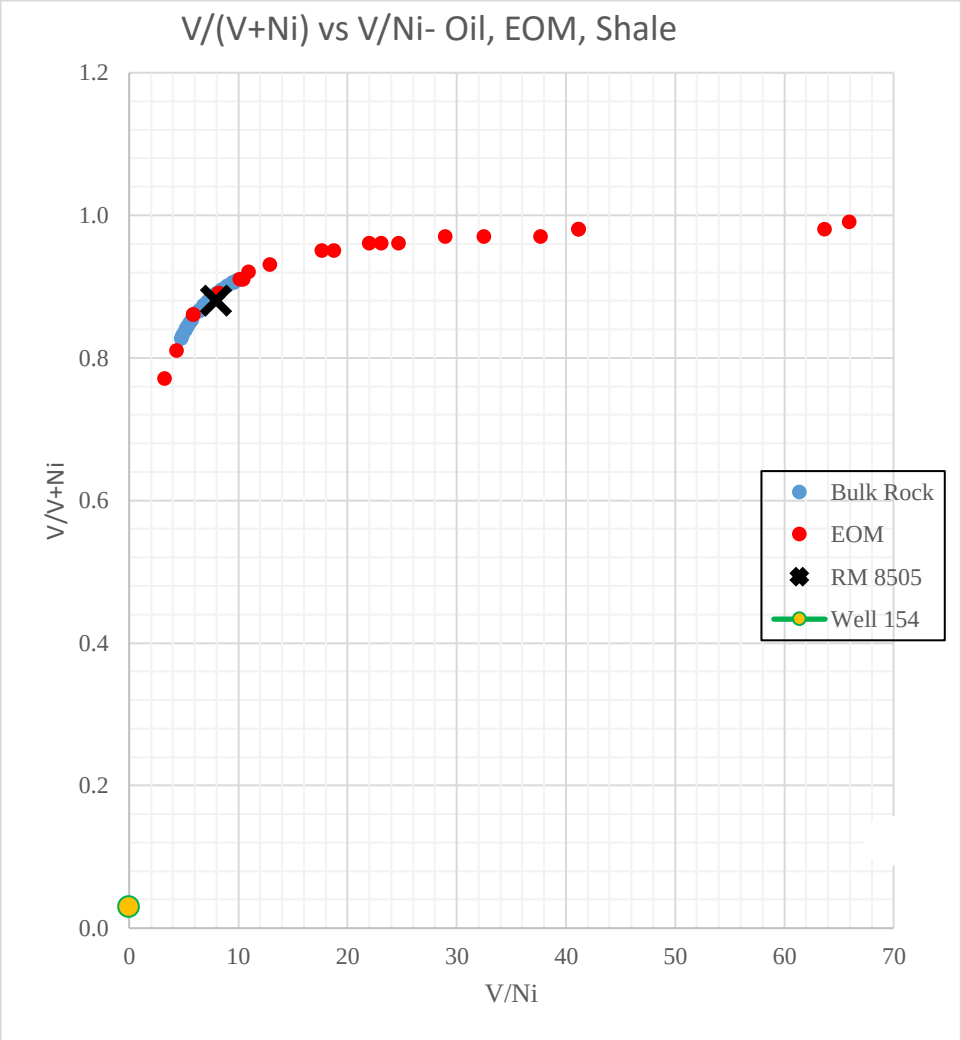

Figure 4.5.3: V/(V+Ni) vs V/Ni forced parabolic trend between the shale, EOM, RM 8505 oil, and the produced crude oil today.

4.6 Vanadium Isotopes

Following trace element data and the trends associated with metal concentrations and elemental ratios, vanadium isotopic analyses for both shales and EOM are presented on selected samples in the core downhole. Vanadium isotopic analyses require very intensive sample preparation involving chromatographic methods previously outlined. While elemental abundances provide important information, they are prone to such uncertainties such as water content and variations in initial source concentration (Gao et al., 2017), so it is of interest to combine both elemental data with isotopic data (Figure 4.6.1; Table 4.6.1; Table 4.6.2). In order to perform vanadium isotopic analysis, the samples were selected based on adequate vanadium content and obtaining a broad spectrum of samples throughout the core to create downhole profiles. There are fewer EOM samples analyzed than bulk shale due to the fact that the EOM samples had very low vanadium concentrations; some too low to analyze without very large and multiple solvent extractions of the same samples. In order to measure the $\delta^{51}V$, you need around 1 microgram of vanadium to run a sample once.

Table 4.6.1: Bulk rock shale sample, depth (ft), V (µg/g) and $\delta^{51}V$

Rock (shale)	Depth (ft)	V (µg/g)	$\delta^{51}V$
EP8	17.23	385	-0.15
EP16	39.2	877	-0.21
EP18	44.69	854	-0.23
EP22	55.69	540	-0.14
EP24	61.18	649	-0.6
EP26	66.67	577	-0.23
EP28	72.16	713	-0.6
EP30	77.65	1056	-0.71
EP32	83.1	155	-0.87
EP34	88.64	529	-0.55
EP36	94.08	546	-0.85
EP38	99.6	363	-0.57
EP44	116.06	252	-0.39

Table 4.6.2: EOM sample, depth (ft), V (ng/g) and $\delta^{51}V$

EOM	Depth (ft)	V (ng/g)	$\delta^{51}V$
EP 8	17.23	1437	-0.96
EP 16	39.2	3345	-1.56
EP 18	44.69	2026	-2.28
EP 22	55.69	1634	-1.71
EP 26	66.67	4742	-1.15
EP 30	77.65	3481	-1.08
EP 44	116.06	3436	-0.74

Figure 4.6.1 shows the isotopic data for both the bulk shale and EOM samples plotted against core depth. The BSE (bulk silicate earth), modern-day seawater, and a less mature oil with similar (V/V+Ni) characteristic from Venezuela deposited at about the same time as Eagle Ford Shale (La Luna Source - RM 8505 crude oil), are plotted as reference lines (Prytulak et al., 2013; Gao et al., 2017; Wu et al., 2019). As shown in the figure 4.6.1, the bulk shale and EOM samples show a very wide range of values. The EOM values range from $\delta^{51}V$ (-2.28±-0.3‰ to -0.74±0.3‰) and the bulk shale values range from $\delta^{51}V$ (-0.87±0.3‰ to -0.14±0.3‰). Therefore, the EOM samples tend to be more isotopically light values and the bulk shale samples tend to be more isotopically heavy values.

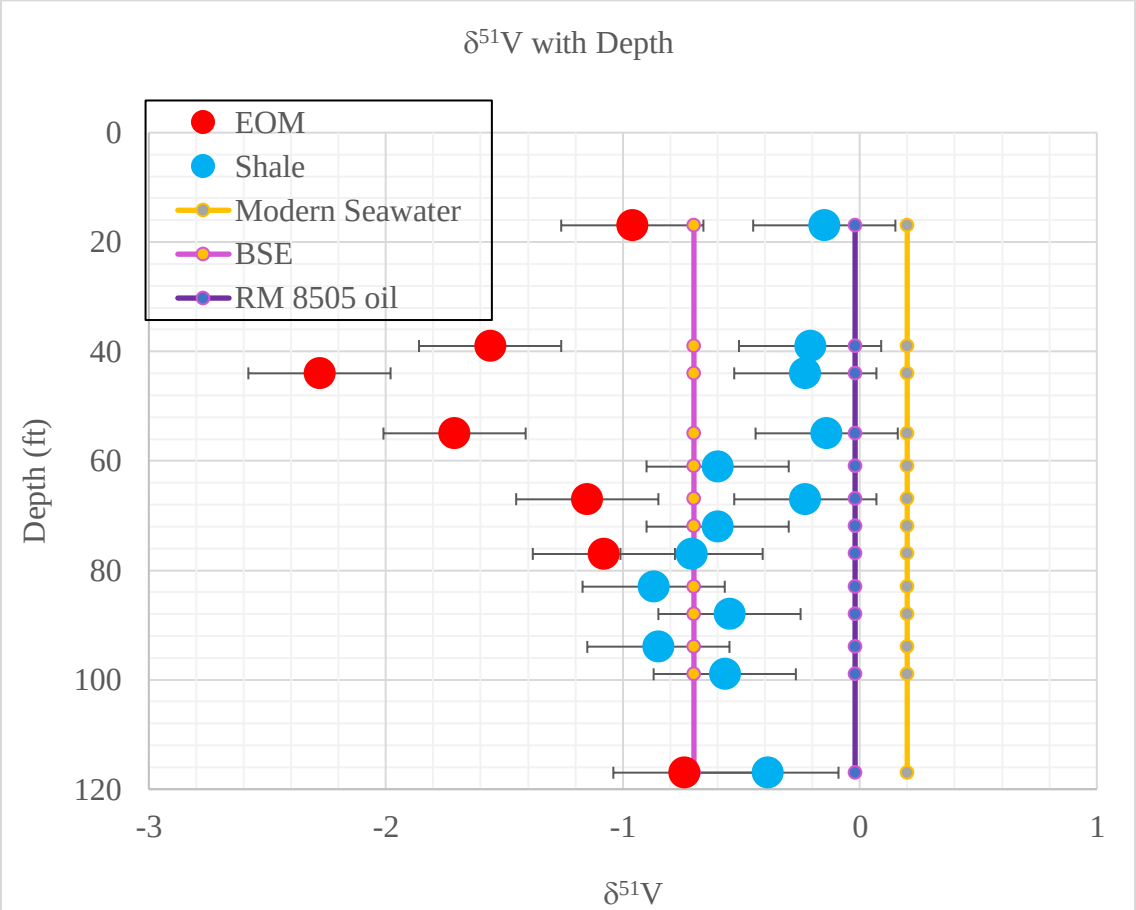

Figure 4.6.1: Vanadium Isotopic Analysis of bulk rock shale samples and EOM samples. The references used are bulk silicate earth (BSE), the immature oil, RM 8505, and modern day seawater. Depth profiles display a modified depth, not true depth. (Prytulak et al., 2013; Gao et al., 2017; Wu et al., 2019)

The reason for the very wide range of values associated with the EOM and bulk shale is due to the fact that stable isotopic fractionation is inversely related to temperature. As stated previously, organic matter and shales in the Eagle Ford samples analyzed have progressed from low temperature depositional and diagenetic processes to processes related to compaction, thermal and high maturity, i.e., increases from very low to higher temperature catagenesis in the oil window (~50°-150 °C) (Figure 4.6.2; Tissot

& Welte, 1984; Hunt, 1996; Seewald, 2003). Thus, crude oils are formed at low temperatures (Ro =1.1) compared to many other earth materials so far analyzed for their V isotope compositions. These other materials are dominated by high temperature rocks. It is therefore not surprising that a larger variation or fractionation is observed for the bulk shale and EOM compositions analyzed here when compared to their high temperature counterparts (igneous and metamorphic rocks). At very high temperatures, the isotopic fractionation would diminish to near zero.

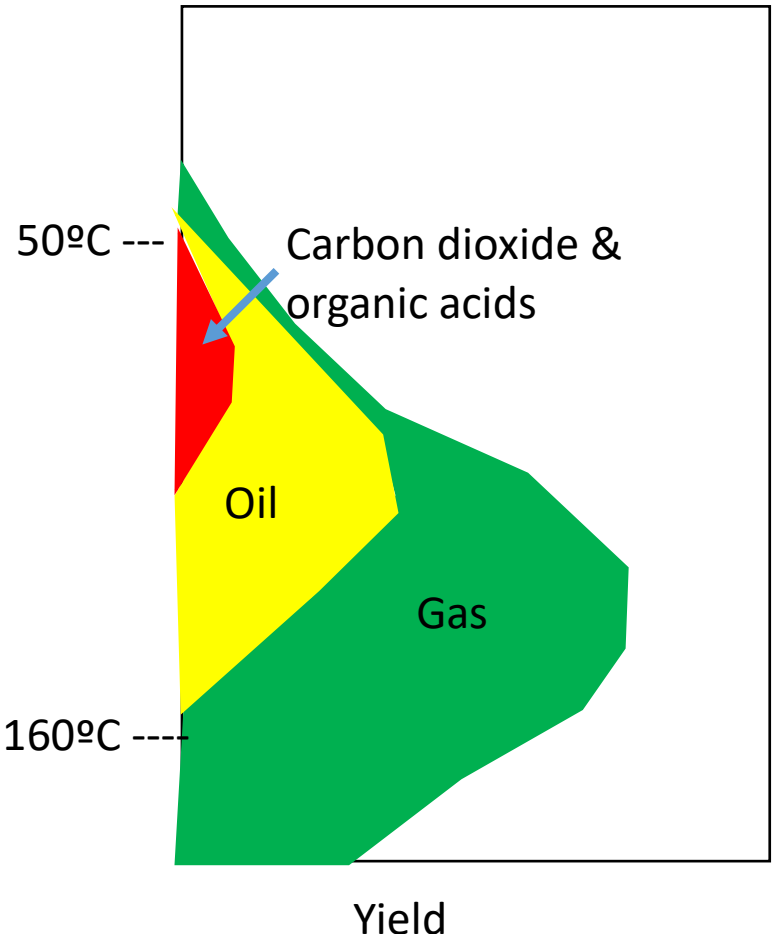

Figure 4.6.2: Timing of organic products generated during burial in sedimentary basins. Oil formation occurs around 60-160° C. (Redrafted from Seewald, 2003; Tissot & Welte, 1984; Hunt, 1996)

4. 7 Terrestrial and Extraterrestrial Isotopic Data

Figure 4.7.1, shows the bulk shale and EOM vanadium isotopic data analyzed in this study (top two rows) with vanadium isotopic data from all sources available at this time. As shown, the crude oils, EOM and bulk shale show the largest variability.

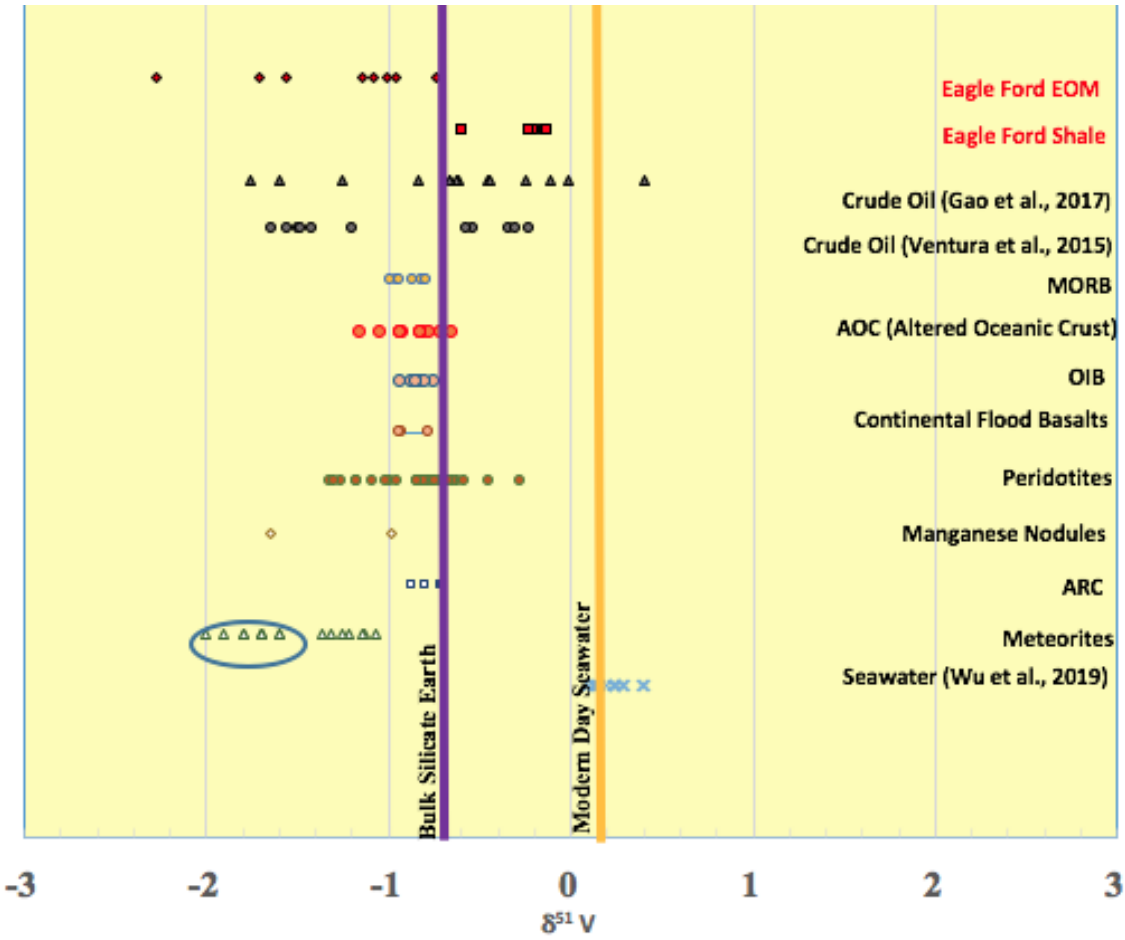

Figure 4.7.1: All recorded terrestrial and extraterrestrial vanadium isotopic data. (Klein and Langmuir 1987; Fisk and Kelley 2002; Wanless et al., 2012, Gannoun et al., 2012; Prytulak et al., 2013; Nielsen et al., 2014; Gale et al., 2014; Ventura et al., 2015; Wu et al., 2016; Schuth et al., 2017; Gao et al., 2017; Wu et al., 2019)

Terrestrial sources, including mid ocean ridge basalt (MORB), altered oceanic crust (AOC), ocean island basalt (OIB), continental flood basalts, mantle peridotites, manganese nodules, arcs, and meteorites show more restricted values due to lower

amounts of fractionation, as they are high temperature sources. In general, they each have a much narrower range of values. MORB values range from $\delta^{51}V$ (-0.8‰ to -1.04‰). AOC values range from $\delta^{51}V$ (-0.71‰ to -1.16‰). OIB values range from $\delta^{51}V$ (-0.7‰ to -1.3‰), continental flood basalts range from $\delta^{51}V$ (-0.7‰ to -0.9‰), peridotites range from $\delta^{51}V$ (-0.3‰ to -1.4‰), manganese nodules range from $\delta^{51}V$ (-1‰ to -1.65‰), and Arcs range from $\delta^{51}V$ (-0.65‰ to -0.85‰) (Klein and Langmuir, 1987; Fisk and Kelley, 2002; Wanless et al., 2012; Gannoun et al., 2012; Prytulak et al., 2013; Nielsen et al., 2014; Gale et al., 2014; Ventura et al., 2015; Wu et al., 2016; Schuth et al., 2017; Gao et al., 2017; Wu et al., 2019). The terrestrial sources are also very similar to the value of BSE $\delta^{51}V$ (-0.7±0.2‰) (Prytulak et al., 2013). The extraterrestrial meteorites are grouped in two separate arrays. The group with isotopically lighter values, circled in blue, is the vanadium isotopic data from Nielsen et al 2013., and indicates the first published values. But in 2018, Nielsen published new meteorite data taking into account the large sulfur interference pointed out in Gao at al., 2017 based on a new chromatography method. After taking sulfur into account, the meteorite values become heavier isotopically $\delta^{51}V$ (-1.2‰) than the original data set (Nielsen et al., 2018). Lastly, the modern seawater values from Wu et al., 2019 are plotted showing that the present-day oceans are very homogenous with values near $\delta^{51}V$ (+0.2±0.12‰). Whether the seawater values are appropriate for the Cretaceous depositional period of the Eagle Ford is questionable, but the average value is plotted simply for a reference point of possible seawater compositions.

The spread of vanadium isotope values in the Eagle Ford shale observed here (a single drill hole) shows greater variation than any other data sets presented in Figure 4.7.1 and is similar to the wide variation in the combined global crude oil data sets of Ventura et al., 2015 and Gao et al., 2017. The higher temperature terrestrial and extraterrestrial data shows a narrower range of isotopic variation and exhibits slight isotopic fractionation mainly due to redox conditions, volatilization, partial melting, and magmatism processes (Prytulak et al., 2013; Nielsen et al., 2014; Wu et al., 2019).

4.8 Downhole variations of Bulk Rock and EOM isotopic compositions

In Figure 4.8.1, the bulk shale and EOM show an overall trend. The deepest samples show bulk shale and EOM values somewhat similar to one another, and similar to Bulk Silicate Earth (BSE) values. In the upper portions of the core, bulk shale and EOM values seem to diverge from one another (Figure 4.8.1). The EOM values become isotopically lighter than BSE and the bulk shale values become isotopically heavier than BSE up section in the hole. The bulk shale values in the lower core are very similar to the BSE value of $\delta^{51}V$ -0.7±0.2‰ (Prytulak et al., 2013). In the upper core, the bulk shale values become isotopically heavier and diverge away from Bulk Silicate Earth (BSE).

Figure 4.8.1 suggests there is possible fractionation that could be occurring causing the EOM and bulk rock shale samples to exhibit more highly disparate values. The bulk rock shale and EOM samples show almost identical vanadium isotopic composition in the deep portion of the core, which are also very similar to BSE. Migrating up core, the bulk rock shale values become isotopically heavier and the EOM values become isotopically more significantly lighter. Fractionation processes causing

this difference could be due to speciation and bonding at the sea bottom, fractionation due to oil formation by heating, fractionation due to oil expulsion of early formed crude oils, and/or during the process of catagenesis with demetalation.

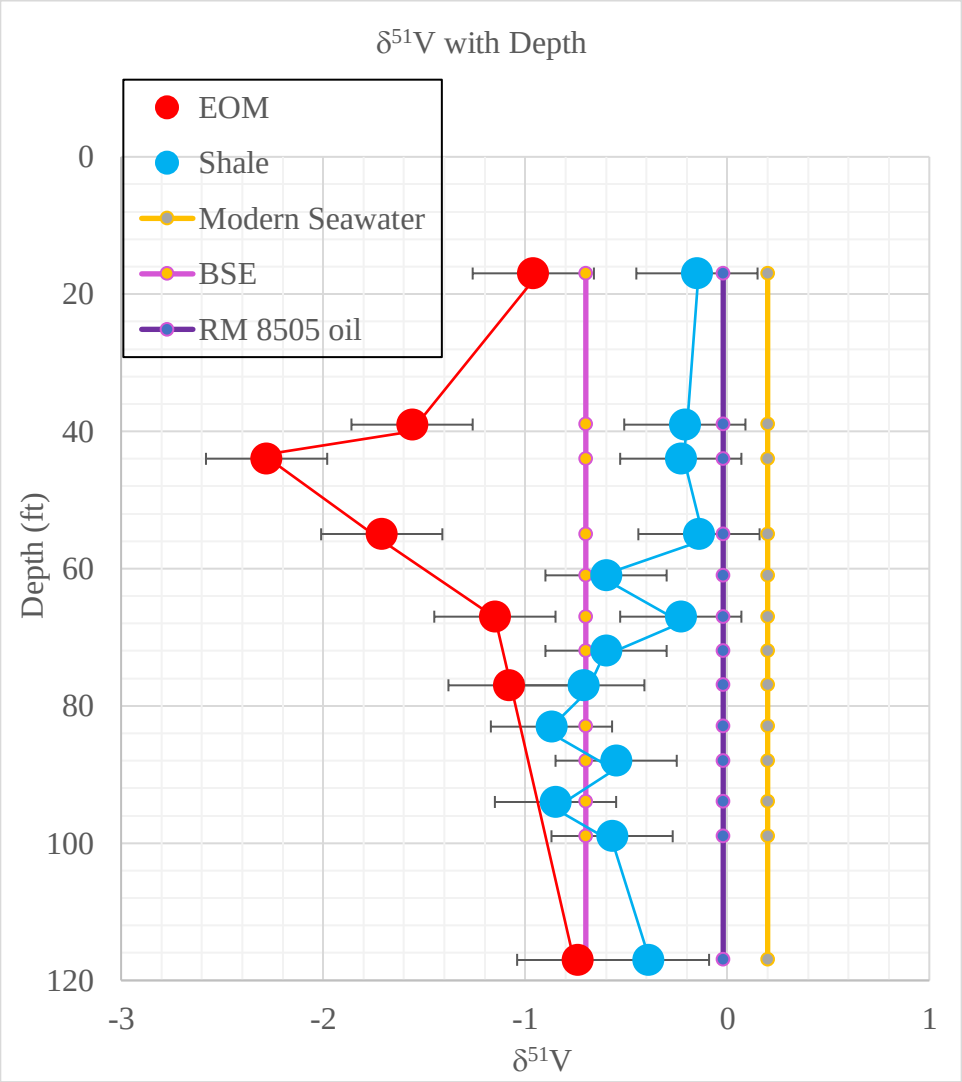

Figure 4.8.1: Vanadium Isotopic Analysis of bulk rock shale samples and EOM samples. The references used are bulk silicate earth (BSE), the immature oil, RM 8505, and modern day seawater. Depth profiles display a modified depth, not true depth. (Prytulak et al., 2013; Gao et al., 2017; Wu et al., 2019)

CHAPTER 5:

DISCUSSION:

The relationship between vanadium and total organic carbon (TOC) is evident by their strong correlation in marine shales of the Eagle Ford. The correlation likely reflects the affinity of vanadium to organic matter and the favorability of depositional conditions that favor preservation of organic matter in partitioning dissolved vanadium from seawater to shales. During petroleum generation, vanadium organic complexes can migrate with petroleum out of the shale, but it appears that a significant amount of vanadium is retained either in refractory organic matter (kerogen) or authigenic clay minerals. The results presented here are the first vanadium isotopic analysis performed on both EOM and bulk rock carbonaceous marine shale. They indicate that there are large and significant variations between EOM and bulk shale vanadium isotope compositions. Therefore, fractionation processes that are causing these differences need to be examined and understood. Before addressing the possible fractionation processes that could be causing the differences, I examined the vanadium reservoirs that could be involved in both the enrichments and depletions in vanadium abundances and/or isotopic fractionations. The organic matter–rich shales may be regarded as an open system with respect to seawater, pore fluids, oil formed and oil expulsed. The vanadium now within the EOM and bulk shale may have involved vanadium exchanged within several reservoirs: seawater, pore waters, oxides, authigenic and detrital clay, kerogen, and progressively formed in situ (EOM) and extracted oil and fluids. The geochemical processes such as reduction/oxidation, adsorption, and complexation during deposition, diagenesis, burial and hydrocarbon formation and expulsion, and their effects on

vanadium transport and accumulation are not completely established. The three primary sources of vanadium in shales are 1) the detrital fraction derived from continental weathering of terrigeneous material, 2) a biologic fraction assimilated by organisms during their life cycle and retained following degradation in the water column and within sediments, and 3) an authigenic fraction that can reflect redox processes during early diagenesis (Cole et al., 2017). The authigenic fraction is likely largely responsible for hyper-enrichments of vanadium in the Eagle Ford shales (Cole et al., 2017).

5.1 Reservoirs of Vanadium

Fractionation processes can cause vanadium to change or transform from one reservoir entity to another. Vanadium can reside in: seawater, pore water, detrital siliciclastics, EOM (movable oil), kerogen (organic matter), or in the already extracted oil and pore fluids (Figure 5.1.1). Below, a brief review of what is known about each of these reservoirs and transformations will be described in relation to vanadium abundances and isotopic compositions.

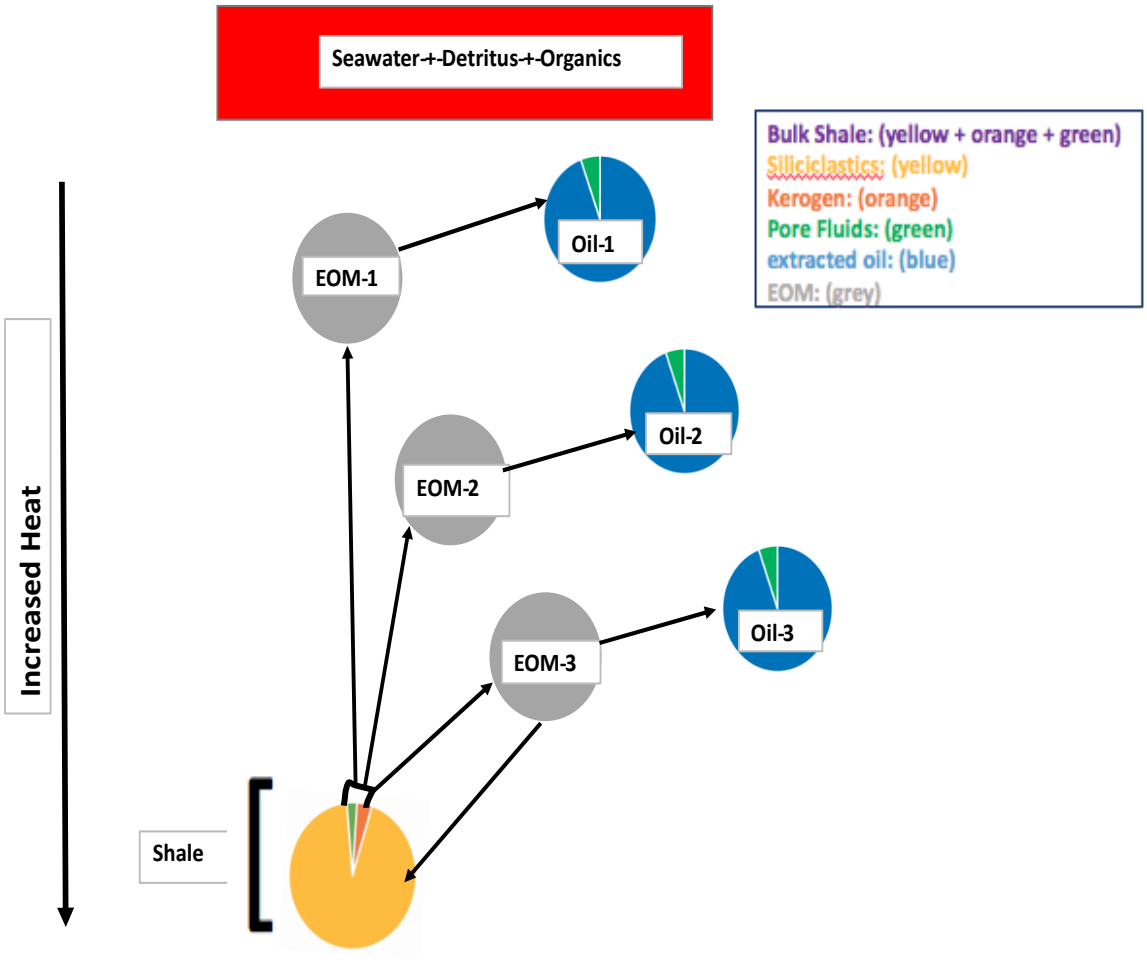

Figure 5.1.1: Cartoon depicting the reservoirs containing vanadium: seawater, pore fluids, EOM, kerogen, shale, or already expulsed fluids.

Seawater Reservoir

Vanadium enters the oceans mainly by riverine transportation. The overall vanadium concentration of the ocean is rather homogenous and low ~2 ng/g (Wu et al., 2019; Wedepohl, 1971; Gao et al., 2017). The residence time of vanadium is 50 kyr, much longer than the mixing rate of the oceans (Tribovillard, 2006; Gao et al., 2017). In oxic waters, vanadium exists as soluble V(V), but as waters become anoxic, and in some cases euxinic (high H_2S), vanadium is reduced to V(IV) and forms vanadyl ions (Lewan, 1984). Further reduction of V (IV) to V (III) under even more elevated H_2S activities (exceeding 0.29 mM) in bottom or pore waters is possible. This may lead to hyper-enrichments of V consistent with reduction to V(III) (Breit and Wanty, 1991). If vanadium is in its reduced state, the vanadyl ions can form strong bonds with organic molecules (e.g., porphyrins) at the sea bottom or within the sediments, and be further buried. Thus reduction, adsorption, diffusion and complexation of dissolved vanadium favor addition of vanadium to sediments rich in organic matter.

Organic Matter Evolution

Vanadium can be bound to organic matter as well as siliciclastics. The vanadium existing in both components (organic matter and siliciclastics) together are measured as the bulk shale composition reported in chapter 4. Over time, as the bulk shale is buried and heated, the organic matter is first transformed to kerogen. As the kerogen is progressively buried, it is transformed to hydrocarbons of oil and gas. As oil is formed, increasing pore pressures could lead to several stages of expulsion from the system. As hydrocarbons are expulsed and kerogen is transformed to EOM progressively during

catagenesis, EOM may be of variable composition as early V enriched and isotopically heavier oils yield to V poor and V-isotopically lighter oils or EOM. This movable EOM and residual kerogen left behind are components of the bulk rock analysis presented. With burial, the residual kerogen and rock are subjected to higher temperatures. As the organic matter reaches higher maturities and temperatures, a further process of demetallation will also occur. The high temperatures create the cracking of more complex vanadium-bearing organic molecules releasing vanadium metal ions. During the demetallation process, vanadium in its V(IV) state in the organic-metallic molecules may be further reduced to V(III) and absorbed or incorporated in the structure of authigenic clays or released to pore fluids (Lewan, 1984; Gao et al., 2017).

Concentrations in the different reservoir entities have large variations, indicating elemental fractionation. Vanadium concentrations in seawater are extremely low, averaging around 2 ng/g (Wedepohl, 1971; Wu et al., 2019). The bulk silicate earth vanadium concentrations, which are considered to approximate the silicate portion of the earth (mantle and crust) are much higher averaging ~97 µg/g (Prytulak et al., 2013). The vanadium abundances of average shale vanadium were determined by Turekian and Wedephole, 1961 to be ~130 µg/g. The bulk shale compositions included in this study range from 155 µg/g to 1056 µg/g, averaging 526 µg/g. Thus in general, shales are considerably more enriched in the Eagle Ford section than average shales (Turekian and Wedephole, 1961). In addition, because V concentrations in modern sediments are below 500 µg/g (Scholtz et al., 2011), many values like those in the Eagle Ford section sampled here exceed enrichments in modern-day sediments (maximum 500 µg/g) (Scholtz et al., 2011). Those with higher abundances are characterized as “hyper-enriched” with respect

to V. On the contrary, the EOM vanadium concentrations are much lower. The EOM vanadium concentrations range from only 554 ng/g to 6613 ng/g, averaging 2575 ng/g. The oil that has been produced from the well has even smaller vanadium mass fractions than the EOM sampled, averaging ~ 20 ng/g.

While the concentrations within these different reservoirs have large variations, the isotopic composition measured here and in the recent literature are similarly different. The data presented here suggests isotopic fractionation is indicated by differences between bulk shale and extracted EOM. The average vanadium isotopic composition of modern day seawater is $\delta^{51}V$ (0.20±0.12‰) (Wu et al., 2019). The average bulk silicate earth value is around $\delta^{51}V$ (-0.7 ± 0.2‰) (Prytulak et al., 2013). In comparison, the vanadium isotopic composition of sampled EOM range from $\delta^{51}V$ (-0.74 ±0.3‰ to -2.28 ± 0.3‰) with an average of $\delta^{51}V$ (-1.35 ±0.3‰), which is significantly lighter than seawater or BSE. These sampled EOM values, in fact, represent the lightest values yet recorded for any earth materials. The bulk shale, in turn, ranges from $\delta^{51}V$ (-0.14 ±0.3‰ to -0.87±0.3‰) with an average of $\delta^{51}V$ (-0.47 ±0.3‰), on average closer to BSE and heavier than EOM in the same samples. The EOM values are thus significantly isotopically lighter than the bulk rock shale values. The modern day seawater value, which may not necessarily reflect Cretaceous seawater values, exhibits a heavier value compared to the EOM and bulk rock shale. The crude oil produced from the borehole sampled here is very mature, R_o =1.1 and has obviously demetallized significantly due to extremely low vanadium concentrations (20 ng/g). Therefore, it was not practical to measure vanadium isotopic compositions of the crude oil produced. However, as a

comparison we utilize RM 8505 crude oil produced from the La Luna source rock in Venezuela, which has the same age and V/(V+Ni) ratios of the Eagle Ford Shales. It should be noted that the RM 8505 crude is metal rich (V=391 µg/g) and sulfur rich (2.17 wt %) representing an immature crude oil that we liken to early formed oils of the Eagle Ford shale (Gao et al., 2017). The RM 8505 $\delta^{51}V$ value (-0.02±0.3‰) was reported by Gao et al. 2017 and is significantly heavier than EOM sampled here. It is suggested that early immature crude oils expulsed from the Eagle Ford section analyzed may have had a similar heavier isotopic composition to La Luna crude oils. This is compared with the much lighter EOM values reported here.

5.2 Vanadium Isotopic Fractionation

The V abundances and isotopic signatures listed above are indicative of both elemental and isotopic fractionations at relatively low temperatures. There are many different ways that vanadium can fractionate during the process of deposition through catagenesis. Fractionation could be due to speciation and redox conditions occurring in the water column, at the sea bottom, and within the near-bottom sediment and formation of authigenic minerals. It could also occur once vanadium has been incorporated into the sediment during burial and heating, upon oil formation, during oil extraction, and during demetallation processes.

5.3 Fractionation via bonding and speciation at seafloor

Elemental and isotopic fractionation can occur because of change in the types of vanadium bonds, Eh-pH and redox conditions. Vanadium exists in marine environments in two oxidation states as largely unreactive vanadium (V) in oxic seawater and in a reduced state as particle reactive vanadium (IV) under moderately reducing conditions (Wanty and Goldhaper, 1992). Vanadium incorporation into minerals where H_2S activity is very high may cause further reduction from vanadium (IV) to vanadium (III) in bottom waters or pore waters within the sediments (Breit and Wanty, 1991; Wanty and Goldhaper, 1992; Scott et al., 2017). Equilibrium isotope fractionation is most likely controlled by bond strength (Bigelieson and Mayer, 1947; Urey, 1947; Wu et al., 2015). Species with shorter bond lengths with vanadium have stronger bonds and higher vibrational frequencies and therefore favor preferential incorporation of heavier isotopes in aqueous solutions (Wu et al., 2015). The longer the bonds the weaker

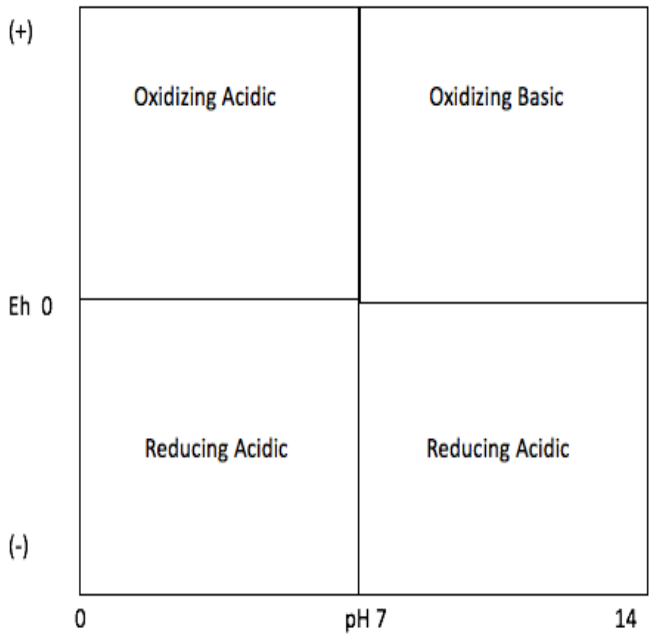

Figure 5.3.1: Eh/pH conditions in water. Reducing conditions exist when Eh conditions are below 0, and oxidizing conditions exist when Eh conditions are above 0. Acidic conditions exist when the pH ranges from 0-7, and alkaline conditions exist when the pH ranges from 7-14.

the bonds, and therefore these bonds favor lighter isotopes relative to heavier isotopes in aqueous solutions (Wu et al., 2015). Wu et al., 2015 showed that V species with high valence states show shorter V-O bond length in aqueous solutions. Therefore, the shortest and strongest bonds exist between vanadium existing as a V(V) and the longest and weakest bonds would exist between vanadium existing as a V(III) in aqueous solutions. A complete understanding of the oceanic V flux and isotope mass balance will be the key to developing the use of V isotope geochemistry as a reliable paleoredox indicator.

Eh-pH conditions refer to the stability of minerals or species in terms of hydrogen ions (pH) and electron activity (Eh). In natural waters, Eh conditions range from -400 to 600 milivolts, and pH conditions 1-10. In Figure 5.3.1, Eh vs pH conditions are demonstrated that show the depositional environment (reducing and oxidizing conditions) relative to acidic or basic water conditions. Where Eh conditions are below zero and exhibit a pH of 0-7, reducing acidic conditions prevail. As the pH climbs above 7 to 14, reducing alkaline or basic conditions exist. On the contrary, where Eh conditions are above zero and exhibit a pH of 0-7, oxidizing acidic conditions exist. As the pH climbs above 7 to 14, the water becomes more basic under oxidizing conditions.

Vanadium speciation in aqueous solutions depends on the pH and Eh conditions. In Figure 5.3.2, vanadium exists as V(V), V(IV), and as V(III). Vanadium exists in the V(III) state when Eh conditions are below zero and the pH ranges from 3-9 (Gustafsson et al., 2018). This is the most reduced state of vanadium in natural conditions. Vanadium exists in the V(IV) state when the Eh ranges from -100 to 600 milivolts and the pH

ranges from 3-6.5 (Gustafsson et al., 2018). As vanadium becomes more reduced it transitions from V(IV). To V(III). Vanadium exists in the V(V) state at all Eh conditions but with restricted pH conditions of 9-11 (Gustafsson et al., 2018).

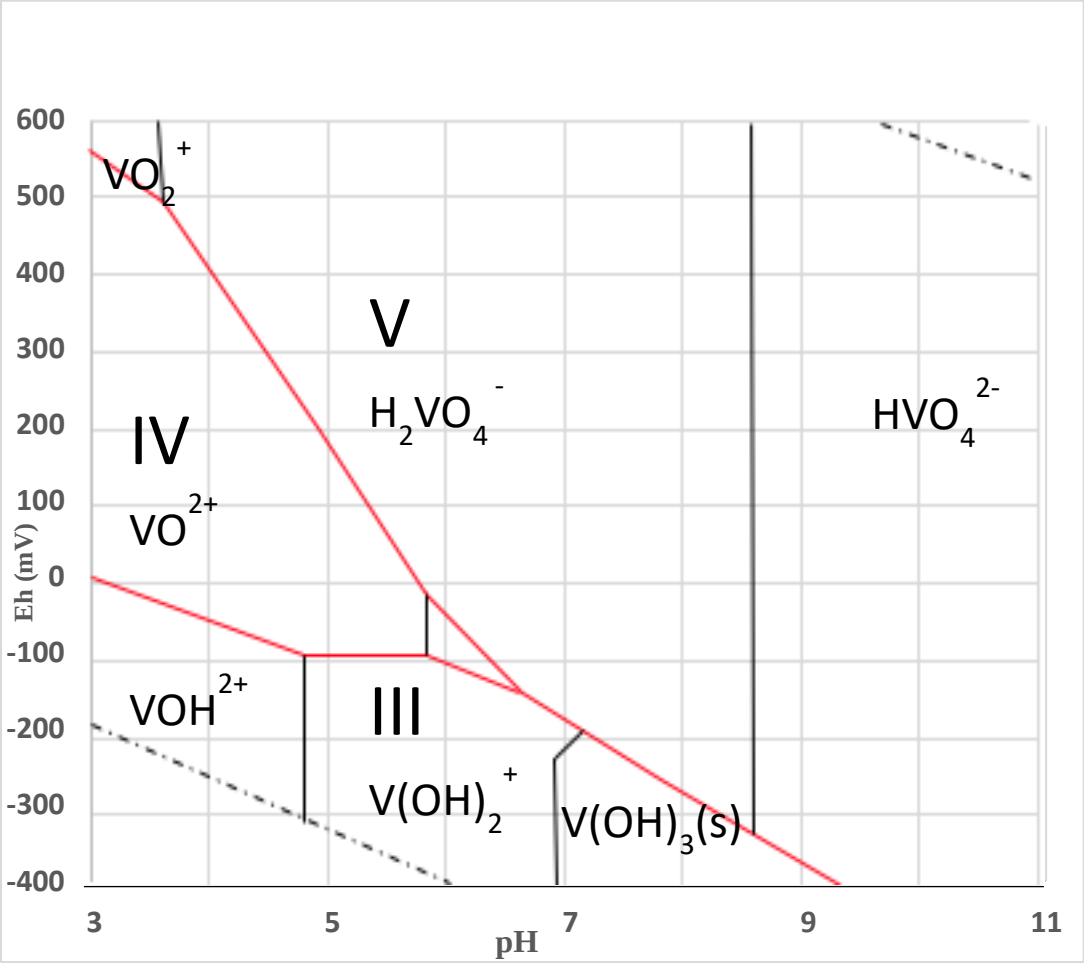

Figure 5.3.2: Vanadium speciation Eh/pH conditions in aqueous solutions. Vanadium exists in a +5 state when pH conditions are >9 and Eh conditions are >600 mV. Vanadium exists as a +4 state when the pH ranges from 3-6.5 and Eh from 0-600mV. Vanadium exists as a +3 state when the pH ranges from 3-9.2 and the Eh is below 0. (Modified from Gustafsson et al., 2018).

In 1984, Lewan proposed three regimes where vanadium exists in different species under differing pH and Eh conditions under natural conditions (Figure 5.3.3). Regime I at elevated Eh and pH conditions represents vanadium occurring as a quinquivalent anion V(V) where soluble vanadyl cations V (IV) are not available for metalation into the sediment because of hydroxides in the water hindering the bonding to organic matter (Lewan, 1984). On the contrary, nickelous cations are available for metalation giving rise to an overall low V/(V+Ni) or V/Ni ratio, and low sulfur content in the organic matter and likely in the derivative crude oil. In regime II at more acidic low pH and elevated Eh, both highly reactive vanadyl, V (IV) and nickelous cations are available for metalation (Lewan, 1984) of organic matter. In regime II, in basic (high pH) conditions, nickelous cations dominate for metalation due to the vanadyl ions hindered by hydroxide ions. In acidic (low pH) conditions, hydroxide ions do not hinder vanadium, therefore allowing for vanadyl and nickelous cations to be available for metalation of organic matter. Lastly in regime III, at low Eh reducing and low to moderate pH acidic conditions, vanadyl ions are available for metalation, but nickel is hindered by reduced sulfate and sulfide formation (Lewan, 1984). In this regime, sulfate is reduced by sulfate reducing bacteria and nickelous cations have an affinity to bind to the reduced sulfur (sulfide minerals). This results in high V/(V+Ni) and high sulfur content in organic matter and the generated crude oil (Lewan, 1984). Lewans' 1984 Figure 5.3.4 shows the three regimes in terms of V/(V+Ni) and sulfur wt % which is useful generally for immature oils (i.e., where significant demetallation has not ensued because of high maturities) (Figure 5.3.4). We have plotted the EOM samples in comparison of to an immature Venezuelan crude oil on this diagram. The diagram shows an oil, RM 8505,

which is an immature oil from the La Luna formation source rock in Venezuela of the same age as the Eagle Ford. It may have been similar to an immature oil in the Eagle Ford as it has similar V/V+Ni to the EOM from the Eagle Ford. The La Luna Formation is also a marine shale thought to be formed in a silled basin like the Eagle Ford sampled here based on data collected at UH (Casey and Gao, personal communication). The Eagle Ford EOM samples analyzed here are also plotted, but are much more mature (R_o =~1.1)

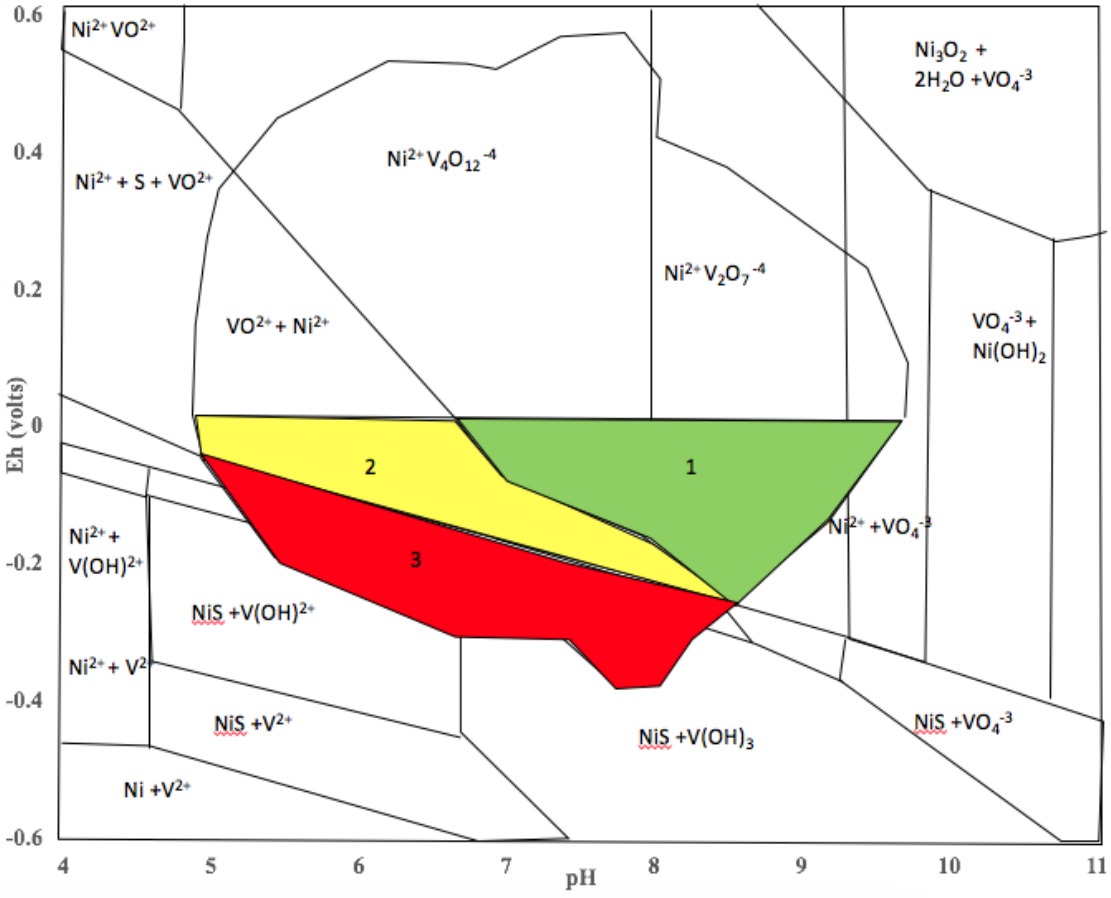

Figure 5.3.3: Three Regimes comparing Eh vs pH for vanadium and nickel speciation. Regime one (green) indicates Ni ions for metalation over V ions. Regime two (yellow) indicates Ni and V ions available for metalation depending indicates Ni and V ions available for metalation depending on pH conditions. Regime three (red) indicates V ions available for metalation over Ni due to sulfate reduction. (Modified from Lewan, 1984).

and not well suited for plotting on this diagram. The EOM is likely to have nearly maintained or altered slightly the original high V/V+Ni ratio of an immature precursor oil like RM 8505.

However, the V and S abundances are likely to have undergone severe loss upon maturation and demetallation upon maturation. RM 8505 exhibits a high V/(V+Ni) and high sulfur wt %, which is typical of immature oils from regime III, indicative of a more anoxic-euxinic (H_2S -rich), and acidic depositional environment. The bulk rock samples and EOM samples likewise show a very similar and high V/(V+Ni) like RM 8505, suggesting that these ratios may have changed only slightly upon maturation. However, the EOM samples show low sulfur and V contents indicating metal loss likely because of their high maturity. As maturity increases, the V/(V+Ni) stays nearly constant, but V, Ni and S contents decrease (Gao et al., 2017). In EOM, metals are significantly depleted in V and Ni, while maintaining a high V/(V+N) ratio. Therefore,

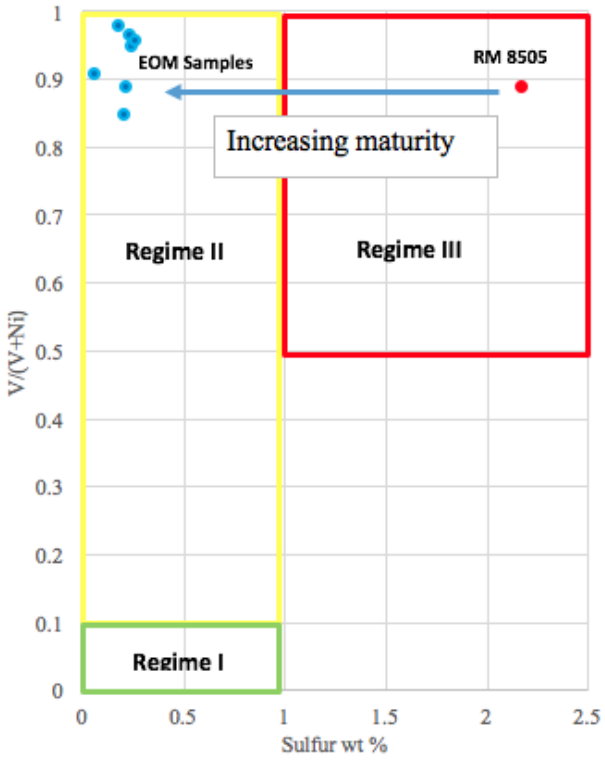

Figure 5.3.4: Three Regimes-V/(V+Ni) vs Sulfur wt %. Regime three (red) indicates high sulfur content and high V/(V+Ni). Regime two (yellow) indicates low sulfur and variable V/(V+Ni). Regime one (green) indicates low sulfur and low V/(V+Ni). EOM samples plotted along with immature Cretaceous sourced Venezuelan crude oil, NIST RM 8505. EOM samples and RM 8505 oil show similar V/(V+Ni) ratio but differing metal contents (Lewan 1984).

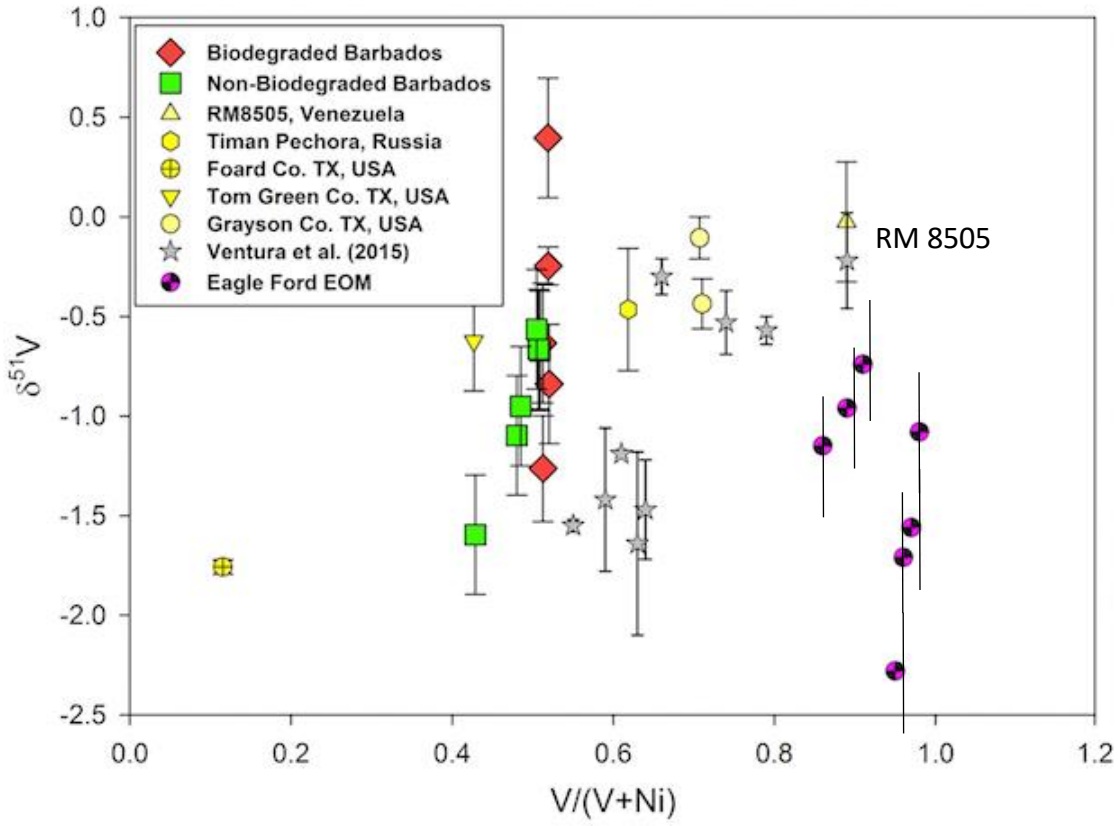

Figure 5.3.5: $\delta^{51}V$ vs V/(V+Ni) for global crude oil set. RM 8505 is plotted exhibiting a heavy isotopic value. The EOM samples are also plotted showing a very similar V/(V+Ni) ratio to RM 8505, but a wide range of isotopic values. (Modified from Gao et al., 2017; Ventura et al., 2015)

the metal concentrations are interpreted to have significantly decreased in the EOM samples, compared with a precursor low maturity oil, like the Late Cretaceous RM8505, which originated in a similar silled basin setting.

Figure 5.3.5 shows the $\delta^{51}V$ vs V/(V+Ni) ratio of RM 8505 alongside a global set of crude oils. The EOM samples are also plotted showing a very similar V/(V+Ni) ratio to the RM 8505 Cretaceous La Luna oil. However, the $\delta^{51}V$ isotopic signature varies in

the EOM from the Eagle Ford sampled in this study. The isotopically heavier EOM samples show the most similar V/(V+Ni) ratios and isotopic compositions to RM8505, the La Luna derived crude oil. The isotopically lighter EOM samples from the Eagle Ford show elevated V/(V+Ni) ratios and are noticeably lighter than RM 8505.

Combining the speciation diagrams and high V/(V+Ni) ratios, it is evident that the metalation of the organic matter likely occurred when V(IV) existed in abundance and the vanadyl ion dominated the metalation of the organic matter. Vanadyl ions will enter the porphyrin structures or other organic metallic molecules of the organic matter typically at the seafloor or within the sediments under reducing conditions.

Vanadium in seawater in oxic conditions exists as V(V). The oxic sink for V (V) is where it is absorbed by Fe-Mn oxide and deposited under oxic conditions (Tribovillard, 2006; Wu et al., 2015). Given the estimated V isotopic fractionation between seawater and oxic sediment of about 1.2‰ (Wu et al., 2019), the removal of V from seawater under oxic conditions will result in a heavier V isotopic composition of the seawater compared to the V isotopic composition of the main input source, i.e. the riverine input which is estimated to be -0.6±0.3‰ (Wu et al., 2019). However, under reducing and/or anoxic conditions the removal of V is expected to be through the incorporation of vanadyl ions into organic matter and/or the precipitation of V(III) into authigenic clay (Gustafsson, 2019). The bond length for the tetrahedral V-O for the dissolved V(V) in seawater is 1.72 A, 1.588A for the V(IV)-O bond in vanadyl ion, and 1.992 A for the octahedral V(III)-O bond (Gustafsson, 2019). In the marine environment, the V(IV) ionic species may be removed to the sediment by surface adsorption processes or by formation of organometallic ligands (Emerson and Huested, 1991; Morford and Emerson, 1999). In

the diagenetic environment, V(III) readily substitutes for aluminum in the octahedral sites of authigenic clay minerals or in recrystallizing clay minerals (Breit and Wanty, 1991). Given the consideration of the bonding length/strength, the isotopic fractionation between vanadium in the seawater [V(V)] and vanadium in the organics [V (IV)] at reducing sea bottoms would most likely shift the vanadium isotopic value somewhat heavier in the V-organic complex and lighter for vanadium in authigenic clays. Vanadium in modern-day seawater V(V) has an isotopic composition of $\delta^{51}V = 0.20 \pm 0.12‰$, which is heavier than its main input source, namely the riverine flux due to the preferential removal of V^{50} by Fe and Mn oxides (Wu et al., 2019). The bulk rock and EOM sampled here are lighter than RM 8505 and modern seawater (Figure 5.3.6).

Whereas modern-day seawater has an isotopic composition of $\delta^{51}V$ 0.20 ±0.12‰, however, the global seawater composition during the Cretaceous is unknown. The Cretaceous period was known, however, for anoxic ocean expansion (Takashima et al., 2011). If in fact the global seawater in the Cretaceous was more anoxic or euxinic globally, vanadium could either be removed under reduced conditions by clays as V(III) or by organometallic complexes as V(IV). If vanadium was removed by clays, this would shift the global seawater value heavier as removal to clays lends itself to a lighter isotopic composition for the clays. If vanadium was removed by organics as reduced vanadyl species, the global seawater value would become lighter, as removal to organics lends itself to a heavier isotopic composition for the organic matter. However, if global seawater in the Cretaceous was more like it is today, which is overall oxic, V^{50} would be incorporated into Fe-Mn oxides under oxic conditions shifting the seawater isotopic value to heavier values than the values of today's seawater (Figure 5.3.6; Wu et al., 2019).

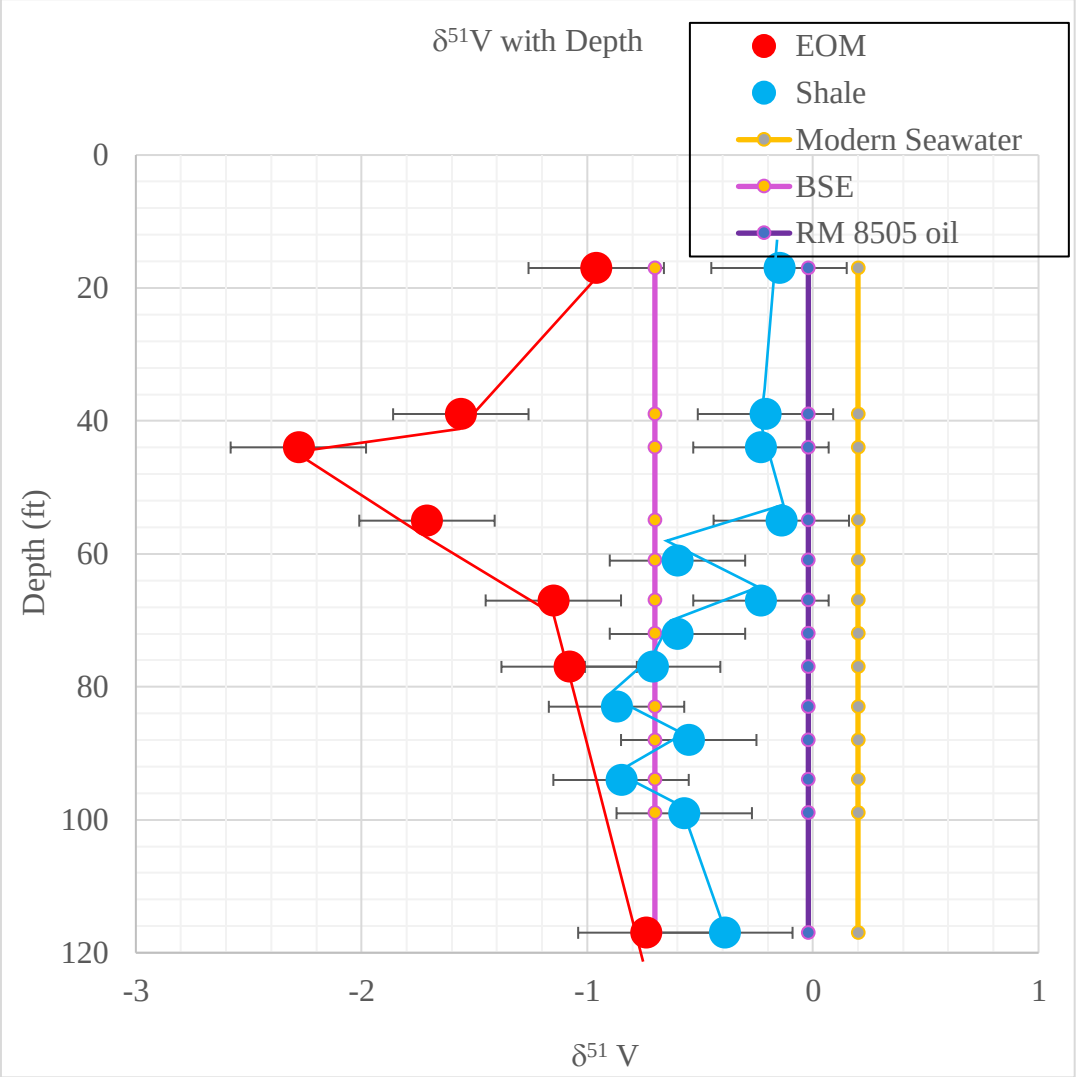

Figure 5.3.6: $\delta^{51}V$ isotopic composition of EOM and bulk rock shale samples. Modern seawater, bulk silicate earth and RM 8505 oil are used as references. Depth profiles display a modified depth, not true depth. (Prytulak et al., 2013; Gao et al., 2017; Wu et al., 2019)

Bottom Water Conditions

There are patterns that suggest factors that influence the uptake of authigenic trace metals, creating enrichments of metals in sediment. Molybdenum and vanadium are two trace metals that are similar in the following ways. In oxic conditions, they are both soluble in seawater, but once anoxia or sulfidic anoxic conditions prevail, they are reduced and become insoluble (Takahashi et al., 2014). Molybdenum exists as soluble MoO_4^{2-} in oxic waters, and becomes reduced insoluble Mo (IV) (Takahashi et al., 2014). Vanadium undergoes a two-step reduction process from oxic to anoxic and then anoxic to euxinic (sulfidic). Vanadium exists as soluble HVO_4^{2-} in oxic conditions and under mildly reduced conditions converts to V(IV) and forms the reactive vanadyl ion (Takahashi et al., 2014). Under more strongly reduced conditions vanadium can be further reduced to V(III) and precipitate as a solid oxide or hydroxide (Takahashi et al., 2014). In 2009, Algeo et al. postulated factors that could influence the uptake of Mo authigenic trace metals in sediment. The factors include: benthic redox conditions and the operation of a particulate shuttle. Because Mo and V operate similarily, these factors could contribute to the enrichments in molybdenum and vanadium in the bulk rock shales and high V/V+Ni ratios seen in the EOM and bulk shale samples.

The first and most important factor is benthic redox conditions, which most likely affect the majority of the trace metal enrichment in sediment (Algeo et al., 2009). Waters can range from oxic to sulfidic. In terms of Mo and U, oxic conditions exhibit no enrichment in sediment, suboxic conditions exhibit U/Mo ratio enrichment and sulfidic conditions exhibit Mo/U ratio enrichment (Morford and Emerson,1999; Zheng et al., 2002a; Morford et al., 2005; Algeo et al., 2009). In suboxic conditions, the reason for the

U/Mo ratio enrichment has to do with U(VI) reduced at the Fe(II)-Fe(III) redox boundary prior to sulfate reduction (Algeo et al., 2009). Under anoxic-sulfidic conditions as the chemocline becomes shallower relative to the sediment water interface, Mo is reduced to thiomolybdates which are particle reactive and enhance the uptake by the sediment of authigenic Mo (Takahashi et al., 2014). This creates high enrichments of Mo/U ratios. This phenomenon by Algeo et al. (2009) could be representing vanadium as well indicating that very high enrichments of metals and metal ratios (>0.9) are indicative of very sulfidic, high H_2S bottom waters (Lewan, 1984; Figure 5.3.7).

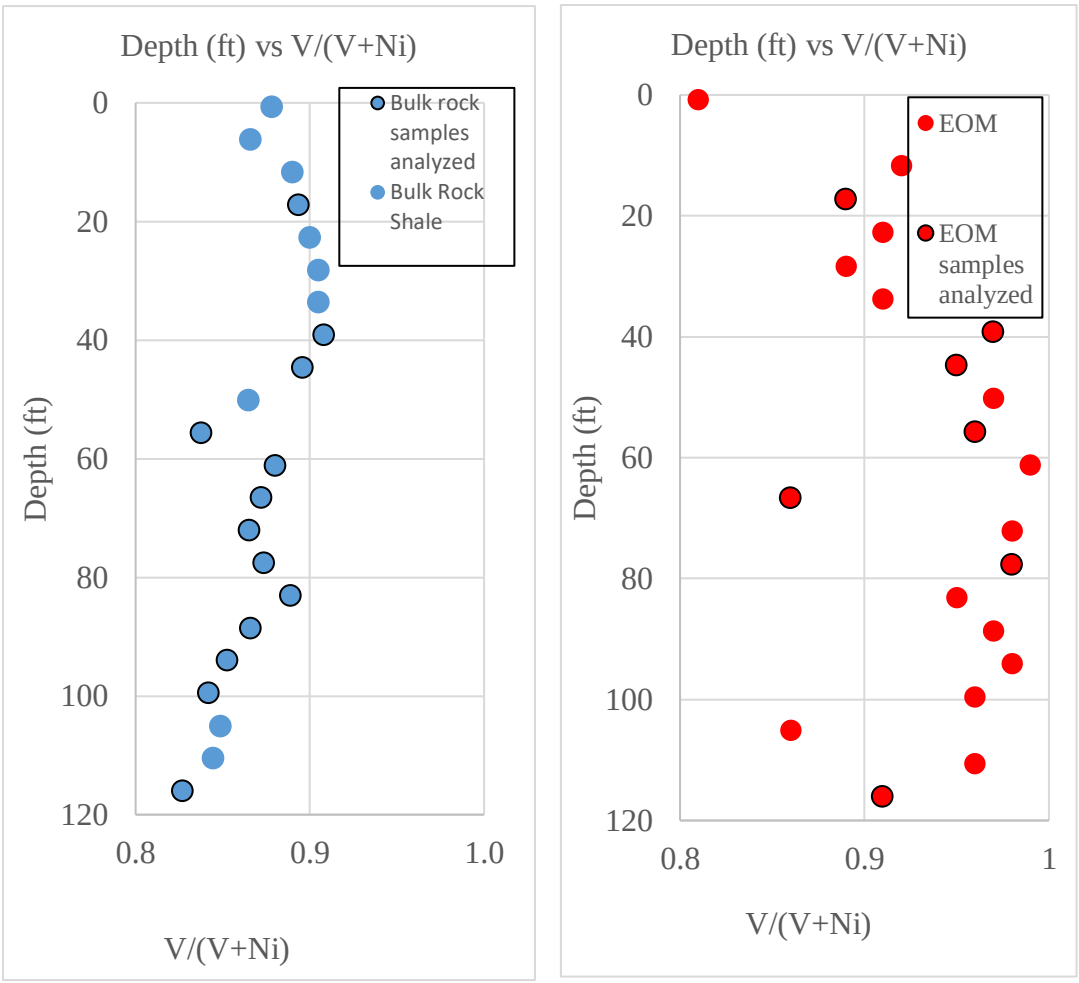

Figure 5.3.7: Depth (ft) vs V/(V+Ni) ratio for both the bulk rock shale and EOM samples. Both bulk rock shale and EOM show very high ratio values indicative of strongly reducing conditions. The solid samples indicate all bulk rock and EOM data. The black circled samples indicate the samples that were analyzed for $\delta^{51}V$ in this study. Depth profiles display a modified depth, not true depth.

The second factor controlling benthic redox conditions is the Mn-Fe particulate shuttle (Calvert and Piper, 1984; Wehrly and Stumm 1989; Algeo et al., 2009). Manganese forms an insoluble MnO_2 in oxic conditions and then becomes soluble in anoxic/sulfidic conditions (Broecker and Peng, 1982; Tribovillard, 2006). In terms of the particulate shuttle, the chemocline location is very important (Algeo et al., 2009). The

chemocline separates oxic conditions from sulfidic conditions. The highest enrichments will reside where the chemocline is closer rather than farther from the sediment water interface or sediment bottom (Algeo et al., 2009). Mn existing as an insoluble ion in oxic conditions adsorbs Mo as well as V, which can incorporate Mo and V into the sediment in oxic condition. However, when the chemocline is encountered, the MnO_2 breaks down as Mn becomes soluble again. Meanwhile the Mo and V transition from the soluble ion in oxic waters to become highly reactive and insoluble (Algeo et al., 2009). As increases in H_2S are encountered and depending on the location relative to the sediment, the highest amounts of Mo and V are available to be taken up by the organic matter and sediment as V(IV) or V(III), respectively (Lewan, 1984).

Figure 5.3.8 shows how geochemical processes affect the abundance and speciation of vanadium (Breit et al., 1991) at the seafloor and below. In oxic waters, vanadium exists in the +5 valence state, V(V). High concentrations of vanadium exist in oxic waters because vanadium is soluble and does not bind to organic matter. Therefore, in oxic global seawater, vanadium concentrations are rather homogenous. As vanadium is reduced from V(V) to V(IV) in anoxic waters, vanadium exists as vanadyl ions and binds to (or reacts with) the available organic matter in the water column. Vanadium concentrations decrease in the water, if in fact, replenishment is low due to the fact that vanadium is now binding to organic matter. However, if there is replenishment of metals, then metal concentrations should not change much in the water column. As vanadium is reduced even further to V(III) in euxinic conditions, H_2S causes vanadium to bind to organic matter along with bonding to authigenic clays in higher amounts. The vanadium at the seafloor is bound to organic matter in the V(IV) state, but it is possible that

vanadium can be reduced to V(III) and absorbed or complexed to clays well before catagenesis begins (Breit et al., 1991). Vanadium may continue to be reduced to a V(III) state after sufficient burial and high temperatures. As predicted by Wu et al. (2015), reduction of V and incorporation into organic molecules with shorter bond lengths or in clay minerals with longer bond lengths in the sediment should cause progressively heavier V isotopic compositions in organics or lighter V isotopic compositions in clays.

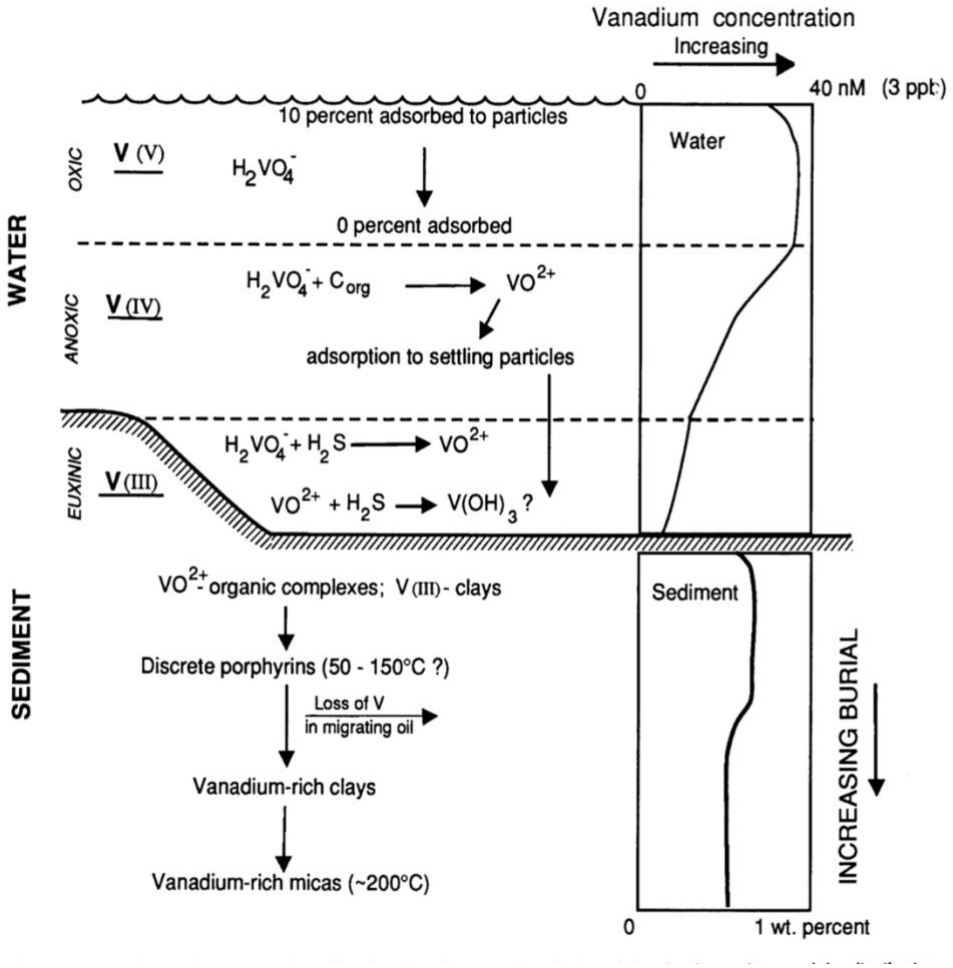

Figure 5.3.8: Vanadium speciation at and below the seafloor depending on geochemical processes. Within the water column, vanadium can exist in a +5, +4, and even a +3 state. As vanadium is incorporated into the sediment and buried vanadium reduces to a +3 state and binds to clays and siliciclastics. (Taken from Breit et al., 1991)

As vanadium under reducing conditions exists at the seafloor as vanadyl ions in organic matter, and as V(III) in clays are buried in the sediment, vanadium is subjected to higher temperatures upon burial that may cause vanadium to isotopically or elementally fractionate further At around 50-150 ºC, oil formation occurs and vanadium can undergo elemental or isotopic fractionation due to formation of oil from kerogen, which has likely

more enriched in V content (Odermatt and Curiale, 1991) as well as through the extraction of early V-rich oil upon expulsion. Expulsion can create a decrease in bulk vanadium concentration existing in the buried matured sediment. Vanadium is also subjected to high enough temperatures where demetallation can occur and the larger vanadium organic-metallic molecules break down, releasing vanadium. Porphyrin type can also change from DPEP (deoxophylloerythroetioporphyrin) to ETIO (etioporphyrin) where demetallation occurs (Didyk et al., 1975; Mackenzie et al., 1980; Barwise and Park, 1983; Barwise and Roberts, 1984; Barwise, 1987; Sundararaman et al., 1988; Sundararaman and Hwang, 1993). As the temperature and demetallation increases, vanadium can be released and fractionate into the clays and lastly form micas at around 200 ºC.

Another factor to take into account is vanadium residing in pore waters which is where most of the free vanadium is taken up by free-base porphyrins in the organic matter. Depending on whether the chemocline exists either at the sea bottom or below, vanadium can be reduced either above the seafloor or below. If the H_2S exists above or at the sediment water interface, then metalation of vanadium to organics or sediments could occur at the sea bottom (Tribovillard, 2006). If the bottom waters are oxic or suboxic at the sea bottom, and the H_2S exists beneath the surface, then the H_2S is limited to pore waters (Tribovillard, 2006). In this case where the chemocline exists below the sea bottom, vanadium can be further reduced below the sea bottom.

5.4 Fractionation Mechanisms- Seafloor, Diagenesis, Burial, Oil Formation/Extraction, Demetallation

The Cretaceous period was known for anoxic ocean expansion (Takashima et al., 2011). If in fact the global seawater was anoxic or euxinic, vanadium could either be removed by clays as V(III) or by organometallic complexes as V(IV). If vanadium was removed by clays, this would shift the isotopic global seawater value heavier as removal to clays lends to a lighter isotopic composition in clay. If vanadium was removed by organics V(IV), the isotopic global seawater value would become lighter, as removal to organics lends to a heavier isotopic composition in the organics. However, if the global seawater was more like it is today, which is oxic, V(V) would be incorporated into Fe-Mn oxides shifting the seawater isotopic value to heavier values than today. (Figure 5.3.6; Wu et al., 2019).

As vanadium is bound to the organic matter, fractionation could occur between oil/kerogen with sufficient burial, heating and transformation of kerogen to oil during catagenesis. As the bulk rock shale is heated and buried, the kerogen is progressively transformed to oil. Once oil has formed, there are extraction mechanisms leading to oil expulsions as pore pressures increase. First, there could be no extraction of oil meaning that the kerogen is transformed to oil and no oil has left the system. Second, there could be a single oil extraction or expulsion, and third, there could be multiple oil extractions occurring over time. Once oil is formed, overpressure and natural fracking can cause oil to expulse and fill nearby pore spaces. In the case of the Eagle Ford, the oil reservoirs in the overlying Austin Chalk may suggest multiple expulsion events from the Eagle Ford

(Dawson et al., 1995). We assume the first oils to expulse will be vanadium-rich and heavier isotopically, like sample RM8505 from the La Luna source rock in Venezuela.

As isotopically heavier oils are expulsed, and more extractions occur, the more depleted the residual oil/EOM/kerogen in situ will likely become as the oil removes heavier isotopes. The EOM samples will eventually show lower concentrations of vanadium (like Eagle Ford EOM, 554 ng/g to 6613 ng/g) with a very isotopically light signature ($\delta^{51}V$ -0.74±0.3‰ to -2.28± 0.3‰). The oil from the well sampled, which is the oil produced today, also shows even lower vanadium concentrations (20 ng/g), typical of highly mature oil. However, the early oil was likely more enriched in V and heavier in isotopic composition. RM 8505 is a similar age oil to the Eagle Ford Shale from Venezuela with similar V/(V+Ni) and high vanadium concentrations (391 µg/g),

Table 5.4.1: RM 8505 oil from Gao et al., 2017. This sample is resembling a similar age immature oil from the Eagle Ford Shale formation

Sample	Vanadium (ug/g)	$\delta^{51}V$	V/(V+Ni)	Sulfur
RM 8505	391	-0.02 ± 0.3‰	0.89	2.17 wt %

as well as a heavy isotopic signature ($\delta^{51}V$ -0.02±0.3‰) (Table 5.4.1). Therefore, the first Eagle Ford oil expulsed likely contained abundant vanadium with a heavier $\delta^{51}V$ leaving the system, if similar to the La Luna, RM 8505. Ultimately this leads to lighter $\delta^{51}V$ and lower vanadium concentration in the residual EOM. The first oil that left the system was likely a very isotopically heavy oil that was slightly V-isotopically lighter than modern

day seawater, if the RM 8505 analogue is appropriate. After the first oil left the system, the kerogen/EOM reservoir became lower overall in vanadium concentration, and lighter isotopically due to the large amount of vanadium removed from the system. With time and with progressive burial and heating, oil continues to form and is expelled. This would create a system that is not replenished and becomes more depleted in vanadium and lighter in isotopic ratios, as seen in the EOM sampled. This is especially observed up hole with the EOM vanadium isotopic signature becoming very light (Figure 5.4.1). The subsequent oil extractions likely become isotopically lighter and even more isotopically lighter progressively upon multiple extractions to resemble the well sampled, which is the oil that is being produced today, exhibiting a very low vanadium concentration. Although the isotopic composition of the well crude oil has not been measured, it most likely exhibits a very light isotopic signature, probably similar to the lightest EOM.

My hypothesis is that the isotopically heavier oil left the system and multiple expulsions of oil occurred leading to the final or residual present-day $\delta^{51}V$ (EOM) as the lightest (Figure 5.3.9 top). Where the $\delta^{51}V$ (EOM) is the isotopically heaviest in the section, this indicates that perhaps there has been less expulsion of isotopically heavy oil or that fewer expulsion events have occurred (Figure 5.3.9 top). There does seem to be a positive correlation between $\delta^{51}V$ and TOC in five of the EOM samples. Lower TOC values correspond with lighter isotopic EOM values, and higher TOC values correspond with heavier isotopic EOM values (Figure 5.3.9 top), suggesting lower amounts of oil expulsed. Where the EOM shows the lowest TOC and is isotopically the lightest, in the positive trend, could indicate that the isotopically heaviest oil has been extracted or that multiple extractions occurred. With all the oil leaving the system, lower TOC values

occur in the bulk rock itself. Where the TOC is the highest, the positive trend could indicate fewer extractions or lower amounts of isotopically heavy oil left the system. The TOC values are higher because either less organic matter was transformed to hydrocarbons or the oil was simply not expulsed. Figure 5.3.9 (bottom) indicates the $\Delta\delta^{51}V$, which is the difference in the isotopic composition of the shale and the EOM. Where the $\Delta\delta^{51}V$ is the largest indicates a large difference in the isotopic composition of the bulk rock and the EOM. Where the difference is the largest could indicate where the isotopically heaviest oil has left the system and multiple extractions occurred indicating large fractionation, shifting the EOM isotopic values lighter and the bulk rock shale isotopic values heavier (Figure 5.3.9 bottom). Where the difference is the smallest, could indicate fewer expulsions or more isotopically heavier oil or kerogen still exists in the rock. In this case, the bulk rock and EOM isotopic composition are very similar. There is a negative correlation with the $\Delta\delta^{51}V$ vs TOC (Figure 5.3.9 bottom). The samples in the trend with the lowest TOC values show the greatest $\Delta\delta^{51}V$(shale-EOM) value. This is where the multiple expulsions of isotopically heavy oil left the system. The samples in the trend with the highest TOC values show the lowest $\Delta\delta^{51}V$ (shale-EOM) value. This is where fewer expulsions or less isotopically heavy oil left the system. Now the samples without a positive or negative correlation, correspond to the top most and bottom most sample of the core. These samples might not have had enough TOC to produce hydrocarbons. There seems to be a threshold of around ~7-8% TOC. These samples therefore have not encountered multiple expulsions and have had less isotopically heavy oil leaving the system.

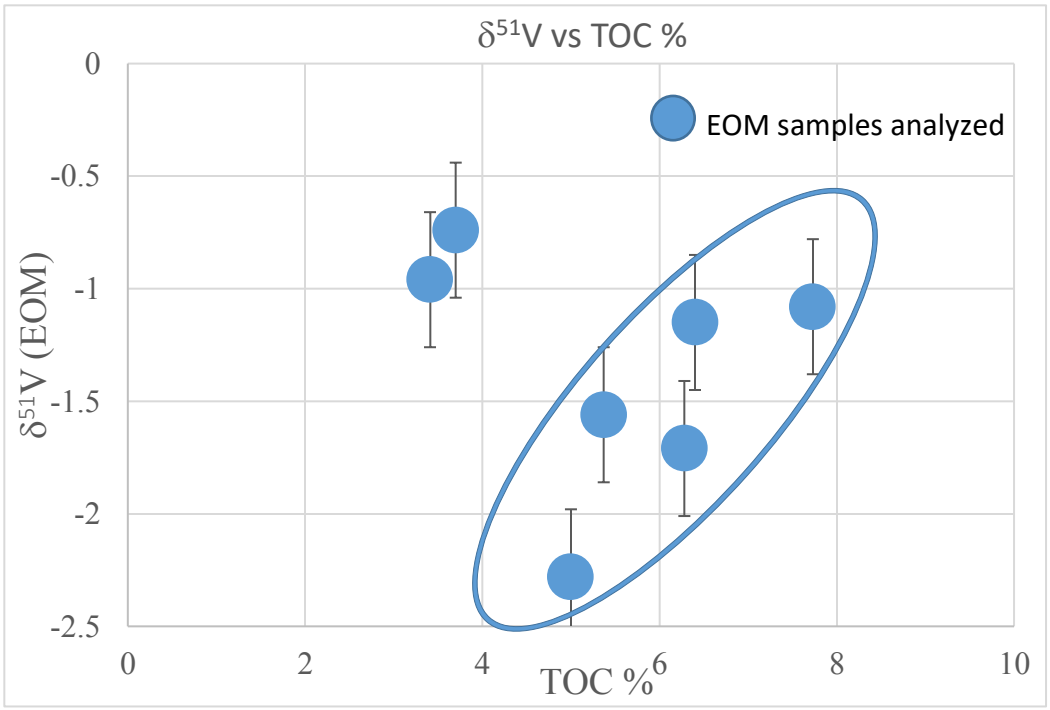

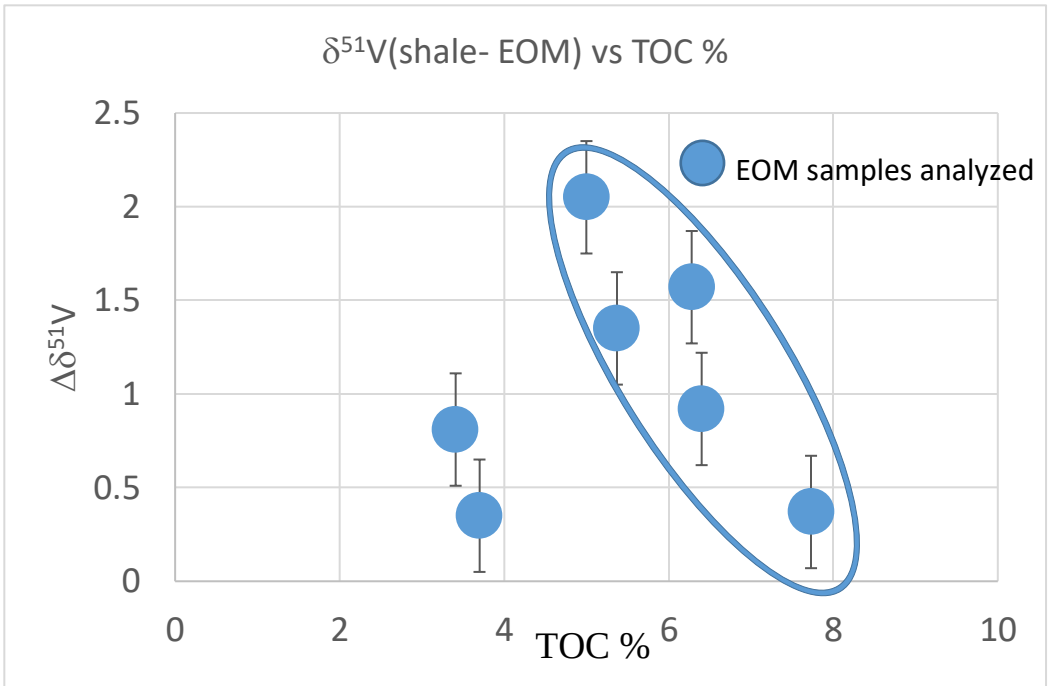

Figure 5.3.9: (TOP) $\delta^{51}V$(EOM) vs TOC. The lighter EOM values indicates isotopically heavier oil left the system or multiple expulsions occurred. The heavier the EOM values indicates isotopically heavier oil still in the rock or fewer expulsions occurred. (BOTTOM) $\delta^{51}V$ vs TOC. The higher the $\delta^{51}V$, the lower the TOC indicating more isotopically heavier oil expulsed, and the lower the $\delta^{51}V$, the higher the TOC indicating less isotopically heavier oil expulsed. TOC precision +/- 0.107.

There are several uncertainties in the equation of mass balance that make it difficult to account for all the vanadium. First, the kerogen concentration and kerogen isotopic signature are unknown. As previously mentioned, it is proposed that the isotopically heaviest, V rich oils left the system first, with subsequent oils exhibiting isotopically lighter values and are V poor. If the isotopically heaviest oils left the system first, with later oils isotopically lighter, then we should see a similar pattern in the kerogen as we do with the EOM. In other words, the kerogen should become isotopically lighter with time. As the kerogen becomes isotopically lighter with time, the bulk rock should become isotopically lighter overall. The large amounts of isotopically heavy vanadium leaving the system should shift the whole system (bulk rock, kerogen, EOM) isotopically lighter as light vanadium is left in situ.

Another uncertainty to take into account is other fluids that are present in the reservoir/pore spaces. Fluids other than oil, such as water and hydrothermal fluids can remove or incorporate vanadium in the system.

Lastly, we assume that the first oils extracted were isotopically heavy, high vanadium concentration oils, and that the oils being produced now are relatively isotopically light, and low in vanadium concentration. However, we do not know about the intermediate oils. We assume that they are isotopically lighter and lower V concentration than RM 8505, but isotopically heavier and more V-rich than the well producing today. Based on the EOM sampled, we see a very isotopically light, low V concentrated oils being extracted today. Once again, a very high reliance is being placed on RM 8505 oil being a good analog for early Eagle Ford oil.

As the EOM/kerogen values become isotopically light, it is evident that the bulk rock shale becomes isotopically heavier up hole ($\delta^{51}V$ -0.87±0.3‰ to -0.14±0.3‰). It would be expected that with the EOM/kerogen becoming isotopically lighter with time, the bulk rock would become isotopically lighter overtime as well. However, it is possible that the bulk rock did become isotopically lighter at first with the beginning isotopically heavy oil expulsions and then shifted isotopically heavier later.

There are several scenarios that can shift the bulk rock isotopically heavier even though the EOM/kerogen is isotopically light. First, if the isotopically lighter oils expulsed contained V(III). In this case, abundant isotopically light vanadium is leaving the system, shifting the bulk rock shale isotopically heavier. Second, a process of demetalation could be occurring where vanadyl ions are removed from the EOM/oil and bind to the inorganic component of the bulk rock. This would cause the bulk rock to become isotopically heavier as isotopically heavy vanadium (V(IV)) is being incorporated into the siliciclastics component and the EOM/oil becomes isotopically lighter. Lastly, isotopically light vanadium could be removed via fluids (formation waters, pore waters, hydrothermal fluids) or isotopically heavy vanadium from fluids are incorporated into the rock shifting the bulk rock isotopically heavier.

In other words, in order for the bulk rock to become isotopically heavier, there has to be abundant isotopically light vanadium removed either by oil or fluids, or an incorporation of abundant isotopically heavier vanadium has to be bound to the siliciclastics/clays.

5.5 Conclusion

Vanadium related to source rock shales can reside in several different reservoirs including: seawater, pore water, detrital siliciclastics, EOM (movable oil), kerogen (immovable organic matter) in shales and can be removed in the already produced oil and the pore fluids extracted and expulsed by natural processes.

The $\delta^{51}V$ global seawater value today is the result of a generally oxic open ocean, however the isotopic value during the Cretaceous is unknown. If in fact the Cretaceous global seawater was anoxic or euxinic, vanadium could either be removed by clays as reduced V(III) or by organometallic complexes as reduced V(IV). If vanadium was removed dominantly by clays, this would shift the global seawater value isotopically heavier as removal to clays lends to a lighter isotopic composition in clay. If vanadium was removed by organic molecules dominantly as V(IV), the global seawater value could have become isotopically lighter, as removal to organics lends itself to a heavier isotopic composition in the organics. However, if the global seawater was more like it is today, which is oxic, isotopically light V(V) would be incorporated into Fe-Mn oxides shifting the seawater isotopic value to heavier values as found today. (Figure 5.3.6; Wu et al., 2019).

As vanadium tends to be bound to the organic matter at the sea bottom during or shortly after deposition, vanadium isotopes can be significantly fractionated from seawater where reducing conditions exist. Isotopic fractionation can also occur subsequently between oil/kerogen/EOM and shale with sufficient burial, heating and transformation of kerogen to oil during catagenesis. As the bulk rock shale is heated and buried, the kerogen will progressively transform to oil.

It is evident that with time, burial, and oil expulsion, the EOM studied here from the Eagle Ford Formation becomes isotopically lighter and the bulk rock shale becomes isotopically heavier. RM 8505 was modeled as an example or proxy of isotopically heavy oil that may have been expulsed from the Eagle Ford during early stages of catagenesis. With RM 8505 used as a reference of the first oils expulsed, isotopically heavy, V rich oils likely first expulsed from the Eagle Ford source rocks. This expulsion would render the residual organic matter to be isotopically lighter. The well producing today indicates a V poor oil because of high maturity. If the first oils expulsed were isotopically heavy, V rich, and the later oils were V poor, then the later oils probably resembled the light isotopic signature like the EOM studied here. Where the EOM is isotopically lightest in the source rocks sections studied, we suggest that more expulsion events of isotopically heavier oil have occurred. On the contrary, where the EOM is the heaviest isotopically, it resembles more the RM 8505 isotopic values, indicating less expulsions of the isotopically heavy oil occurred. This could be interpreted to indicate oil reservoirs are more enriched in liquid oil where the EOM is isotopically heaviest and has been efficiently expulsed from areas where the EOM is isotopically lightest. This provides a hypothesis that is testable based on production from the various horizons drilled in the section.

Although we interpret that the EOM/kerogen become isotopically lighter with time and the progression of catagenesis and expulsion, the bulk rock shale becomes isotopically heavier. In order for the bulk rock shale to become isotopically heavier with time, abundant isotopically light vanadium must be removed from the system. This could occur by the isotopically lighter oils demetallizing, causing a removal of vanadium in a

more reduced lighter form of vanadium (III), and removal with the crude oil expulsion. In addition, demetallizing isotopically heavy V(IV) to the clays or by removal of isotopically light vanadium via fluids expulsed or delivery of high V concentrations and isotopically heavy vanadium from fluids into the clays. The bulk shales and EOM $\delta^{51}V$ values obtained in the shale and EOM sampled here have produced the broadest set of isotopic values from any earth materials sampled to date. This indicates that relatively low temperature fractionation of ^{51}V can be an important process in earth materials.

5.6 Future Work

Because this is the first time that EOM and bulk rock shale have been analyzed for vanadium isotopes in the same petroleum system, it is difficult to compare data and pinpoint the exact fractionation process(es) that could be contributing to the distinct shift in the isotopic signatures. Previously, vanadium isotope ratios had only been analyzed for crude oils, not the source rocks. One major drawback to this data set is that we cannot account for all the reservoirs containing the vanadium, and thus there are many unknowns about the vanadium content and isotopic values of potential reservoirs for vanadium. For example, the Cretaceous global seawater $\delta^{51}V$ is unknown, the kerogen concentrations and their isotopic signatures have not been analyzed, and the Eagle Ford Shale oil isotopic signature is unknown.

The next step to this study would be to analyze the kerogen for its isotopic signature and to acquire Eagle Ford shale oil. An issue with the Eagle Ford Shale oil is that the vanadium concentrations of highly mature and demetallized oils from that area are so low in vanadium abundance, that it may be difficult to extract enough V to

measure isotopic abundances. Therefore, we would require abundant amounts of oil to be able to perform the isotopic analysis, which could be very hard to come by and extremely expensive to process and prepare for isotopic analysis. To put it in perspective, the oil producing out of the Eagle Ford shale today has a vanadium concentration of ~20 ng/g. In order to perform the isotopic analysis on an oil, we need approximately one microgram of vanadium. In other words, we would need around 50 g of the Eagle Ford shale oil. In one digestion, we can digest about 0.4 g of oil, which would equal around 100 digestions overall. The better alternative is to acquire an oil from a less mature updip section of the Eagle Ford shale or to sample the overlying Austin Chalk crude oil in a less mature area. The lower maturities would yield higher vanadium concentrations and could be more easily measured.

5.7 References

Aleshin, G.N., Altukhova, Z.P., Antipenko, V.R., Marchenko, S.P., and Kamyanov, V.F., 1984. Distribution of vanadium and vanadyl porphyrins in petroleum distillates of different chemical types. Petroleum Chemistry, 24, 191–195.

Algeo, T. J., and Rowe, H., 2012. Paleoceanographic applications of trace-metal concentration data. Chemical Geology, 324-325, 6-18.

Algeo, T., and Tribovillard, N., 2009. Environmental analysis of paleoceanographic systems based on molybdenum-uranium covariation. Chemical Geology, 268 (3-4), 211-225

Amorim, F.A.C., Welz, B., Costa, A.C.S., Lepric, F.G., Vale, M.G.R., and Ferreira, S.L.C., 2007. Determination of vanadium in petroleum products using atomic spectrometric techniques. Talanta, 72, 349–359.

Anbar, A.D., and Knoll, A., 2002. Proterozoic ocean chemistry and evolution: a bioinorganic bridge. Science, 297, 1137–1142.

Anbar, A. D., and Rouxel, Oliver., 2007. Metal Stable Isotopes in Paleoceanography. Earth and Planetary Sciences Letters, 35, 717-746.

Baker, E.W., and Palmer, S.E., 1978. Geochemistry of porphyrins. In: Dolphin, D. (Ed.), The Porphyrins. Academic Press, New York, 1, 486–552.

Barwise, A., 1990. Role of nickel and vanadium in petroleum classification. Energy & Fuels, 4, 647–652.

Barwise, A.J.G., 1990. Role of nickel and vanadium in petroleum classification. Energy Fuels, 4, 647–652.

Barwise, A., and Park, P., 1983. Petroporphyrin finger- printing as a geochemical marker. In: BJOROY, M. ET AL. (eds) Advances in Organic Geochemistry 1981. Wiley, Chichester, 1, 668–674.

Barwise, A. and Roberts, I., 1984. Diagenetic and catagenetic pathways for porphyrins in sediments. Organic Geochemistry, 6, 167–176.

Bigeleisen, J. and Mayer, M.,1947. Calculation of Equilibrium Constants for Isotopic Exchange Reactions. The Journal of Chemical Physics, 15(5), 261-267.

Breit, G. and Wanty, R., 1991. Vanadium accumulation in carbonaceous rocks: A review of geochemical controls during deposition and diagenesis. Chemical Geology, 91(2), 83-97.

Breit, G., Wanty, R., and Tuttle, M., 1991. Geochemical Control on the Abundance of Vanadium in Black Shales and Other Carbonaceous Rocks in Metalliferous Black Shales and Related Ore Deposits. U.S. Geological Survey Circular, 1058, 6-8.

Broecker, W.S., and Peng, T.H., 1982. Tracers in the Sea. Eldigio Press, Columbia University, Palisades, NY. 689 pp.

Calvert, S.E., and Piper, D.Z., 1984. Geochemistry of ferromanganese nodules: multiple diagenetic metal sources in the deep sea. Geochimica et Cosmochimica Acta, 48, 1913–1928.

Casey, J.F., Gao, Y., Thomas, R., and Yang, W., 2016. New approaches in sample preparation and precise multi element analysis of crude oils and refined petroleum products using single-reaction-chamber micro- wave digestion and triple-quadrupole ICP-MS. Spectroscopy, 31, 11–224.

Cole, D., Zhang, S. and Planavsky, N., 2017. A new estimate of detrital redox-sensitive metal concentrations and variability in fluxes to marine sediments. Geochimica et Cosmochimica Acta, 215, pp.337-353.

Constantinides, G., Arich, G., and Lomi, C., 1959. Detection and behavior of porphyrin aggregates in petroleum residues and bitumens. 5th World Petroleum Congress, 131–142.

Didyk, B.M., Alturki, Y.I., Pillinger, C.T., and Eglinton, G., 1975. Petroporphyrins as indicators of geothermal maturation. Nature, 256, 563–565,

Dawson, B. J. and Katz, V. D. Ro., 1995. Austin Chalk Petroleum System: Upper Cretaceous, Southeastern Texas: ABSTRACT. AAPG Bulletin, 79, 157-163.

Donovan, A. D., and S. Staerker., 2010, Sequence stratigraphy of the Eagle Ford (Boquillas) Formation in the subsurface of South Texas and the outcrops of West Texas: Gulf Coast Association of Geologic Societies Transactions, 60, 861–899.

Donovan, A. D., T. S. Staerker, A. Pramudito, W. Li, M. J. Corbett, C. M. Lowery, A. M. Romero, and R. D. Gardner., 2012, The Eagle Ford outcrops of West Texas: A laboratory for understanding heterogeneities within unconventional mudstone reservoirs: Gulf Coast Association of Geological Societies Journal, 1, 162–185.

Elston, H., 2014, Mineralogical and Geochemical Assessment of the Eagle Ford Shale: Ohio State University, p 1-32.

Emerson, S.R., and Huestes, S.S., 1991. Ocean anoxia and the concentrations of molybdenum and vanadium in seawater. Marine Chemistry, 34, 177–196.

Filby, R.H., 1994. Origin and nature of trace element species in crude oils, bitumens and kerogens: implications for correlation and other geochemical studies. In: Parnell, J. (Ed.), Geofluids: Origin, Migration and Evolution of Fluids in Sedimentary Basins. Geological Society London Special Publications, 78, 203–219.

Fisk, M., and Kelley, K.A., 2002. Probing the Pacific's oldest MORB glass: mantle chemistry and melting conditions during the birth of the Pacific Plate. Earth and Planetary Science Letters, 202, 741–752.

Galaragga, F., Reatugui, K., Martinez, A., Martinez, M., Llamas, J., and Marquez, G., 2008. V/Ni ratio as a parameter in paleo environmental characterization of nonmature medium-crude oils from several Latin American basins. Journal of Petroleum Science and Engineering, 61, 9–14.

Gannoun, A., Burton, K.W., Parkinson, I.J., Alard, O., Schiano, P., and Thomas, L.E., 2007. The scale and origin of the osmium isotope variations in mid-ocean ridge basalts. Earth and Planetary Science Letters, 259, 541–556.

Gardner, R., Pope, M., Wehner, M., and Donovan, A., 2013. Comparative Stratigraphy of the Eagle Ford Group Strata in Lozier Canyon and Antonio Creek, Terrell County, Texas. Gulf Coast Association of Geologic Societies Transactions Journal, 2, 42-52.

Gale, A., Langmuir, C.H., and Dalton, C.A., 2014. The global systematics of ocean ridge basalts and their origin. Journal of Petrology, 55, 1051–1082.

Gannoun, A., Burton, K.W., Parkinson, I.J., Alard, O., Schiano, P., and Thomas, L.E., 2007. The scale and origin of the osmium isotope variations in mid-ocean ridge basalts. Earth and Planetary Science Letters, 259, 541–556.

Gao, Yongjun and Casey, John and M. Bernardo, Luis and Yang, Weihang and K. (Adry) Bissada, K., 2017. Vanadium isotope composition of crude oil: effects of source, maturation and biodegradation. Geological Society London Special Publications, 468, 83-103.

Hammes, U., Eastwood, R., McDaid, G., Vankov, E., Gherabati, S., Smye, K., Shultz, J., Potter, E., Ikonnikova, S. and Tinker, S., 2016. Regional assessment of the Eagle Ford Group of South Texas, USA: Insights from lithology, pore volume, water saturation, organic richness, and productivity correlations. Interpretation, 4(1), SC125-SC150.

Harbor, R., 2011. Facies Characterization and Stratigraphic Architecture of Organic-Rich Mudrocks, Upper Cretaceous Eagle Ford Formation, South Texas: Master's Thesis, University of Texas at Austin, 195 p.

Hentz, T.F., and Ruppel, S.C., 2010, Regional lithostratigraphy of the Eagle Ford Shale: Maverick Basin to East Texas Basin: Gulf Coast Association of Geological Societies Transactions, 60, 325-337.

Hoefs, J., 2008. Stable Isotope Geochemistry. Springer Science & Business Media, Berlin.

Hunt, J. M., 1996. Petroleum Geochemistry and Geology (W.H. Freeman, San Francisco).

Klein, E.M., and Langmuir, C.H., 1987. Global correlations of ocean ridge basalt chemistry with axial depth and crustal thickness. Journal of Geophysical Research., Solid Earth, 92, 8089–8115.

Lewan, M.D., 1980. Geochemistry of Vanadium and Nickel in Organic Matter of Sedimentary Rocks. Ph.D. Dissertation, University of Cincinnati, 353.

Lewan, M.D., and Maynard, J.B., 1982. Factors controlling enrichment of vanadium and nickel in the bitumen of organic sedimentary rocks. Geochimica et Cosmochimica Acta, 46, 2547–2560.

Lewan, M.D., 1984. Factors controlling the proportionality of vanadium and nickel in crude oils. Geochimica et Cosmochimica Acta, 48, 2231–2238.

Lipiner, G., Willner, I., and Aizenshtat, Z., 1988. Correlation between geochemical environments and controlling factors in the metalation of porphyrins. Organic Geochemistry, 13 (4–6), 747–756.

Louda, J.W., Li, J., Liu, L., Winfree, M.N., and Baker, E.W., 1998. Chlorophyll-a degradation during cellular senescence and death. Organic Geochemistry, 29 (5–7), 1233–1251.

Magoon, L. B., 1988. Petroleum Systems of the United States. U.S. G. P.O.

Mackenzie, A.S., Patience, R., Maxwell, J., Vanden-Broucke, M. and Durand, B., 1980. Molecular parameters of maturation in the Toarcian shales, Paris Basin, France – I. Changes in the configurations of acyclic isoprenoid alkanes, steranes and triterpanes. Geochimica et Cosmochimica Acta, 44, 1709–1721.

Martin, R., Baihly. J.D., Malpani, R., Lindsay, G.J., and Atwood, W.K., 2011. Understanding Production from Eagle Ford-Austin Chalk System: SPE Annual Technical Conference and Exhibition, p. 1–28.

Maylotte, D., Wong, J., Peters, R.S., Lytle, F. and Greegor, R., 1981. X-ray absorption spectroscopic investigation of trace vanadium sites in coal. Science, 214, 554–556.

McGarity, H., 2013. Facies and Stratigraphic Framework of the Eagle Ford Shale in South Texas: Master's thesis, University of Houston, 96 p.

Moldowan, J.M., Sundararaman, P. and Schoell, M., 1986. Sensitivity of biomarker properties to depositional environment and/or source input in the Lower Toarcian of SW-Germany. Organic Geochemistry, 10, 915–926.

Morford, J.L., and Emerson, S., 1999. The geochemistry of redox sensitive trace metals in sediments. Geochimica et Cosmochimica Acta, 63, 1735–1750.

Morford, J.L., Emerson, S.R., Breckel, E.J., and Kim, S.H., 2005. Diagenesis of oxyanions (V, U, Re, and Mo) in pore waters and sediments from a continental margin. Geochimica et Cosmochimica Acta, 69, 5021–5032.

Murphy, Eric, et al., 2013. A Workflow to Evaluate Mineralogy, Porosity, TOC, and Hydrocarbon Volume in the Eagle Ford Shale. SPE Unconventional Resources Conference and Exhibition- Asia Pacific.

Niederer, F., Papanastassiou, D. and Wasserburg, G., 1985. Absolute isotopic abundances of Ti in meteorites. Geochimica et Cosmochimica Acta, 49, 835–851.

Nielsen, S.G. 2015. Stable Vanadium Isotopes in Crude Oils and Their Source Rocks: A New Tool to Under- stand the Processes Governing Petroleum Generation. Report DN12, American Chemical Society, https://acs webcontent.acs.org/prfar/2013/Paper12260.html

Nielsen, S.G., Prytulak, J. and Halliday, A.N., 2011. Determination of precise and accurate V-51/V-50 isotope ratios by MC-ICP-MS, Part 1: chemical separation of vanadium and mass spectrometric protocols. Geostandards and Geoanalytical Research, 35, 293–306.

Nielsen, S.G., Prytulak, J., Wood, B.J. and Halliday, A.N., 2014. Vanadium isotopic difference between the silicate Earth and meteorites. Earth and Planetary Science Letters, 389, 167–175.

Nielsen, S.G., Owens, J.D. and Horner, T.J., 2016. Analysis of high-precision vanadium isotope ratios by medium resolution MC-ICP-MS. Journal of Analytical Atomic Spectrometry, 31, 531–536.

Nielsen, S., Auro, M., Righter, K., Davis, D., Prytulak, J., Wu, F. and Owens, J. (2019). Nucleosynthetic vanadium isotope heterogeneity of the early solar system recorded in chondritic meteorites. Earth and Planetary Science Letters, 505, 131-140.

Odermatt, J.R., and Curiale, J.A., 1991. Organically bound metals and biomarkers in the Monterey Formation of the Santa Maria Basin, California. Chemical Geology, 91 (2), 99–113.

Peters, K.E. and Moldowan, J.M. 1993. The Biomarker Guide: Interpreting Molecular Fossils in Petroleum and Ancient Sediments. Prentice Hall, Englewood Cliffs, NJ.

Premović, P.I., 1984. Vanadyl ions in ancient marine carbonaceous sediments. Geochimica et Cosmochimica Acta, 48, 873–877.

Premovic, P.I., Allard, T., Nikolic, N.D., Tonsa, I.R., and Pavlovic, M.S., 2000a. Estimation of vanadyl porphyrin concentration in sedimentary kerogens and asphaltenes. Fuel, 79 (7), 813–819.

Premović, P.I., Đorđević, D., and Pavlović, M., 2002. Vanadium of petroleum asphaltenes and source kerogens (La Luna Formation, Venezuela): isotopic study and origin. Fuel, 81, 2009–2016.

Prytulak, J., Nielsen, S.G., and Halliday, A.N., 2011. Determination of high precision $^{51}V/^{50}V$ isotope ratios by MC-ICP-MS, Part 2: verification of precision and accuracy for standard reference materials. Geostandards and Geoanalytical Research, 35, 307–318.

Prytulak, J., Nielsen, S.G., Ionov, D.A., Halliday, A.N., Harvey, J., Kelley, K.A., Niu, Y.L., Peate, D.W., Shimizu, K., and Sims, K.W.W., 2013. The stable vanadium isotope composition of the mantle and mafic lavas. Earth and Planetary Science Letters, 365, 177–189.

Schauble, E., Rossman, G. and Taylor, H., 2001. Theoretical estimates of equilibrium Fe-isotope fractionations from vibrational spectroscopy. Geochimica et Cosmochimica Acta, 65, 2487–2497.

Scholz, F., Hensen, C., Noffke, A., Rohde, A., Liebetrau, V. and Wallmann, K., 2011. Early diagenesis of redox-sensitive trace metals in the Peru upwelling area – response to ENSO-related oxygen fluctuations in the water column. Geochimica et Cosmochimica Acta, 75(22), 7257-7276.

Schuth, S., Horn, I., Brüske, A., Wolff, P. and Weyer, S., 2017. First vanadium isotope analyses of V-rich minerals by femtosecond laser ablation and solution-nebulization MC-ICP-MS. Ore Geology Reviews, 81, 1271-1286.

Scott, C, et al., 2017. The Hyper-Enrichment of V and Zn in Black Shales of the Late Devonian-Early Mississippian Bakken Formation (USA). Chemical Geology, 452, 24-33.

Seewald, J.S., 2003. Organic-Inorganic interactions in petroleum- producing sedimentary basins. Nature, 426, 327-333.

Shields, W.R., Murphy, T.J., Catanzaro, E.J. and Garner, E.L., 1966. Absolute isotopic abundance ratios and the atomic weight of a reference sample of chromium. Journal of Research of the National Bureau of Standards A, 70, 193–197.

Sundararaman, P., Biggs, W.R., Reynolds, J.G. and Fetzer, J.C. 1988. Vanadyl porphyrins, indicators of kerogen breakdown and generation of petroleum. Geochimica et Cosmochimica Acta, 52, 2337–2341.

Sundararaman, P., Schoell, M., Littke, R., Baker, D., Leythaeuser, D. and Rullkotter, J., 1993. Depositional environment of Toarcian shales from northern Germany as monitored with porphyrins. Geochimica et Cosmochimica Acta, 57, 4213–4218.

Takahashi, S., Yamasaki, S., Ogawa, Y., Kimura, K., Kaiho, K., Yoshida, T., and Tsuchiya, N., 2014. Bioessential element- depleted ocean following the euxinic maximum of the end- Permian mass extinction. Earth and Planetary Science Letters, 393, 94-104.

Takashima, R., Nishi, H., Yamanaka, T., Tomosugi, T., Fernando, A., Tanabe, K., Moriya, K., Kawabe, F. and Hayashi, K., 2011. Prevailing oxic environments in the Pacific Ocean during the mid-Cretaceous Oceanic Anoxic Event 2. Nature Communications, 2(1), 1-5.

Tissot, B.P. and Welte, D.H., 1984. Petroleum Formation and Occurrence. Springer Verlag, Germany.

Treibs, A., 1934. Chlorophyll und Häminderivate in bituminösen Gesteinen, Erdölen, Erdwachsen und Asphalten. Justus Liebigs Annalen der Chemie, 510, 42–62.

Treibs, A., 1936. Chlorophyll und Häminderivate in organischen Mineralstoffen. Angewandte Chemie, 49, 682–686.

Tribovillard, N., Algeo, T.J., Timothy Lyons, T., and Riboulleau, A., 2006. Trace metals as paleoredox and paleoproductivity proxies: an update. Chemical Geology, 232, 12–32.

Turekian, K.K. and Wedepohl, K.H., 1961. Distribution of the Elements in some major units of the Earth's crust. Geological Society of America, Bulletin, 72, 175-192.

Urey, H.C., 1947. The thermodynamic properties of isotopic substances. Journal of the Chemical Society (Resumed), 1947, 562–581.

U.S. Energy Information Administration., 2010. http://www.eia.gov/oil_gas/rpd/shaleusa9.pdf (accessed March 2019).

U.S. Energy Information Administration., 2014. https://www.eia.gov/maps/pdf/EIA%20Eagle%20Ford%20Play%20update%2012-29-14.pdf (accessed March 2019).

Ventura, G.T., Gall, L., Siebert, C., Prytulak, J., Szat- Mari, P., Hurlimann, M. and Halliday, A.N., 2015. The stable isotope composition of vanadium, nickel, and molybdenum in crude oils. Applied Geochemistry, 59, 104–117.

Wang, W.H., 2014. High Precision Determination of Trace Elements in Crude Oils by Inductively Coupled Plasma-Optical Emission Spectrometry and Inductively Coupled Plasma-Mass Spectrometry. University of Houston, Texas, USA.

Wanless, V., Perfit, M., Klein, E., White, S., and Ridley, W., 2012. Reconciling geochemical and geophysical observations of magma supply and melt distribution at the 9 N overlapping spreading center, East Pacific Rise. Geochemistry, Geophysics, Geosystems,13, 1-22.

Wanty, R.B., Goldhaber, M.B. and Northrop, H.R., 1990. Geochemistry of vanadium in an epigenetic, sandstone- hosted vanadium–uranium deposit, Henry Basin, Utah. Economic Geology, 85, 270–284.

Wanty, R.B., and Goldhaber, M.B., 1992, Thermodynamics and kinetics of reactions involving vanadium in natural systems: Accumulation of vanadium in sedimentary rocks: Geochimica et Cosmochimica Acta, 56, 1471-1483.

Wehrly, B., and Stumm, W., 1989. Vanadyl in natural waters: adsorption, and hydrolysis promote oxygenation. Geochimica et Cosmochimica Acta, 53, 69–77.

Wedepohl, K. 1971. Environmental influences on the chemical composition of shales and clays. Physics and Chemistry of the Earth, 8, 305–333.

Whisman M. L. and Cotton F. O., 1971. Bumines data promise help in identifying petroleum-spill sources. Oil and Gas Journal, 27, 111-113.

Wu, F., Qin, T., Li, X., Liu, Y., Huang, J.H., Wu, Z. and Huang, F., 2015. First-principles investigation of vanadium isotope fractionation in solution and during adsorption. Earth and Planetary Science Letters, 426, 216–224.

Wu, F., Qi, Y., Yu, H., Tian, S., Hou, Z., and Huang, F., 2016. Vanadium isotope measurement by MC-ICP-MS. Chemical Geology, 421, 17-25.

Wu, F., Qi, Y., Perfit, M., Gao, Y., Langmuir, C., Wanless, V., Yu, H. and Huang, F., 2018. Vanadium isotope compositions of mid-ocean ridge lavas and altered oceanic crust. Earth and Planetary Science Letters, 493, 128-139.

Wu, F., Owens, J.D., Huang, T., Sarafian, A., Huang, K.F., Sen, I.S., Horner, T.J., Blusztajn, J., Morton, P., and Nielsen, S.G., 2019. Vanadium isotope composition of seawater. Geochemica et Cosmochimica Acta, 244, 403-415.

Zheng, Y., Anderson, R.F., van Geen, A., and Fleischer, M.Q., 2002a. Preservation of non- lithogenic particulate uranium in marine sediments. Geochimica et Cosmochimica Acta, 66, 3085–3092.